

The copyright of this thesis vests in the author. No quotation from it or information derived from it is to be published without full acknowledgement of the source. The thesis is to be used for private study or non-commercial research purposes only.

Published by the University of Cape Town (UCT) in terms of the non-exclusive license granted to UCT by the author.

Sorption of the Platinum-group elements in selected solid matrices

Lídia Velazquez Lopes

B. Environmental Engineering (University of Aveiro, Portugal)

Submitted in partial fulfilment of the requirements for the degree of

Master of Science

in Environmental Geochemistry

Department of Geological Sciences

Faculty of Science

University of Cape Town

January 2003

ABSTRACT

Recent research on the platinum-group elements (PGE) has shown increased concentrations in environmental samples, probably as a result of the widespread use of PGE (Pt, Pd and Rh in particular) as catalysts in the chemical and car industry. Most of the recent research on PGE focuses on the analysis of concentrations in environmental samples exposed to anthropogenic sources of PGE, but there are very few studies that have investigated sorption behaviour of PGE in soils. A lack of knowledge about the sorption behaviour of PGE, especially Pt, Pd and Rh, has motivated the present adsorption study.

Six solid matrices were selected and characterised for their physico-chemical properties: two clay mineral samples (Kaolin and Calcium-bentonite), a windblown sand (Consol sand), a topsoil from the Table Mountain slope (Malm), a wetland sediment (Zandvlei), and a pine forest topsoil (Tokai). Kaolin and Ca-bentonite samples had low and high cation exchange capacity (CEC), respectively, while the Consol sand had very low CEC and no clay or organic material (Corg). The Malm soil consisted predominantly of fine sand and silt with a 6% Corg. In contrast, the wetland sample consisted of clay and silt particles in combination with an elevated Corg (11%). The pine forest topsoil was poor in clay content in comparison to the other soils and extremely rich in organic matter (23% Corg).

Batch adsorption experiments were conducted over 24 hours using each of the solid matrices as sorbent in contact with a solution containing PGE and Au of known concentration (parts per billion range). PGE and Au concentrations in the solid matrices supernatant were analysed over 24h using ICP-MS and pH was monitored at each sampling point. From the patterns obtained in the experiments it was obvious that the most pronounced decrease in concentration occurs within the first 30-60 minutes of reaction time as compared to the following 23 hours. However, not all the elements behaved in the same way. Re, Rh, Os, and Ir do not decrease substantially over time under these experimental conditions, while Au, Pd, Pt, and Ru show a

dramatic decrease in concentration over the equilibration time (24 h) in most solid matrices.

Batch adsorption isotherm experiments were conducted for the calculation of Pt, Pd and Rh distribution coefficients (K_d in L/kg) in the Table Mountain topsoil, wetland sediment and pine forest samples. The obtained adsorption isotherms confirmed the trends observed in the time course experiments at the low concentration range. Freundlich and Langmuir equations were applied to the adsorption data in order to calculate the partitioning coefficients. Since the low C_w concentration (50-500 $\mu\text{g/L}$) is the range of interest for the present study linear isotherms were also plotted with the selected data and the K_d (L/kg) obtained for Pt, Pd, and Rh. K_d values for Pt in the Malm and Zandvlei matrices were 27.09 ($r^2=0.984$) and 43.78 ($r^2=0.994$), respectively. For Pd the K_d values were 727.11 ($r^2=0.993$) and 1405.60 ($r^2=0.649$) in the Malm and Zandvlei matrices, respectively. The K_d value for Rh could only be calculated in interaction with the Zandvlei sample ($K_d=4.54$, $r^2=0.985$) due to the Rh erratic sorption behaviour in the Malm and Tokai samples. The calculated K_d for Rh was the lowest of the three elements studied.

Under the experimental conditions of these experiments it appears that Pt and Pd are adsorbed strongly to solid matrices whilst Rh is practically not adsorbed and therefore remains in solution. This may have important environmental implications since Rh could have a greater tendency to reach the ground water and possibly also be more bio-available for plants and humans. Pt shows a clear preference for organic rich matrices.

More studies are needed to confirm these findings and further investigations are required to understand possible mobilisation of PGE in the natural environment.

ACKNOWLEDGEMENTS

Wish to thank my supervisors Dr A. N. Roychoudhury for the assistance, patience and encouragement during this project and Dr. M. Tredoux for the friendly support and primordial idea of doing a project in this field. I would also like to thank Dr. John Compton and Meris Smith for the encouragement and helpful suggestions during the whole year. Furthermore, Dr. John Rogers and Rochelle Wigley for the permission and help using the settling column in the Marine Geosciences department (UCT) and to the ICP-MS team in the Geological Sciences department (UCT): Dr. Andreas Späth and Fayroosa Raywoot for their help during the intensive laboratorial work. A special thank to Shireen Govender and Prof. Martin Fey for their help and constructive comments. Also the following persons were important for the successful completion of this project: Ernest Rood from *G&W Base* (Johannesburg) for the supply of clay minerals (Ca-bentonite and kaolin); Cliff Doors from the Zandvlei Wetland Reserve (Muizenberg, Cape Province) for the supply of Zandvlei sediment and D. Engelbrecht from *Lafarge Pty.* (Bellville, Cape Town) for the supply of Consol sand.

Not to forget the daily friendly support from Patrick Seas, Ivan and Ernest in many laboratorial procedures.

I enjoyed the company of all honours students and my course colleagues Naadira Haniff, Keir Sodergerg and specially André Smit for the friendly working atmosphere during the whole year.

Last but not least I would like to thank my parents for the financial support and encouragement and my partner Mace Schuurmans, who helped me pursue my aim and supported me in the difficult times.

TABLE OF CONTENTS

<u>Chapter</u>	<u>Page</u>
Abstract	1
Acknowledgements	3
Table of contents	4
List of tables	6
List of figures	10
1. Introduction and background	12
1.1 Anthropogenic PGE.....	13
1.2 PGE in the natural environment: speciation, mobilisation, and bioavailability of PGE.....	16
1.3 Analysis of PGE in environmental samples: interferences and limitations.....	20
1.4 Batch studies to identify and characterise PGE interactions in the natural environment: advantages and limitations.....	21
1.5 Conclusions.....	22
2. Methodology	23
2.1 Sample collection.....	23
2.2 Analytical techniques	24
2.2.1 General characterisation of solid matrices	24
2.2.2 PGE and Au analysis by ICP-MS.....	26
2.3 Batch experiments.....	27
2.3.1 Time course experiments.....	27
2.3.2 Adsorption isotherm experiments	29

3. Results	30
3.1 General characterisation of solid matrices.....	30
3.2 Batch adsorption experiments.....	35
3.2.1 Time course experiments.....	35
3.2.2 Adsorption isotherm experiments.....	40
4. Discussion	46
4.1 General characterisation of solid matrices.....	46
4.2 Time course experiments.....	48
4.3 Pt, Pd and Rh isotherms and K_d calculation.....	52
4.4 Data quality	66
5. Conclusions	67
6. References	70
Appendix	76

LIST OF TABLES

	Page
Table 1 – Summary of some examples of Pt, Pd and Rh concentrations analysed in environmental samples (soil, road dust, air, air dust, plants and human body fluids) reported in recent studies.	14
Table 2 - Typical instrumental operation conditions for the ELAN 6000-Perkin Elmer ICP-MS at the Department of Geological Sciences (UCT).	25
Table 3 - Typical instrumental operation conditions for the Philips X-ray diffractometer at the Department of Geological Sciences (UCT).	26
Table 4 - Summary of solid matrices physico-chemical properties: texture, pH, CEC, LiCl extractable cations, % Corg, mineralogy and SSA-N ₂	30
Table 5 – Average values of total PGE and Au concentrations (µg/kg) in the solid matrices acid digestion leachates determined by ICP-MS.	32
Table 6 – PGE and Au concentration (µg/l) in the reagent solution at the beginning (t ₀) and end (after 1440 minutes) of the time course experiments: (A) using the Kaolin, Ca-bentonite, and Consol sand and (B) using the Malm, Zandvlei and Tokai samples.	35
Table 7 - PGE and Au concentrations (µg/l) in the reagent solutions (A, B, C, D, F, G, H) for the isotherm adsorption experiments determined by ICP-MS.	41
Table 8a - PGE and Au equilibrium concentrations (µg/l) in the Malm subsamples supernatant after 24h interaction with the respective reagent solution A-H (in duplicate: upper/lower panel).	42
Table 8b - PGE and Au equilibrium concentrations (µg/l) in the Zandvlei subsamples supernatant after 24h interaction with the respective reagent solution A-H (in duplicate: upper/lower panel).	43
Table 8c - PGE and Au equilibrium concentrations (µg/l) in the Tokai subsamples supernatant after 24h interaction with the respective reagent solution A-H (in duplicate: upper/lower panel).	44

	Page
Table 9 - Comparison of Pt, Pd and Rh K_d values obtained using the Freundlich, Langmuir and linear isotherm models (when applicable) to describe adsorption behaviour in the batch adsorption experiments. Using $C_w = 0.03$ mg/L).	64
Table 10 - Total data (duplicates) from solid matrices characterisation: CEC, LiCl extractable cations, and organic carbon content (%).	77
Table 11 – pH readings at different electrolyte concentrations for Kaolin, Ca-Bentonite, Consol sand, Malm, Zandvlei, and Tokai samples. Duplicates (D) and triplicates (T) for the 0.01M KCl concentration are presented.	78
Table 12 - Total PGE and Au concentrations ($\mu\text{g}/\text{kg}$) in the solid matrices acid digestion leachates using ICP-MS: Kaolin (single subsample), Ca-bentonite (single subsample), Consol sand (single subsample), Malm (triplicate subsamples), Zandvlei (duplicate subsamples), and Tokai (duplicate subsamples) solid matrices. Triplicate runs in ICP-MS (1, 2, and 3)	80
Table 13a - PGE and Au background concentrations (ng/L) in the Kaolin subsamples supernatant in the time course adsorption experiments. Solid matrix/ MQ water ratio: 3 g: 50 ml.	81
Table 13b - PGE and Au background concentrations (ng/L) in the Ca-bentonite subsamples supernatant in the time course adsorption experiments. Solid matrix/ MQ water ratio: 3 g: 50 ml.	81
Table 13c - PGE and Au background concentrations (ng/L) in the Consol sand subsamples supernatant in the time course adsorption experiments. Solid matrix/ MQ water ratio: 3 g: 50 ml.	82
Table 13d - PGE and Au background concentrations (ng/L) in the Malm subsamples supernatant in the time course adsorption experiments. Solid matrix/ MQ water ratio: 3g:50 ml.	82
Table 13e - PGE and Au background concentrations (ng/L) in the Zandvlei subsamples supernatant in the time course adsorption experiments. Solid matrix/ MQ water ratio: 3g: 50 ml.	83
Table 13f - PGE and Au background concentrations (ng/L) in the Tokai subsamples supernatant in the time course adsorption experiments. Solid matrix/ MQ water ratio: 3g: 50 ml.	83

	Page
Table 14a – Average PGE and Au concentrations ($\mu\text{g/l}$) and pH readings and respective standard deviation between duplicate for the Kaolin subsamples supernatant at specific time sampling points (t_i) in the time course experiments.	84
Table 14b – Average PGE and Au concentrations ($\mu\text{g/l}$) and pH readings and respective standard deviation between duplicate for the Ca-bentonite subsamples supernatant at specific time sampling points (t_i) in the time course experiments.	84
Table 14c – Average PGE and Au concentrations ($\mu\text{g/l}$) and pH readings and respective standard deviation between duplicate for the Consol sand subsamples supernatant at specific time sampling points (t_i) in the time course experiments.	85
Table 14d - Average PGE and Au concentrations ($\mu\text{g/l}$) and pH readings and respective standard deviation between duplicate for the Malm subsamples supernatant at specific time sampling points (t_i) in the time course experiments.	85
Table 14e – Average PGE and Au concentrations ($\mu\text{g/l}$) and pH readings and respective standard deviation between duplicate for the Zandvlei subsamples supernatant at specific time sampling points (t_i) in the time course experiments.	86
Table 14f – Average PGE and Au concentrations ($\mu\text{g/l}$) and pH readings and respective standard deviation between duplicate for the Tokai subsamples supernatant at specific time sampling points (t_i) in the time course experiments.	86
Table 15 – PGE and Au concentration ($\mu\text{g/l}$) in the reagent solution at the beginning (t_0) and end (after 1440 minutes) of the time course experiments: (A) using the Kaolin, Ca-bentonite, and Consol sand and (B) using the Malm, Zandvlei and Tokai samples. ICP-MS replicates of duplicate aliquots: upper/lower panel.	87
Table 16 – Masses of each solid matrices (mg) used in the adsorption isotherm experiments for the respective reagent solution concentration (A, B, C, D, E, F, G, H).	87
Table 17 – PGE and Au concentration ($\mu\text{g/l}$) of the respective reagent solution: A, B, C, D, E, F, G, and H used in the adsorption isotherm experiments. ICP-MS replicates of single aliquots: upper/lower panel.	88

	Page
Table 18a – PGE and Au equilibrium concentration ($\mu\text{g/l}$) and standard deviations from replicate ICP-MS analysis, after interaction of the Malm sample with the respective reagent solution (A, B, C, D, E, F, G, and H) in the adsorption isotherm experiments. Duplicate aliquots: upper/lower panel	89
Table 18b – PGE and Au equilibrium concentration ($\mu\text{g/l}$) and standard deviations from replicate ICP-MS analysis, after interaction of the Zandvlei sample with the respective reagent solution (A, B, C, D, E, F, G, and H) in the adsorption isotherm experiments. Duplicate aliquots: upper/lower panel	90
Table 18c – PGE and Au equilibrium concentration ($\mu\text{g/l}$) and standard deviations from replicate ICP-MS analysis, after interaction of the Tokai sample with the respective reagent solution (A, B, C, D, E, F, G, and H) in the adsorption isotherm experiments. Duplicate aliquots: upper/lower panel	91

University of Cape Town

LIST OF FIGURES

	Page
Figure 1 - Potentiometric titration curves for the (a) Kaolin and the (b) Ca-bentonite, (c) Consol sand, (d) Malm, (e) Zandvlei, (f) Tokai samples obtained at four different electrolyte (KCl) concentrations.	33
Figure 2 - Average PGE and Au concentrations ($\mu\text{g/L}$) of replicate analysis and duplicate samples in the supernatant of (a) Kaolin, (b) Ca-bentonite, (c) Consol sand, (d) Malm, (e) Zandvlei and (f) Tokai samples at the correspondent sampling time points. The time plotted (in minutes) indicates the elapsed reaction time since the beginning of the experiment (t_0).	37
Figure 3 - Average pH values of the supernatant for each solid matrix at the correspondent sampling points during the time course experiments. The time plotted (in minutes) indicates the elapsed reaction time since the beginning of the experiment (t_0).	40
Figure 4 - pH of the supernatant of Malm, Zandvlei and Tokai samples after 24h reaction time with the respective PGE and Au reagent solution (A-H) for the adsorption isotherm experiments.	45
Figure 5 - Concentrations of (a) Pt, (b) Pd and (c) Rh ($\mu\text{g/L}$) in the supernatant of Kaolin, Ca-bentonite, Consol sand, Malm, Zandvlei and Tokai samples at correspondent reaction times over 24 h time course experiment.	49
Figure 6 - Adsorption isotherms in duplicate: (a) Pt, (b) Pd and (c) Rh. The adsorbed concentration C_s (mg element adsorbed / kg solid matrix) is plotted against the concentration in equilibrium C_w (mg /L).	53
Figure 7 - Freundlich isotherm converted to the logarithmic form for Pt, Pd and Rh. Pt in the (a) Malm, (b) Zandvlei and (c) Tokai samples; Pd in the (d) Malm, (e) Zandvlei and (f) Tokai samples, and Rh in the (g) Zandvlei sample.	57

	Page
Figure 8 – Langmuir isotherms converted to the linear form $C_w/C_s = bK - KC_w$ for Pt adsorption data in the (a) Malm, (b) Zandvlei and (c) Tokai samples; Pd in the (d) Malm, (e) Zandvlei and (f) Tokai samples, and Rh in the (g) Zandvlei sample.	59
Figure 9 – Linear isotherm for Pt, Pd and Rh selected adsorption data. $C_w = KC_s + b$. for Pt, adsorption data in the (a) Malm, (b) Zandvlei and (c) Tokai samples; Pd in the (d) Malm, (e) Zandvlei and (f) Tokai samples, and Rh in the (g) Zandvlei sample	62
Figure 10 - Correlation between % Corg with the max (a) Pt and (b) Rh adsorbed in the Malm, Zandvlei and Tokai solid matrices studied.	65
Figure 11 – X-ray diffractograms of the solid matrices: (a) X-ray diffractogram for Malm, Zandvlei, Tokai and Consol sand bulk sample (< 2 mm) and (b) X-ray diffractogram for Malm, Zandvlei and Tokai clay fraction.	92
Figure 12 – Plot of $\log a_{Cl^-}$ versus pH for (a) Pt and (b) Pd at 25°C showing the various fields of predominance of the various chloride, hydroxide and mixed hydroxychloride complexes. Source: <i>Wood et al. (1992)</i> .	94

1. INTRODUCTION AND BACKGROUND

The platinum-group elements (PGE) consist of the following six elements: ruthenium, rhodium, osmium, iridium, palladium, and platinum. They are the six densest members of Groups 8 and 10 in the periodic table. They are rare elements: Pt is the most common with an average abundance of 10 parts per billion (ppb) in the Earth crust whereas the others have abundances of 1 ppb to 10 ppb (Cabri, 1989).

The PGE have many useful applications because they exhibit extremely varied chemical behaviour depending on their state of oxidation and chemical environment (Cabri, 1989). PGE are widely used as catalysts in many industrial processes, for example, in the hydrogenation of ethylene for production of acetaldehyde, and oxidation of ammonia to nitric acid.

More recently, the widespread use of catalytic converters in motorcars to reduce emission of pollutant gases like CO and unburned hydrocarbons has resulted in a new and widespread application for these metals. In currently manufactured catalysts, a combination of Pt and Pd is present to induce oxidation of the hydrocarbons by nitrogen oxides (NO_x) at lower temperatures (220°C) than usual thermal oxidation processes. In order to favour nitrogen oxides reduction Rh is also present in lower concentrations (Palacios et al., 2000; Morton et al., 2001). Conventional three way catalytic converters contain about 0.10-0.15% PGE and the ratios of the metals may vary from country to country. For example the ratio of Pt/Pd is 10/1 for the United States (US) and 5/1 for the European Union (EU). Recently Pd has been used increasingly to substitute for both Pt and Rh.

South Africa is one of the world's biggest exporters of PGE because its ore deposits in the Merensky Reef and the UG2 reef parts of the Bushveld complex. Exploration of PGE has been increasing in SA over the last years since the country presents the highest PGE reserves (McLeod, 1996; Jones, 1999). Enrichment of PGE is often associated with several other metals (Au, Ag, Cr, Cu and Ni) in ultramafic intrusions and volcanic rocks (Cabri, 1989; Kucha et al., 1999), and recently has been studied extensively in order to find

conditions and mechanisms for its accumulation in associated sediments (Fletcher et al., 1995; Wood et al., 1996). South Africa is also one of the main catalyst manufacturers although the production is mainly for overseas use. Despite that the local market will soon be increasing the use of catalysts in the automobile industry since recent laws promote the use of catalytic converters and unleaded fuel is readily available.

The increased use of Pt, Rh, and Pd in catalytic converters in motorcars has increased the interest in these rare elements that were previously confined to mining environments and have now become part of our daily life.

1.1 Anthropogenic PGE

Although the use of catalysts in the automobile industry has started just over 20 years ago, its use only became mandatory in the UK at the beginning of 1993 in response to the EU emission standards (Farago et al., 1998) and was enforced by state regulations in Germany in 1994 (Schierl and Fruhmann, 1996). In Mexico City one third of more than 4 million vehicles are equipped with catalytic converters after stricter emissions legislation became effective in 1993 demanding the use of oxidation catalysts in all light vehicles (Morton et al., 2001). In Madrid about 40-50% of the city's cars are equipped with catalytic converters to decrease emission of greenhouse gases according to the new directives of the EU which were implemented there as from 1993 (Gómez et al., 2001). In South Africa the use of catalytic converters is not compulsory but recent legislation encourages their use.

Using PGE to reduce emission of harmful gases to the atmosphere results in the release of very small PGE-containing particles (0.5-10 μ m) due to abrasion and deterioration of catalytic converters (Koenig et al., 1992; Artelt et al., 1999; Artelt et al., 2000). Possible accumulation of these particles in soils, air and air dust has been investigated and are summarised in Table 1. It is evident from these results that concentrations of Pt, Pd and Rh in soils (and other environmental samples) exposed to inputs have clearly increased levels as compared to background concentrations (Table 1).

Table 1 – Summary of some examples of Pt, Pd and Rh concentrations analysed in environmental samples (soil, road dust, road air dust and human body fluids) reported in recent studies.

Sample type	Element	Concentration	Method	Detection limit	Reference	Observations
Earth crust, soils or road dust	Pt	7.17-24.3 (ng/g)	Pb-FA and ICP-MS	0.1 (ng/g)	Farago et al., 1998	Soil and road dust, major roads (Richmond and Kew)
		0.35-4.92 (ng/g)	Pb-FA and ICP-MS	0.1 (ng/g)	Farago et al., 1998	Soil and road dust, minor roads (Richmond and Kew)
		253 (ng/g)	Ni-FA and ICP-MS	0.5 (ng/g)	Cubelic et al., 1997	Soil near highways (Frankfurt)
		330 (ng/g)	Ni-FA and INAA	0.5 (ng/g)	Heinrich et al., 1996	Soil near highways (Frankfurt)
		1.4 (ng/g)	NiS-FA and ICP-MS	0.4 (ng/g)	Schaefer and Puchelt, 1998	Soil background conc. (average) (SW Germany) ¹
		max 200 (ng/g)	NiS-FA, ICP-MS\GFAAS	0.4 (ng/g)	Schaefer and Puchelt, 1998	Surface soil, adjacent highway (SW Germany)
		67 (µg/l)	Acid diges., ICP-MS	0.043 (µg/l)	Morton et al., 2001	Aver. background levels (SW Mexico City)
		max 300 (µg/l)	Acid diges., ICP-MS	0.043 (µg/l)	Morton et al., 2001	High traffic densities (SW Mexico City)
		min 5.9 (µg/l)	Acid diges., ICP-MS	0.043 (µg/l)	Morton et al., 2001	Low traffic density (SW Mexico City)
		33.0 (ng/l)	Acid diges., Ads V	0.5 (ng/l)	Schierl and Fruhmann, 1996	Airborne dust, dense urban traffic (Munich)
	3.3 (ng/l)	Acid diges., Ads V	0.5 (ng/l)	Schierl and Fruhmann, 1996	Airborne dust (average), less travelled routes (Munich)	
	0.1-57.1 (pg/ m ³)	ICP-MS	0.1 (pg/ m ³)	Gomez et al., 2001	Airborne dust (Madrid)	
	31-2252 (ng/g)	ICP-MS	1.6 (ng/g)	Gomez et al., 2001	Road dust (average) (Madrid)	
	3.63 (ng/g)	ICP-MS	0.07-3 (ng/g)	Ely et al., 2001	Soil background conc. (South Bend, Indiana)	
	64.44 (ng/g)	ICP-MS	0.07-3 (ng/g)	Ely et al., 2001	Surface roadside soil (South Bend, Indiana)	
	Pd	2.0 (ng/g)	NiS-FA and INAA		Schmidt et al., 1997	Estimate of Earth crust abundance
		6.6 (ng/g)	NiS-FA and INAA	0.3 (ng/g)	Heinrich et al., 1996	Soil near highways (Frankfurt)
		0.53 (ng/g)	NiS-FA and ICP-MS	0.4 (ng/g)	Schaefer and Puchelt, 1998	Soils background conc. (average) (SW Germany)
		max 10 (ng/g)	NiS-FA, ICP-MS\GFAAS	0.4 (ng/g)	Schaefer and Puchelt, 1998	Surface soil, adjacent highway (SW Germany)
		22 (µg/l)	Acid diges., ICP-MS	0.088 (µg/l)	Morton et al., 2001	Aver. background levels (Mexico City)
max 70 (µg/l)		Acid diges., ICP-MS	0.088 (µg/l)	Morton et al., 2001	High traffic densities (SW Mexico City)	
min 19 (µg/l)		Acid diges., ICP-MS	0.088 (µg/l)	Morton et al., 2001	Low traffic density (SW Mexico City)	
1.54 (ng/g)		ICP-MS	0.07-3 (ng/g)	Ely et al., 2001	Soil background conc. (South Bend, Indiana)	
18.52 (ng/g)		ICP-MS	0.07-3 (ng/g)	Ely et al., 2001	Surface roadside soil (South Bend, Indiana)	

Note: FA (fire assay); ICP-MS (inductively coupled plasma mass spectrometry); GFAAS (graphite furnace atomic absorption spectroscopy); INAA (instrumental neutron activation analysis); UV digest. (ultra violet digestion/photolysis); Ads V (adsorptive voltametry).

Table 1 (cont.)- Summary of some examples of Pt, Pd and Rh concentrations analysed in environmental samples (soil, road dust, road air dust and human body fluids) reported in recent studies.

Sample type	Element	Concentration	Method	Detection limit	Reference	Observations
Earth crust, soils or road dust (cont.)	Rh	0.38 (ng/g)	NiS-FA and INAA		Schmidt et al., 1997	Estimate of Earth crust abundance
		7.5 (ng/g)	NiS-FA and INAA	0.3 (ng/g)	Heinrich et al., 1996	Soil near highways (Frankfurt)
		0.18 (ng/g)	NiS-FA, ICP-MS	0.1 (ng/g)	Schaefer and Puchelt, 1998	Soils background conc. (average) (SW Germany) ¹
		max 35 (ng/g)	NiS-FA, ICP-MS\ GFAAS	0.1 (ng/g)	Schaefer and Puchelt, 1998	Surface soil, adjacent highway (SW Germany)
		5 (µg/l)	Acid diges., ICP-MS	0.016 (µg/l)	Morton et al., 2001	Aver. background levels (Mexico City)
		max 40 (µg/l)	Acid diges., ICP-MS	0.016 (µg/l)	Morton et al., 2001	Soils from high traffic roads (Mexico City)
		min 1.3 (µg/l)	Acid diges., ICP-MS	0.016 (µg/l)	Morton et al., 2001	Soils from low traffic roads (Mexico City)
		0.2-12.2 (pg/m ³)	ICP-MS	0.2 (pg/ m ³)	Gomez et al., 2001	Road air dust (Madrid)
		11-182 (ng/g)	ICP-MS	0.2 (ng/ g)	Gomez et al., 2001	Road dust (Madrid)
		0.09 (ng/g)	ICP-MS	0.07-3 (ng/g)	Ely et al., 2001	Soil background conc. (South Bend, Indiana)
		3.35 (ng/g)	ICP-MS	0.07-3 (ng/g)	Ely et al., 2001	Surface roadside soil (South Bend, Indiana)
Urine	Pt	0.5-7.6 (ng/l)	UV diges., ICP-MS	0.24 (ng/l)	Begerow et al., 1996	Unexposed population (Dusseldorf)
		< 1 (ng/l)	UV diges., ICP-MS	0.03 (ng/l)	Krachler et al.,1998	Urban and suburban children (Rome)
		0.5-14 (ng/l)	HP Acid diges., AV	0.2 (ng/l)	Messerschmidt et al., 1992	Unexposed persons (Germany)
		21-2900 (ng/l)	HP Acid diges., AV	0.2 (ng/l)	Messerschmidt et al., 1992	Occupationally exposed persons (Germany)
	Pd	10 (ng/l)	UV diges., ICP-MS	0.2 (ng/l)	Krachler et al.,1998	Urban and suburban children (Rome)
	Rh	10 (ng/l)	UV diges., ICP-MS	0.03 (ng/l)	Krachler et al.,1998	Urban and suburban children (Rome)
Blood	Pt	< 5 (ng/l)	HR-ICP-MS	< 1 (ng/l)	Begerow et al., 1997	Unexposed population (Dusseldorf)
		120-140 (ng/l)	Acid diges., ICP-MS	0.03 (µg/l)	Farago et al, 1998	Unexposed population (London)
		150-420 (ng/l)	Acid diges., ICP-MS	0.03 (µg/l)	Farago et al, 1998	Pt refinery workers (London)
		< 0.8-6.9 (ng/l)	HP Acid diges., AV	0.2 (ng/l)	Messerschmidt et al., 1992	Unexposed persons (Germany)
		32-180 (ng/l)	HP Acid diges., AV	0.2 (ng/l)	Messerschmidt et al., 1992	Occupationally exposed persons (Germany)
	Pd	32-102 (ng/l)	UV diges., ICP-MS	< 1 (ng/l)	Begerow et al., 1997	Unexposed population (Dusseldorf)
	Rh	< 15 (ng/l)	UV diges., ICP-MS	< 1 (ng/l)	Begerow et al., 1997	Unexposed population (Dusseldorf)

Note: FA (fire assay); ICP-MS (inductively coupled plasma mass spectrometry; GFAAS (graphite furnace atomic absorption spectroscopy); INAA (instrumental neutron activation analysis); UV digest. (ultra violet digestion/photolysis); Ads V (adsorptive voltametry).

1.2 PGE in the natural environment: Speciation, mobilisation, and bioavailability of PGE

Ultramafic rocks are very rich in PGE, especially in Pt (with concentrations between 8 and 16000 ppb) compared to bulk crustal concentrations. On weathering of ultramafic rocks, dissolved species of PGE are apparently mobilised and seem to accumulate in organic rich soils (Fuchs and Rose, 1974). The involvement of hydrothermal fluids in the genesis of platinum group elements deposits was studied by Mountain and Wood (1988). Thermodynamic calculations of the solubility of 10 ppb concentrations of these metals at 25°C and 300°C were obtained. As a result, predictions about the relevant ligands present in the environment responsible for PGE transport were made. According to these calculations, chloride and hydroxide ligands are likely to be the most important ligands for PGE mobilisation, their relative influences being dependent on pH, fO_2 , T and ligand concentration.

Further research concluded that other complexes such as bisulphide also could be very important for PGE transport under hydrothermal conditions. Wood et al. (1989) also concluded that hydroxide complexes of PGE might contribute significantly to PGE mobilisation in relatively oxidised groundwater with pH varying from 5 to 8. In order to understand the nature of the interactions of dissolved platinum with organic acids in natural waters, Wood (1990) conducted several experiments mixing platinum-containing solutions with either distilled water or solutions of several organic acids at 25°C. Results showed that fulvic and phthalic acids are capable of maintaining a higher proportion of platinum in a soluble form than distilled water at acidic and basic pH. Although there is evidence for interaction between PGE and soil materials, the form in which the PGE are mobile is poorly understood (Wood, 1990). The same author presented a review supporting the role of humic substances in the transport and fixation of metals of economic interest (Wood, 1996). An important conclusion was that PGE are more mobile than predicted by existing thermodynamic data. At temperatures of more than 100°C, humic substances are drastically altered, especially their ability to complex metals.

Wood (1996) concluded that the role of humic substances in complexing metals is probably limited to low temperature environments.

Enrichment of Pt and associated metals in brown coals and black shales raised the importance of organic matter in the accumulation of these elements. Plyusmina et al. (2000) investigated the interaction of thermal decomposed organic matter, in particular some organic acids, with Pt in solution. They found that chemical sorption onto organic matter lowers the Pt content in aqueous solutions by about two orders of magnitude relative to organic-free systems at 200–400°C and 1 kbar total pressure. Sorption due to metal-organic complexing is assumed to be the main mechanism of PGE accumulation in carbonaceous rocks. However, the complexity of the Pt-water-organic matter system and the increased Pt-organic speciation makes it difficult to decide on the mechanisms responsible for the transport of Pt in organic-rich environment (Plyusmina et al., 2000). These mechanisms seem to be important for high temperature environments. For low temperature environments, very little data is available regarding the mobilisation of PGE.

The speciation of platinum is best studied of all the PGE because of its higher abundance in natural deposits and its economical and industrial importance. Platinum is an excellent example of the significance of speciation in metal toxicity (Farago et al., 1998; Gebel, 2000). Platinum allergy is confined to some charged compounds that contain reactive ligand systems and the most effective is known to be the chloride ligands (WHO, 1991) while metallic platinum is considered non-allergenic. However, emission of mainly metallic Pt particles from the exhaust fumes of automobiles (Nachtigall et al., 1996) can be deposited in the roadside soils and be oxidised into bioavailable species through interactions with the soil (Lustig et al., 1996). The behaviour of platinum compounds in a clay-like humic soil was investigated by Lustig et al. (1996). Different Pt compounds (Pt black, Pt-tunnel-dust, PtO₂, Na₂PtCl₆ and K₂PtCl₄) with concentrations in the ppb range, were added to soil in the absence (dry) or presence (wet) of water. Solubilities at several reaction times (3 to 60 days) were obtained by analysing Pt soluble species formed through the interaction with the soil. In order to identify formation of soluble species or immobilisation within the soil elution with solvents of different polarities were

performed. This was done because the bioavailability of platinum compounds can be dependent on the complexing agents present in the soil. Their findings suggest that recomplexation processes in the soil lead to the formation of a more stable and insoluble complex (Lustig et al., 1996). This experiment also shows the importance of using a real sample (Pt tunnel-dust) to detect the possible mechanisms happening in the environment. The presence of a large amount of complexing agents in the Pt-tunnel-dust matrix seems to enhance the transformation capacity of the humic fraction in the soil as well as the smaller particle size of Pt-tunnel-dust compared to the one of the Pt black used (Lustig et al., 1996).

Further studies assessing the bioavailability of anthropogenic Pt explored the reaction of material from a used three-way catalyst with soil and/or water (Zeirini et al., 1997). Bulk concentrations of Pt and Rh in the material used were 2045 ppb and 420 ppb, respectively. Speciation of Pt was determined by analysing the soluble fraction formed in the “solubility experiments” changing several parameters such as pH, chloride and sulphur concentrations (Zeirini et al., 1997). The same experiments were conducted using real soil samples. The results obtained in the pH interval 5 to 8 with the soil confirm that the clay fraction as well as the organic fraction of the soil adsorb heavy metals under these experimental conditions. The investigators also concluded that only a small fraction of the metallic Pt and Rh can be dissolved under various environmental conditions (with different pH, sulphur and chloride conditions). Following similar experimental procedures, Lustig et al. (1998) studied and identified the main species, namely resulting from the interaction of the same tunnel dust with a soil during reactions times varying from 3 to 60 days at room temperature. Once again the use of a native sample shows different species patterns when interacting with a soil compared to artificial species. The identification of the species was done by reverse phase high-performance liquid chromatography (RP-HPLC). Formation of Pt species occurred very rapidly within days. A great number of Pt species transformations took place but most of the species were shown to be at very low concentrations and of very short lifetime. As mentioned before the formation of hardly soluble platinum humic acid complexes and immobilisation of these species in the soil

can have direct consequences on the bioavailability of these metals in the environment (Lustig et al., 1996). Bioavailability of Pt species was also investigated by Schafer et al. (1998): PGE distribution in some plants cultivated in soils previously exposed to traffic emissions from catalytic converters was determined. The main result of his studies was a measurable transfer of PGE from the contaminated soil to the plants, palladium being the most biologically available. In the same study the bioavailability of other better-known heavy metals (Pb, Cu, Ni, Cd) was determined in order to compare their behaviour with that of the PGE. The experiments showed that both PGE and other heavy metals were present in higher concentrations in the plants growing in contaminated soils as compared to the plants growing in non-contaminated soils (concentrations below the detection limit). These results indicate that PGE have similar transfer coefficients to well known heavy metals (Schafer et al., 1998).

In order to conclude on health effects of the increase in PGE in the environment, baseline concentrations of PGE in the human body fluids by adsorptive voltametry was determined (Messerschmidt et al., 1992). In the context of occupational exposure to platinum, analysis of urine, blood and blood plasma was performed and concentrations of 21-2900 ng/l, 32-180 ng/l, and 95-280 ng/l respectively were found in occupationally exposed persons. Baseline concentrations in the above mentioned body fluids of non-exposed persons were 0.5 to 14.3 ng/l, 0.8-6.9 ng/l, and 0.8-6.9 ng/l, respectively (Table 1). Farago et al. (1998) complemented the above-mentioned research on Pt and Pd concentrations in road dust and soils with a pilot study on Pt and Pd concentrations in body fluids. The results of the inductively coupled plasma mass spectrometry (ICP-MS) analysis carried out on motorway workers, precious metal workers and Imperial College (London) staff persons, showed that Pt content in the workers' body fluids was the highest both in urine and blood. The levels of Pt in blood were not markedly correlated with the concentrations in urine in this pilot study. It was not possible to conclude with certainty that the traffic emissions were the primary source of PGE in the subjects. Another pilot study presents average Pt, Pd and Rh concentrations in urine in 310 children living in the urban and suburban areas of Rome (Caroli

et al., 2001). The data obtained seemed to support the assumption that the exposure to PGE is rather uniform over larger areas as a consequence of probable transport of very fine particles of car exhaust fumes once these are released into the atmosphere.

1.3 Analysis of PGE in environmental samples: interferences and limitations

Trace concentrations of Pt, Pd and Rh in human blood, plasma, and urine, soils and dust particles have been measured by very sensitive instrumental procedures like ICP-MS, electrothermal atomisation-atomic absorption spectrometry (ETA-AAS) and instrumental neutron activation analysis (INAA). More detailed focus will be given to ICP-MS technique since this was the chosen method for the present study. ICP-MS is a preferred technique for measuring very low concentrations of PGE (Schaefer et al. 1998; Farago et al., 1998; Lustig et al., 1997; Bergerow et al., 1996; Zeirini et al. 1997; Gomez et al., 2001; Plyusnina et al., 2000). This analytical technique is highly attractive because of its high sensitivity and multi-element analysis capacity and usually there is no need of a pre-concentration step (Azoural et al., 2001). Since concentrations in the low parts per billion (ppb) range are expected, the detection limit is supposed to be in the ppt or sub-ppb range, otherwise trace concentrations and slight variations in concentrations will not be detected. As an example this technique was used successfully by Schaefer et al. (1998) to analyse Rh, Pt and Pd content in soil extracts and in plant material (using two different wet-digestion methods). Detection limits in ppb for the analysis of Rh, Pt and Pd in the soil extracts were 0.21, 0.50 and 0.25, respectively. In plant materials detection limits were 0.3-1.05 (Rh), 0.72-2.50 (Pt), 0.35-1.25 (Pd) ppb.

Analytical problems, particularly mass spectral interferences in the determination of very low levels (sub-ng/l) of PGE in urine samples by ICP-MS, were discussed by Krackler et al. (1998) and by Bergerow et al. (1996). Gomez et al. (2000) studied the ultra trace levels of PGE in airborne particulate matter by ICP-MS and concluded that the main interferences are

due to $^{179}\text{Hf } ^{16}\text{O}^+$ for analysis of ^{195}Pt , $^{89}\text{Y } ^{16}\text{O}^+$ for ^{105}Pd , and $^{40}\text{Ar } ^{63}\text{Cu}^+$ for ^{103}Rh . Analysis of the atomic mass units were done for ^{195}Pt , ^{106}Pd , ^{103}Rh by ICP-MS in ashed soil samples and after PGE separation from the matrix by Te precipitation with SnCl_2 was carried by Morton et al. (2001). When PGE are extracted from the soil matrix mass interferences are assumed to be negligible.

1.4 Batch studies to identify and characterise PGE interactions in the natural environment: advantages and limitations

In order to understand the mechanisms involved in the fixation and/or mobilisation of PGE and Au, batch experiments can be very useful to determine metal transformations in soil and soil solution under controlled reaction conditions. The sorption capacity of the soil for a specific ion can be determined by reaction of a known amount of soil with different known concentrations of that ion (McBride, 1994). The possibility of using several solid matrices and varying adsorbate solution concentrations and pH in simultaneous runs is one of the main advantages of using batch studies for the study of sorption behaviour. A further advantage is that the batch experiments are also less time consuming than other types of studies, such as column leaching experiments.

Several adsorption isotherms can be obtained from the relationship between the amount of species sorbed as a function of its concentration in solution and respective adsorption coefficients can be calculated (Langmuir, 1997). Many limitations and assumptions have to be taken into account when concluding on batch adsorption experimental data. Batch experiments do not give representative results of *in situ* conditions since an unreal adsorbent/adsorbate ratio is used. In the same way the system is static: the adsorbent is exposed to a limited mass of ions in solution unlike in a continuous flow system. Moreover, products of reactions are not removed contributing to the inhibition of further adsorbate release and promoting secondary precipitation (Sparks, 1999). In adsorption studies homogenisation provided by uniform mixing of the adsorbent/adsorbate is important so that all

adsorbent surfaces are equally exposed to adsorbate in solution. However, too much mixing can cause abrasion of the adsorbent and alter adsorption properties e.g. specific surface area. At the same time, efficient separation of the solution from the solid suspension is required for quantification of the adsorbate equilibrium concentrations. Even though many experimental constraints limit the conclusions from batch experiments they are widely used for adsorption experiments.

1.5 Conclusions

There is a dramatic increase in the use of PGE in the past 20 years as catalysts in the motorcar industry and in chemical processes. As a consequence there is an enrichment of PGE in the environment. PGE were considered inert metals until recent studies discovered that possible mobilisation of PGE might occur under specific environmental conditions.

Most recent studies focus on the quantification of total Pt, Pd and Rh accumulated in soils near roads with heavy traffic. Other studies focus on the soluble PGE fraction of particles emitted from vehicles in the soil environment. Although the soluble fraction of essentially metallic particles containing Pt, Pd and Rh does not exceed 1% of the total emitted Pt, mobilisation of complexed species has been documented. It is therefore interesting to study the relationship between dissolved metals and soil components known to influence the metal's mobilisation in natural conditions for the example in the presence of organic matter or clay. PGE analysis by ICP-MS has been documented to be a sensitive method not requiring a pre-concentration step.

The knowledge of PGE sorption behaviour is still very scarce under natural soil conditions. PGE accumulation and possible mobilisation in natural systems may well have an impact on biological systems due to known toxicity of these rare elements. Therefore a better understanding of the PGE-soil interactions is needed. This study aims to investigate the sorption behaviour in selected solid matrices with the help of batch experiments. The objective is to compare the different behaviour of the most common PGE used for catalytic converters: Pt, Pd and Rh and suggest possible reasons for their sorption behaviour.

2. METHODOLOGY

2.1 Sample collection

In order to study PGE interactions in the soil environment a set of soils, clays and sediment samples were selected based on differences in organic matter content, mineralogy, and particle size. The soil and sediment samples were collected in August 2002 in different areas of the Cape Peninsula, Western Cape, South Africa.

An individual topsoil sample (Tokai sample) was collected from the Tokai forest in the reserve pine plantation area at about 200 m from the nearest access road and at 700 m from the picnic area. The first top 5-10 cm thick layer was sampled with special care in order to avoid sampling the layer of alluvial sand underneath the dark, organic-rich, and friable top horizon. Roots and bigger barks were excluded. Another sample consisted of 22 cm thick topsoil was collected from the North-facing slope of Table Mountain at about 200 m from the De Waal Drive, Cape Town. The parent material was identified as predominantly Malmesbury shale as it could be identified in the underlying B and C horizons. It was named Malm sample. The vegetation included some fynbos and long grasses as well as pine trees. The Zandvlei sample was taken from the Zandvlei estuarine wetland, near Marina da Gama, Muizenberg, Cape Town. Only the lower 15-40 cm was sampled because it appeared to be fine grained and clay-rich. The site was chosen away from the Marina da Gama residential area to avoid sewage contamination. The "Consol" sand is a quartz sand commercialised by *Lafarge Pty* (Cape Town). It is extracted by the company from the windblown sand deposit in Philippi, Cape Town. Most of this product is sold to a company called *Consol Ltd.* that produces glass in Bellville, Cape Town. The clay minerals used in this study are kaolin (Kaolin sample) and calcium bentonite (Ca-bentonite sample). The Kaolin is mined near Grahamstown in the Eastern Cape Province and supplied by *G&W Base & Industrial Minerals (Pty)*. The Kaolin consists mainly of kaolinite, a dioctahedral two-layer phyllosilicate,

which is a common clay mineral in humid-climate and well-leached acid soils. It is formed by rapid removal of cations from the weathering of primary minerals, frequently from potassium feldspar and muscovite mica present in rocks such as granite. The Ca-bentonite used in this study was also supplied by *G&W Base & Industrial Minerals (Pty)* and is mined from the Blaauwbosch bentonite deposit near Koppies in the northern Free State. Bentonite is a dioctahedral smectite clay constituted mainly of montmorillonite and/or beidellite (Weaver and Pollard, 1973; Langmuir, 1997). Smectite clays are common minerals in arid climates with poor drained alkaline soils, rich in silica and divalent cations and low potassium concentrations (Langmuir, 1997). The Kaolin, Ca-bentonite and the Consol sand represent some of the most common clays and oxide minerals present in soils of the Cape Peninsula, Western Cape Province, South Africa. The Malm, Zandvlei and Tokai samples are examples of some organic rich soils and sediments found in the Cape Peninsula.

2.2 Analytical techniques

2.2.1 General characterisation of solid matrices

Solid matrices were characterised for their size, pH, cation exchange capacity (CEC), LiCl extractable cations, organic carbon content, mineralogy, and specific surface area (SSA-N₂). All the soils and sediments were air dried and sieved through a 2 mm stainless steel sieve. Only the less than 2 mm fraction was used for subsequent characterisation and analysis. The soil and sediment samples were used without any chemical pre-treatment, the only exception being the Consol sand. This sample was deliberately washed with 2% HCl solution and distilled water through a stainless steel sieve in order to remove silt and clay size particles as well as possible organic matter coated in the sand particles. More aggressive chemical treatment such as H₂O₂ was not necessary.

The basic particle size distribution of the soils and sediments was determined by physical separation through stainless steel sieves. The sand fraction of the

Malm soil, Zandvlei and Consol sediments was characterised by the settling column method. The sand fraction of the Tokai sample was characterised using stainless steel sieves since the excessive organic content did not allow the use of the settling column. Silt fraction was separated from the clay fraction in the soil samples using the Stoke's Law for calculation of the settling time. The supplier of both clay minerals provided information on the average particle size.

The general mineralogy of the bulk samples and clay fractions was obtained by X-ray diffraction using a Philips X-ray diffractometer. Bulk samples were ground in an agate mortar and then pressed in an aluminium slide for analysis. The preparation of an oriented clay mineral mount was obtained for the clay fraction of Malm, Zandvlei and Tokai samples by suspension of collected clay in a small amount of distilled water. Typical instrumental details of X-ray diffractometer used are presented in Table 2.

Table 2 – Typical instrumental operation conditions for the Philips X-ray diffractometer at the Department of Geological Sciences (UCT)

	Bulk sample	Clay fraction
Scan type	continuous	continuous
Scan range	60.95	35.95
Wavelength (nm)	1.54	1.54
2θ angle	57.48	21.99
Time per step	0.5	0.5
1st angle	5.03	4.01
Step width	0.05	0.025

Potentiometric acid-base titrations of each of the solid matrices were performed using KOH (0.1M) for the base and HCl (0.1M) for the acid additions at four different electrolyte (KCl) concentrations (Gubevu, 1997). KCl was used as supporting electrolyte solution for acid base titrations since it does not interact strongly with the mineral surfaces and is able to maintain a constant ionic strength (Drever, 1997). At least duplicate pH readings were performed for the 0.01M KCl concentration to access the error on pH readings and because a medium ionic strength is common in soil systems (Table 11 in Appendix).

Specific surface area was determined by the BET technique (Carter et al., 1989) using a Micromeritics ASAP 2010 instrument and N₂ as the adsorption gas.

Cation exchange capacity and the major extractable cations (Ca²⁺, Mg²⁺, Na⁺ and K⁺) were determined by the LiCl method (Soil Science Society of SA, 1990). LiCl serves as an extractant for soluble and exchangeable cations saturating the sample exchangeable complex with Li⁺. Adsorbed cations are subsequently displaced with calcium Ca(NO₃)₂ and the cation exchange capacity is obtained by measuring the Li released using inductively coupled plasma mass spectrometry (ICP-MS).

Total organic carbon content of the soil samples was determined using the Walkley-Black wet digestion method (Nelson and Sommers, 1992).

In order to quantify the background concentration of PGE and Au in the solid matrices, HF/HNO₃ digestions of all solid matrices were performed. On complete acid digestion leachates were then analysed using ICP-MS for determination of PGE and Au concentrations.

All the analysis involved in the characterisation of the selected solid matrixes were performed by the student at the Department of Geological Sciences, University of Cape Town except for the analysis of LI extractable cations determined by the FAAS team at Chemical Engineering at the University of Cape Town and surface area at the University of Stellenbosch, Department of Chemical Engineering.

2.2.2 PGE and Au analysis using ICP-MS

Analyses of PGE and Au concentrations performed in the time course and in the adsorption isotherm experiments were all done by the student and the ICP-MS team at UCT, Department of Geological Sciences using an Perkin Elmer Elan 6000 instrument. Some of the typical operational conditions are summarised in Table 3. The external standard concentration range and the internal standard additions are mentioned in detail in the description of the respective methodology.

Table 3 – Typical instrumental operation conditions of the ELAN 6000-Perkin Elmer ICP-MS at the Department of Geological Sciences (UCT) for PGE and Au analysis.

Analysed isotopes	¹⁰² Ru, ¹⁰³ Rh, ¹⁰⁵ Pd, ¹⁸⁷ Re, ¹⁹² Os, ¹⁹³ Ir, ¹⁹⁵ Pt, and ¹⁹⁷ Au
Nr. of replicates	2
Internal standard	¹¹⁵ In
Washing time	120s

Supernatant aliquots for PGE and Au analysis were preserved with 5% HNO₃ purified by subboiling distillation. All water for reagent solution preparation and material cleaning was purified by a milli-Q-device (MQ) (Millipore®, Bedford, USA).

2.3 Batch adsorption experiments

Sorption phenomenon among PGE was observed in time course experiments and in static adsorption isotherm experiments. The time course experiments involved a sequential sampling of supernatant after interaction of a single concentration of PGE and Au reagent solution with a subsample of each solid matrix (sorbent). The sampling was performed at different time points over 24 h total reaction time. In the isotherm batch experiments several PGE and Au reagent solutions are left equilibrating with subsamples of each solid matrix and a single aliquot of the supernatant is sampled after 24 h. Au was included in the analysis of PGE experiments because it occurs naturally in conjunction with the PGE elements.

2.3.1 Time course experiments

Time course experiments were performed using all six solid matrices. Duplicate subsamples (approximately 3.0 g) of all solid matrices were weighed in 50 ml PP centrifuge vials using a Denver D200 weighing scale. A reagent solution containing 120 µg/L PGE was prepared just before the experiment. This solution was prepared by dilution of SpecPure® 100 mg/l PGE and Au stock solution (in 20% HCl) with MQ water without pH

adjustments. Before addition of the PGE and Au solution to the solid matrix a 600 μl aliquot (in duplicate) of the reagent solution was sampled for the analysis of the initial PGE and Au concentration (at t_0 = start of experiment). This aliquot was preserved with HNO_3 5% (10 times dilution) and was analysed for PGE and Au at the end of the experiment.

A 3 g:50 ml solid matrix/reagent solution ratio was prepared and the time point of reagent addition to each solid matrix subsample was recorded as t_0 (start of experiment). In order to quantify the background PGE and Au content in the solid matrices soil solution, a blank was prepared with each of the solid matrices with 3 g solid matrix: 50 ml MQ water. All samples were kept in suspension by shaking on a horizontal shaker, facilitating the contact of all solid surfaces with the solution. A 600 μl aliquot of the supernatant was taken from each vial at specific time points measured in minutes from the start of the experiment (t_{30} , t_{60} , t_{90} , t_{155} , t_{200} , t_{270} , t_{360} , t_{700} , and t_{1440}) after centrifuging the vial at 5500 rpm for 3 minutes. The pH of the supernatant was measured at each sampling step using a 691 Metrohm pH meter. Each aliquot was immediately diluted ten times with 5% pure HNO_3 .

Analysis of all aliquots was performed immediately after the last aliquot (t_{1440}) was sampled. Special care was taken to avoid contamination and either new or aqua-regia washed glass and PP plastic ware was used at all times. All sample preparation was done in a clean laboratory. Four external standards of 0, 190, 480, and 960 ng/l concentrations were prepared for calibration. Prior to analysis 150 μl of 3 mg/l of ^{115}In internal standard solution was added to all vials for calibration.

Since the reagent solutions used in the adsorption experiments were prepared with MQ water without pH adjustments, stability of this solution over 24 h had to be assessed. In order to assess the reagent solution stability and to quantify PGE and Au concentration of the reagent solution analysis of an aliquot (in duplicate) of the reagent solution at t_0 and at t_{1440} was included as part of the time course experiments.

2.3.2 Adsorption isotherm experiments

Due to the lack of time and budget constraints adsorption isotherm experiments were conducted for the Malm, Tokai and the Zandvlei sediments only. For that purpose 1.5 g of each of these solid matrices were weighed in duplicate in 50 ml PP centrifuge vials using a Sartorius R200D weighing scale. Eight different PGE and Au solutions were prepared by dilution of the SpecPure® 100 mg/l PGE and Au stock solution (in 20% HCl) with MQ water to have the following approximate concentrations: 50, 100, 150, 500, 1000, 1500, 3000 and 5000 µg /l. A 200 µl aliquot of each solution was sampled, diluted 50 times with 5% pure HNO₃ and kept for later analysis, correspondent to initial adsorbate concentration (t_0). 25 ml of each reagent solution was pipetted to the selected solid matrices, achieving the same sorbent/sorbate ratio as in the previous time course experiments. All centrifuge vials were manually agitated every 3 to 6 h during the 24 h reaction time experiment. After 24 h a 200 µl aliquot was sampled from each vial after centrifuging at 5500 rpm for 4 minutes and then diluted 50 times with 5% pure HNO₃. PGE and Au analysis was performed after ¹¹⁵In internal standard addition to each aliquot.

3. RESULTS

3.1 General characterisation of solid matrices

The basic physico-chemical properties of the selected soils, sediments and clays were determined. Particle size analysis (texture), pH, CEC, LiCl extractable cations, organic carbon content, mineralogy and specific surface area are presented in Table 4. Coarse to medium sand size particles are predominant in the Consol sand and Tokai samples. In contrast fine sand, silt and clay size particles predominate in the Zandvlei and Malm samples. The pH of the solid matrices in a 3 g solid:50 ml MQ water suspension ranges from pH 5.0 in the Tokai pine forest soil to pH 8.3 in the Ca-bentonite clay. The CEC ranges from 1040 mmol/kg soil in the Ca-bentonite sample to 12 mmol/kg in the Consol sand. CEC values in the Zandvlei and Tokai samples were of similar order of magnitude, 304 and 234 mmol/kg, respectively. The predominant extractable cations were found to be Ca^{2+} , Mg^{2+} in the all the solid matrices except in the Zandvlei sample where Mg^{2+} and Na^+ predominates. The organic carbon content is 6% in the Malm sample, twice as much in the Zandvlei sediment and about four times higher in the Tokai forest topsoil (23%).

The predominant clay minerals are kaolinite and mica as observed by the clay mineralogy XRD analysis of the soils and sediments (Fig. 12 in Appendix). The clay mineralogy of Kaolin and Ca-bentonite samples was supplied by G&W base (Pty). Mineral impurities present in the Kaolin sample were mica (illite) and quartz (Table 4). These are known to be the most frequent mineral impurities in Kaolin. The Ca-bentonite is constituted by smectite dioctahedral, mica and quartz (trace).

Potentiometric titrations of all solid matrices at four different electrolyte (KCl) concentrations are presented in Fig. 1.

Table 4 – Solid matrices physico-chemical properties: Texture, pH, CEC, LiCl extractable cations , %Corg, mineralogy and SSA-N₂.

Property	Sample ID					
	Kaolin	Ca-Bentonite	Consol sand	Malm	Zandvlei	Tokai
Texture* (%)						
Very coarse sand	-	-	4	4	2	14
Coarse sand	-	-	67	6	>1	32
Medium sand	-	-	26	13	6	22
Fine sand	-	-	3	20	26	18
Very fine sand	-	-	>1	9	32	5
Silt			0	42	10	2
Clay	98-100	98-100	0	6	24	7
pH	6.0-7.5	7.8-8.3	7.1-8.2	6.2-7.4	6.3-7.8	5.0-7.2
CEC (mmol/kg soil)	59	1040	12	97	304	232
LiCl extract. cations (mmol/kg soil)						
Ca ²⁺	20.86	244.01	7.16	61.81	113.27	58.71
Mg ²⁺	4.06	364.68	0.26	33.15	163.08	50.34
Na ⁺	3.42	37.89	6.43	4.25	287.25	5.50
K ⁺	2.19	8.67	0.08	5.63	10.45	5.02
Corg (%)	0	0	0	6	11	23
Mineralogy Bulk (<2mm)			Quartz (1)	Quartz (1)	Quartz (1), calcite (3) chlorite (2)	Quartz (1)
Clay fraction	Kaolinite (1), mica (2), quartz (3)	Smectite dioct. (1), mica (2), quartz (3)		Kaolinite (1) Mica (2)	Kaolinite (1)	Kaolinite (1)
SSA-N₂ (m ² /g)	12.2	85.2	0.2	7.3	5.0	**

Note: (1) predominant, (2) presence, (3) trace; SSA (specific surface area); CEC (cation exchange capacity). *only the < 2mm fraction was characterised and used for further experiments. **not determined because high Corg interfered with degassing process in BET method.

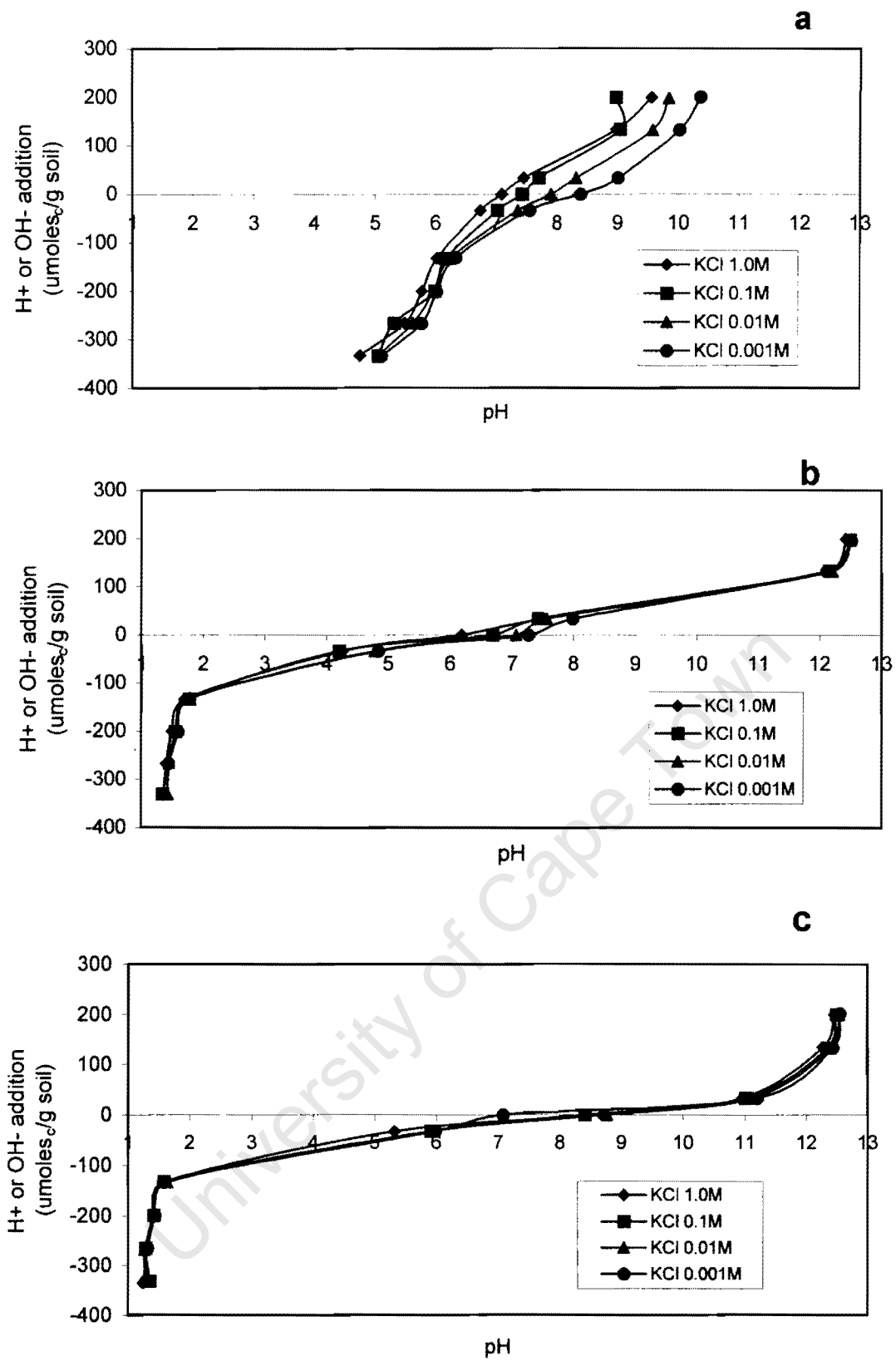


Figure 1 - Potentiometric titration curves for the (a) Ca-bentonite, (b) Kaolin, (c) Consol sand, (d) Malm (e) Zandvlei and (f) Tokai samples obtained at four different electrolyte (KCl) concentrations. Acid (0.1M HCl) and base (0.1M KOH) additions are presented as $\mu\text{moles/g}$ soil).

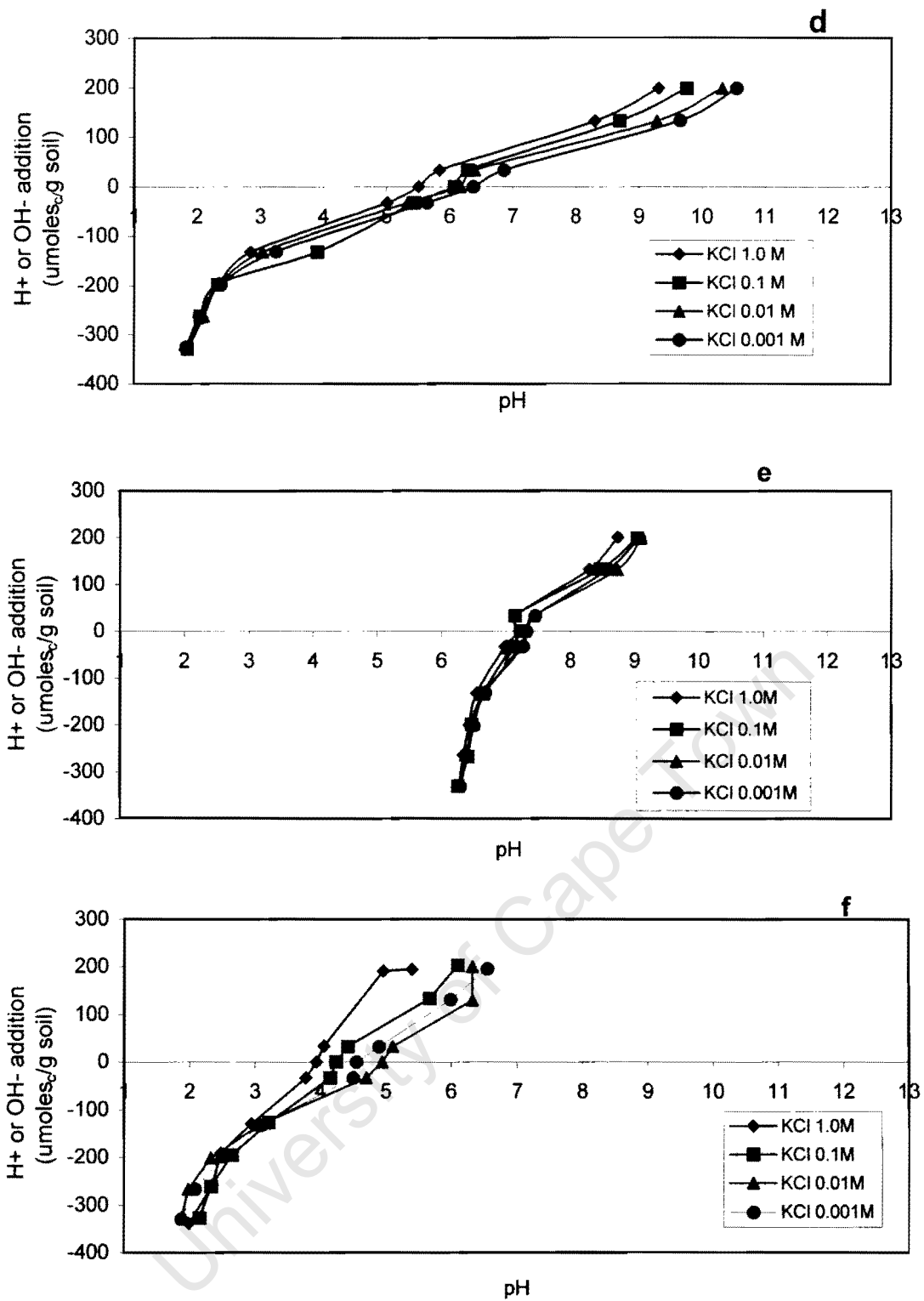


Figure 1 (cont.) - Potentiometric titration curves for the (a) Ca-bentonite, (b) Kaolin, (c) Consol sand, (d) Malm (e) Zandvlei and (f) Tokai samples obtained at four different electrolyte (KCl) concentrations. Acid (0.1M HCl) and base (0.1M KOH) additions are presented as $\mu\text{moles}_e/\text{g}$ soil).

The pH measured after a 12 h equilibration time with four KCl solutions (1.0M, 0.1M, 0.01M, and 0.001M) is plotted as a function of acid and base additions to 10 subsamples of each solid matrix. It can be observed how the ionic strength of the supporting solution (KCl) influences the distribution of the charge: the higher the KCl concentration the lower the pH of the supernatant (Drever, 1997).

Background PGE and Au content in the selected solid matrices were determined using ICP-MS analysis (Table 5). The concentrations ($\mu\text{g}/\text{kg}$) represent the total concentration of PGE and Au in the solid matrices and are determined in order to predict possible contaminations during the batch adsorption experiments.

Table 5 – Average values of total PGE and Au concentrations ($\mu\text{g}/\text{kg}$) in the solid matrices acid digestion leachates determined by ICP-MS.

Element	Sample ID					
	Kaolin	Ca-bentonite	Consol sand	Malm	Zandvlei	Tokai
Ru	bdl	76.01	bdl	36.88	22.08	12.19
Rh	bdl	bdl	bdl	bdl	10.95	bdl
Pd	bdl	bdl	bdl	bdl	41.26	10.79
Re	bdl	bdl	bdl	bdl	bdl	bdl
Os	772.1	105.7	bdl	272.2	169.4	113.3
Ir	33.3	bdl	bdl	22.01	bdl	bdl
Pt	bdl	bdl	bdl	bdl	bdl	bdl
Au	46.80	bdl	bdl	25.14	15.43	36.75

Note: bdl = below detection limit if concentration < 1 ppb

The acid digestion leachates analysis of the solid matrices shows PGE and Au concentrations below the detection limit for most of the analysed elements. For the elements of interest (Pt, Pd, Rh) only Pd and Rh concentrations are above the detection limit in the Tokai sample and Rh is detectable in the Zandvlei sample. Total Os concentrations in the solid matrices are higher than all the other elements analysed. Pt concentration is below the detection limit in all samples (Table 12 in Appendix).

3.2 Batch adsorption experiments

3.2.1 Time course experiments

Time course batch experiments were performed using subsamples of all solid matrices in contact with a PGE and Au solution. The stability of the reagent solution was evaluated analysing PGE and Au concentrations in the reagent solution prepared at the beginning and end of the time course experiment without interaction with the solid matrices (Table 6). Due to large amount of aliquots for PGE and Au analysis, the methodology described in 2.2.1 was followed in two separated experiments: using the clays and Consol sand subsamples (experiment A) and using the Malm, Zandvlei and Tokai matrices (experiment B).

Table 6 – PGE and Au concentration ($\mu\text{g/l}$) in the duplicates of reagent solution at the beginning (t_0) and end (after 1440 minutes) of the time course experiments: (A) using the Kaolin, Ca-bentonite, and Consol sand and (B) using the Malm, Zandvlei and Tokai samples.

A			B	
Element	t_0	t_{1440}	t_0	t_{1440}
Ru	126.95	113.99	111.30	113.42
Rh	129.36	116.35	113.40	114.45
Pd	126.58	112.72	109.30	110.38
Re	130.03	118.11	113.54	112.94
Os	124.21	108.25	114.51	121.40
Ir	127.01	114.90	111.81	111.58
Pt	129.18	115.33	113.06	112.50
Au	84.50	65.09	67.28	62.32
Element	t_0	t_{1440}	t_0	t_{1440}
Ru	115.98	115.57	112.38	112.98
Rh	117.01	116.89	114.28	114.87
Pd	114.99	114.36	110.64	111.72
Re	117.44	117.98	114.74	114.65
Os	120.02	115.35	116.43	125.07
Ir	115.61	116.34	113.33	113.17
Pt	116.33	116.77	114.76	114.73
Au	66.08	70.99	75.95	75.25

For most PGE the concentrations are near the desired concentration of 120 $\mu\text{g/L}$ at t_0 , the exception is Au concentration being approximately half that value. The decrease in PGE and Au concentration over 24h shown in experiment A (top left) may be caused by pipetting errors during the sampling

procedure. Since there is no significant change in the elements' concentration over the experimental time (24h), the initial concentration for each element was calculated as an average of the duplicates concentrations at t_0 and t_{1440} for the correspondent experiment (A and B).

The following figures show the variation of PGE and Au concentrations in the supernatant after interaction with each solid matrix (Figure 2a-f). From the patterns obtained in the time course experiments it is obvious that the more pronounced decrease in concentration occurs within the first 30-60 min. of reaction time suggesting a fast adsorption process capable of removing the PGE and Au from solution (Fig. 2a-f). However, not all the elements behave in the same way. According to the adsorption behaviour in the time course experiments two different groups of elements could be distinguished: (1) Elements with inert behaviour (IB) namely Re, Rh, Os, and Ir. These elements seem to be less adsorbed under these experimental conditions than (2) the elements with reactive behaviour (RB), which were found to be Au, Pd, Pt, and Ru. Concentrations of RB elements decrease rapidly over the equilibration time (24 h) in all solid matrices reaching a 24-hour concentration that is less than 50% of the initial concentration. One exception to this rule is the interaction of these elements (RB) with Kaolin and Consol sand which showed a slower decrease of some of their concentrations (in the supernatant) over time than was observed with the other matrices (Fig. 2a, c). For example this exception is visible in Fig. 2a for Pd and Pt, and in Fig 2c for Ru and Pt. The IB elements also show a decrease in the first 30 min. but this is partly reversed in the following 60-200 min.

This pattern of concentration over time observed in the Kaolin, Malm, and Tokai samples suggests a non-linear ion exchange process (Fig. 2a, d, and f). An exception within the group of IB elements was Ir that showed strong adsorption in the Ca-bentonite sample (Fig. 2a). The RB elements show a faster and stronger decrease over time in the Zandvlei sample as opposed to their less dramatic decrease in the other two soil samples (Malm, Tokai) (Fig. 2e). Interestingly, there are also two IB elements that show a more reactive behaviour in the Zandvlei sample: Rh and Os decrease to less than 50% of the initial concentration by the end of the experiment (Fig. 2e).

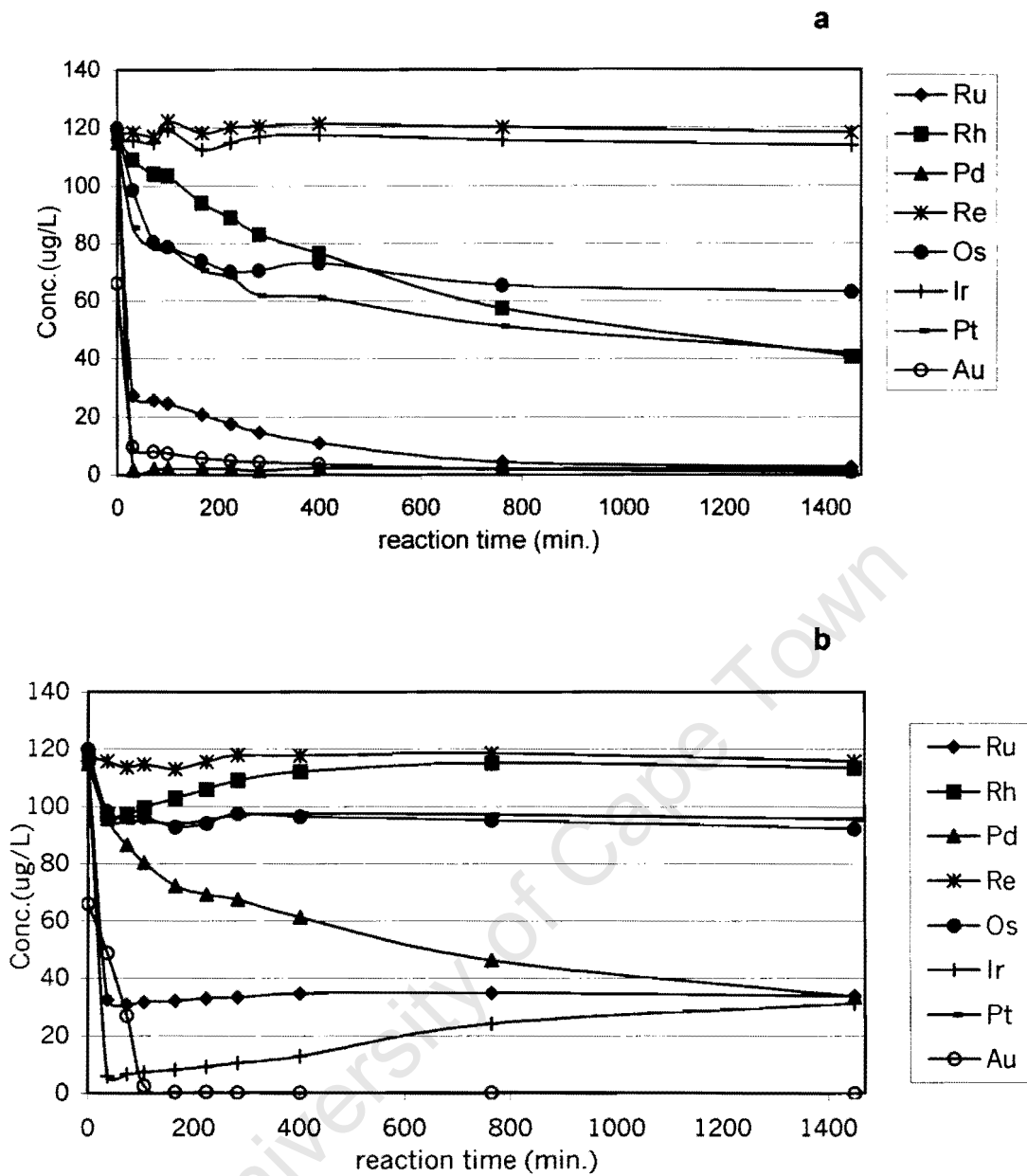


Figure 2 - Average PGE and Au concentrations ($\mu\text{g/L}$) of replicate analysis and duplicate samples in the supernatant of (a) Kaolin, (b) Ca-bentonite, (c) Consol sand, (d) Malm, (e) Zandvlei and (f) Tokai samples at correspondent sampling time points. The time plotted (in minutes) indicates the elapsed reaction time since the beginning of the experiment (t_0).

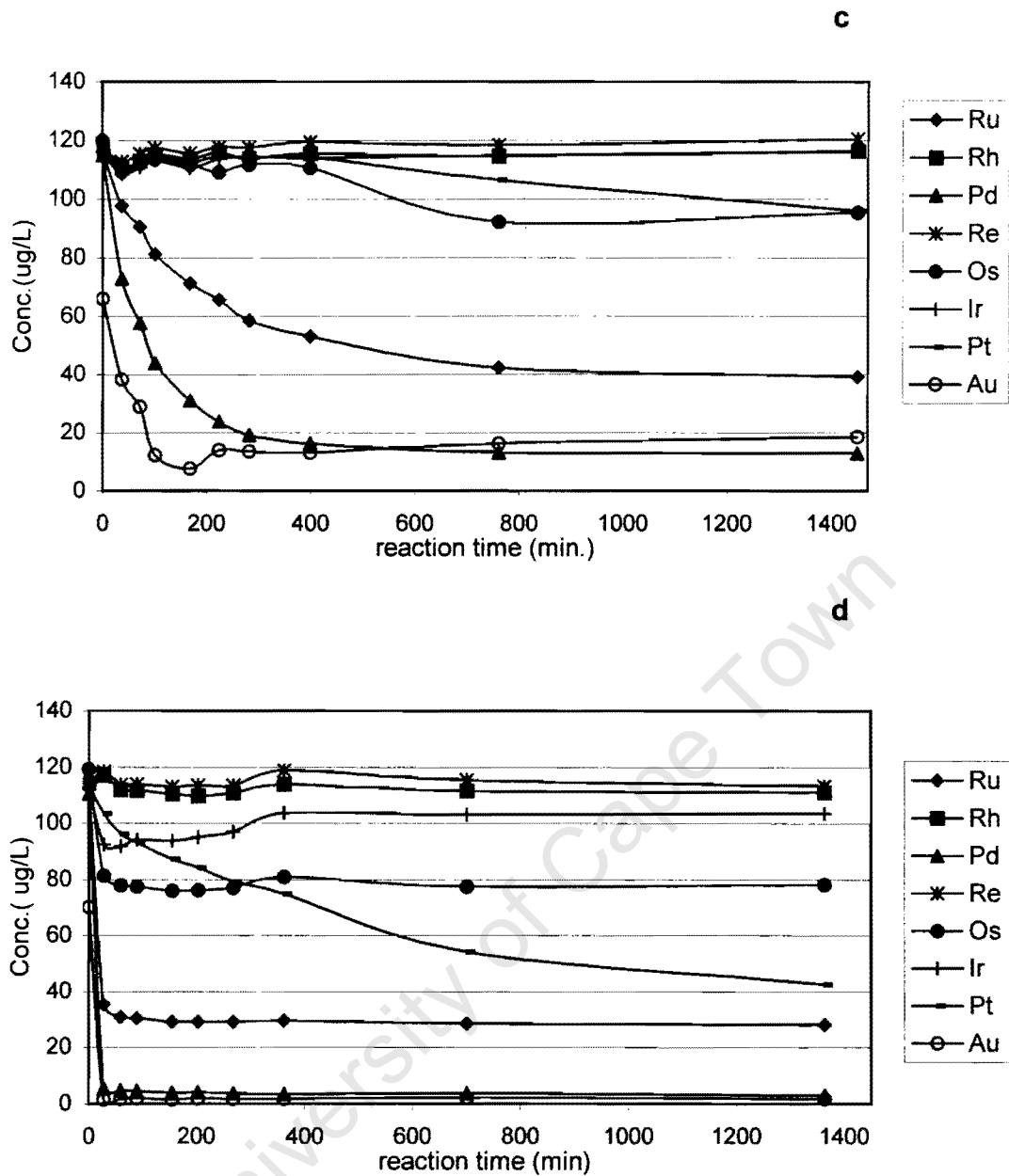


Figure 2 (cont.) - Average PGE and Au concentrations ($\mu\text{g/L}$) of replicate analysis and duplicate samples in the supernatant of (a) Kaolin, (b) Ca-bentonite, (c) Consol sand, (d) Malm, (e) Zandvlei and (f) Tokai samples at correspondent sampling time points. The time plotted (in minutes) indicates the elapsed reaction time since the beginning of the experiment (t_0).

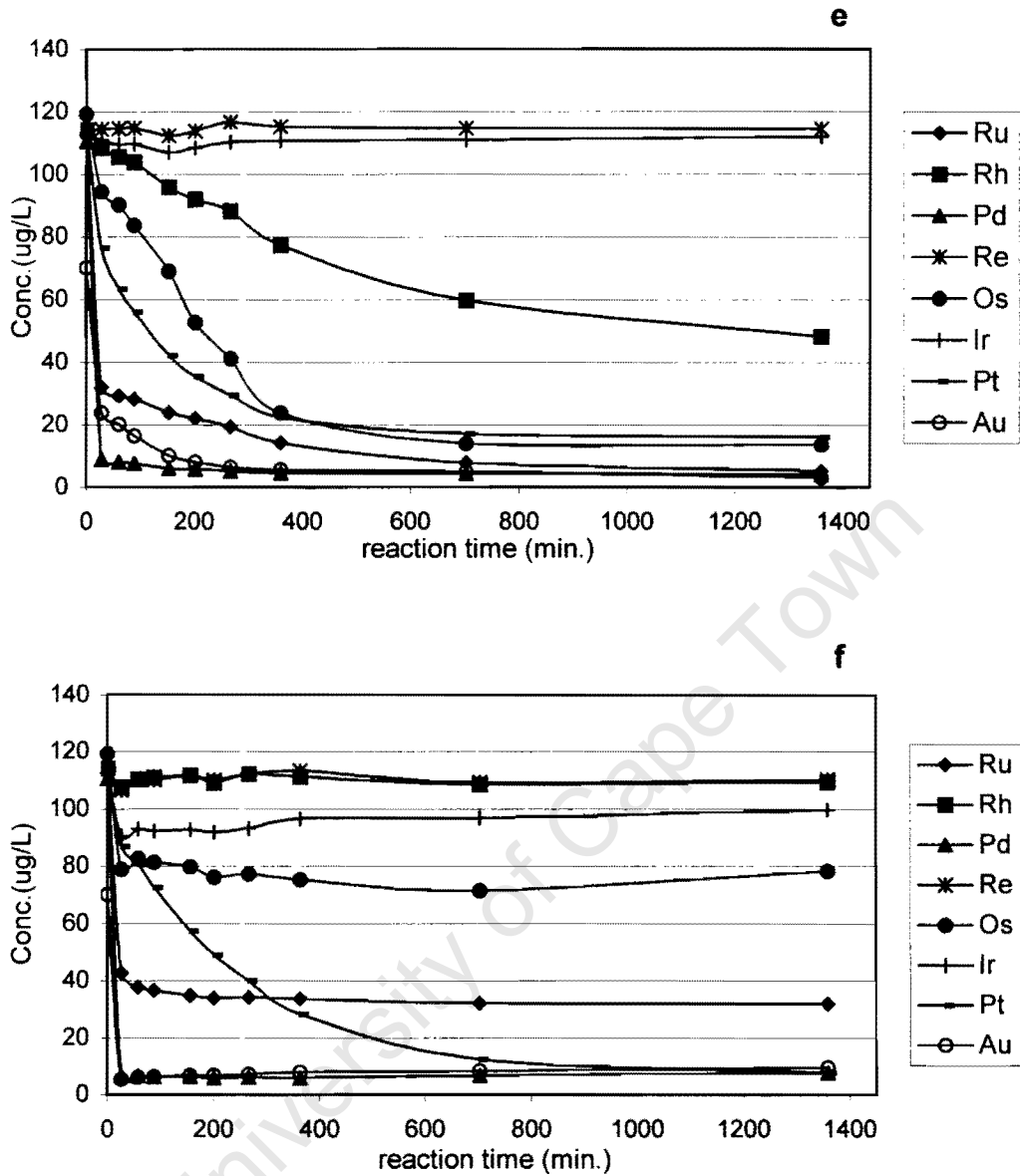


Figure 2 (cont.) - Average PGE and Au concentrations ($\mu\text{g/L}$) of replicate analysis and duplicate samples in the supernatant of (a) Kaolin, (b) Ca-bentonite, (c) Consol sand, (d) Malm, (e) Zandvlei and (f) Tokai samples at correspondent sampling time points. The time plotted (in minutes) indicates the elapsed reaction time since the beginning of the experiment (t_0).

As part of the time course experiments the pH of the supernatant was measured after sampling the aliquot from each vial (in duplicate). Average values of the solution pH for each of the solid matrices are presented in Fig. 3 (Table 14a-f in Appendix).

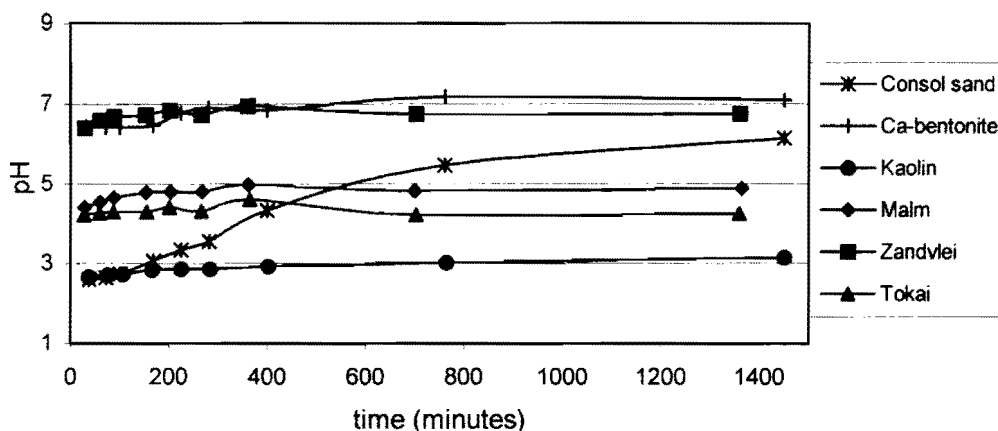


Figure 3 - Average pH values of the supernatant for each solid matrix at the correspondent sampling points during the time course experiments. The time plotted (in minutes) indicates the elapsed reaction time since the beginning of the experiment (t_0).

The pH of the supernatant decreases by 0.5 to 3.5 pH units in relation to solid matrix pH (Table 4) due to the effect of the HCl in the reagent solution. The supernatant pH stayed fairly stable over the 24h experiment for all solid matrices except for the Consol sand sample where initial pH, after reagent solution, decreases abruptly and seems to stabilise only in the latter part of the experiment.

3.2.2 Adsorption isotherm experiments

Prior to the batch experiments PGE and Au concentrations were determined in the eight stock solutions A-H in the 50-5000 $\mu\text{g/L}$ concentration range (Table 7). The results are averages of replicate ICP-MS runs in one single aliquot sampled at the t_0 reaction time (Table 17 in Appendix).

Table 7 - PGE and Au concentrations ($\mu\text{g/l}$) in the reagent solutions (A, B, C, D, F, G, H) for the isotherm adsorption experiments quantified by ICP-MS analysis.

Reagent solution				
Element	A	B	C	D
Ru	42.86	94.61	141.61	436.46
Rh	47.45	95.57	140.92	441.67
Pd	46.98	94.72	138.93	441.74
Re	48.03	97.46	144.95	449.91
Os	94.32	102.76	93.33	601.28
Ir	47.40	94.44	139.96	432.20
Pt	47.84	95.98	141.65	439.06
Au	27.15	64.52	74.33	421.06
Element	E	F	G	H
Ru	920.29	1425.29	3016.58	4918.33
Rh	928.24	1441.05	3065.86	4469.19
Pd	898.75	1388.02	3012.38	4873.48
Re	936.79	1446.98	3116.42	4717.63
Os	1321.73	1784.59	4620.16	7784.06
Ir	925.76	1439.65	3104.86	4660.75
Pt	927.79	1438.72	3048.16	4968.84
Au	921.31	710.03	3217.92	5318.84

Concentrations are once again near the desired values for most elements except for Os and Au. These values were assumed as initial PGE and Au concentrations for posterior adsorption calculations in Chapter 4.

Table 8a - PGE and Au equilibrium concentrations ($\mu\text{g/l}$) in the Malm subsamples supernatant after 24 h interaction with the respective reagent solution A-H (in duplicate: upper/lower panel).

Reagent solution								
Element	A	B	C	D	E	F	G	H
Ru	8.46	25.47	40.36	219.06	576.81	960.96	2589.75	4143.40
Rh	38.50	94.81	139.42	440.97	816.53	1229.70	2816.33	3903.30
Pd	1.87	4.26	4.93	13.20	20.45	51.42	372.94	822.15
Re	41.83	98.88	142.56	422.22	736.08	1096.28	2536.75	3739.84
Os	577.43	606.99	607.33	182.47	337.47	554.50	2036.16	2964.06
Ir	39.09	89.20	120.03	154.10	240.16	432.69	1375.87	2638.09
Pt	19.51	57.05	82.28	178.06	369.79	619.29	1958.18	3453.29
Au	0.81	0.90	0.54	0.83	0.85	2.13	9.96	18.73
Element	A	B	C	D	E	F	G	H
Ru	9.84	26.16	41.58	197.98	556.32	1073.35	2440.83	3924.92
Rh	41.82	95.52	140.68	409.03	788.24	1342.10	2645.28	3739.64
Pd	1.99	4.69	6.11	10.01	23.10	59.19	231.24	702.77
Re	45.46	98.77	142.15	387.10	715.15	1221.85	2337.53	3522.80
Os	589.06	609.37	608.77	169.57	327.41	668.75	1803.65	2766.77
Ir	42.55	90.90	119.82	142.23	232.37	488.50	1254.06	2395.37
Pt	23.98	56.48	79.05	160.27	367.68	728.22	1795.49	3220.47
Au	0.77	0.93	0.72	0.71	1.20	1.90	3.61	10.44

Table 8b - PGE and Au equilibrium concentrations ($\mu\text{g/l}$) in the Zandvlei subsamples supernatant after 24 h interaction with the respective reagent solution A-H (in duplicate: upper/lower panel) in the adsorption isotherm experiments.

Reagent solution								
Element	A	B	C	D	E	F	G	H
Ru	3.09	9.28	17.98	60.90	182.85	424.98	1332.26	4143.40
Rh	20.69	53.57	91.64	306.94	721.69	1128.88	2271.04	3903.30
Pd	5.67	7.65	10.00	13.20	13.40	11.94	9.71	822.15
Re	44.73	98.26	148.46	415.07	901.33	1331.57	2567.69	3739.84
Os	601.35	618.40	81.58	332.06	942.20	2111.79	2612.52	2964.06
Ir	42.41	93.27	144.25	400.87	868.81	1302.55	2447.16	2638.09
Pt	20.20	43.52	63.51	140.03	286.54	387.33	743.05	3453.29
Au	4.79	9.20	24.03	45.57	58.41	51.24	18.63	18.73
Element	A	B	C	D	E	F	G	H
Ru	4.13	9.19	17.71	65.55	177.31	448.23	1318.03	3924.92
Rh	22.40	55.04	90.36	318.35	707.78	1042.25	2343.74	3739.64
Pd	4.57	7.47	10.92	12.02	12.86	11.43	9.31	702.77
Re	49.64	97.63	145.62	435.32	885.39	1230.20	2680.32	3522.80
Os	608.35	618.80	81.59	328.91	983.22	2284.39	2560.14	2766.77
Ir	46.87	94.40	142.69	421.94	858.14	1190.18	2559.71	2395.37
Pt	21.65	44.96	61.16	135.64	256.14	377.09	562.27	3220.47
Au	2.79	11.99	23.37	35.64	55.79	45.32	22.16	10.44

Table 8c - PGE and Au equilibrium concentrations ($\mu\text{g/l}$) in the Tokai subsamples supernatant after 24 h interaction with the respective reagent solution A-H (in duplicate: upper/lower panel) in the adsorption isotherm experiments).

Reagent solution								
Element	A	B	C	D	E	F	G	H
Ru	16.28	34.90	53.03	118.79	391.20	726.07	2045.85	3655.39
Rh	44.59	96.47	136.39	357.81	836.66	1231.21	2537.60	3864.42
Pd	9.44	11.02	13.89	7.16	13.96	20.54	56.02	89.79
Re	46.44	98.64	137.97	347.47	780.82	1109.63	2307.59	3692.74
Os	608.19	612.68	87.99	148.00	56.87	603.13	1366.51	2326.81
Ir	43.09	88.29	114.76	128.28	209.19	335.41	967.31	1724.98
Pt	13.45	29.54	36.61	15.61	42.41	107.65	641.01	1360.60
Au	4.83	4.32	7.81	1.46	3.75	3.73	5.78	5.74
Element	A	B	C	D	E	F	G	H
Ru	16.04	32.14	51.56	142.90	368.06	596.84	1964.79	3825.54
Rh	46.53	95.86	139.20	411.17	769.98	1053.51	2533.27	3992.48
Pd	8.76	11.42	13.71	8.11	13.07	16.35	48.30	113.18
Re	48.07	96.85	141.70	396.75	712.50	956.55	2299.95	3844.03
Os	611.40	612.66	86.35	142.28	40.13	294.63	1178.03	2518.43
Ir	45.87	88.88	118.50	146.50	193.09	264.59	873.20	1898.32
Pt	12.33	23.75	32.96	22.13	42.49	75.45	492.91	1471.69
Au	4.92	5.22	7.66	1.17	4.83	2.61	3.68	33.28

The pH of the supernatant of the Malm, Zandvlei and Tokai samples was measured at the end of the adsorption experiment (24h) for each of the adsorbate concentrations (Fig. 4).

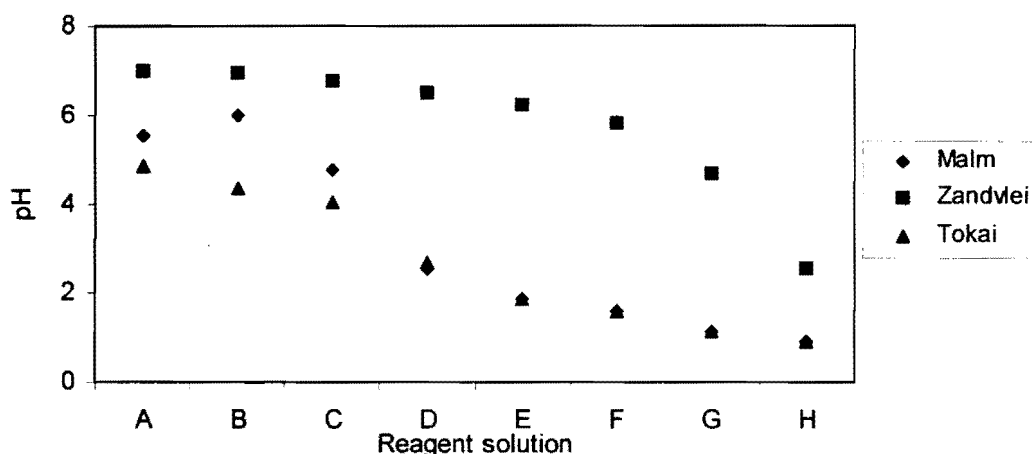


Figure 4 - pH of the supernatant of Malm, Zandvlei and Tokai samples after 24h reaction time with the respective PGE and Au reagent solution (A-H) for the adsorption isotherm experiments.

As it can be observed in Fig. 4 the pH of the supernatant depends on the reagent solution concentration prepared from the SpecPure® PGE and Au stock solution in 20% HCl. The more concentrated the reagent solution the lower the supernatant's pH. The Malm and Tokai samples show the more pronounced decrease in pH for most reagent solutions (D-H) while the Zandvlei sample shows a visible decrease only for the most concentrated reagent solutions (H).

4. DISCUSSION

Six solid matrices were selected and characterised for their general geochemical properties in order to study adsorption of PGE and Au using batch experiments. The study focused on Pt, Pd, and Rh since these are widely used in catalytic converters and therefore of special interest from an environmental point of view. Correlations between the Pt, Pd and Rh adsorption coefficients and selected sorbent properties were also performed in order to conclude on the relevant sorbent properties for the mobilisation of Pt, Pd and Rh in the soil environment.

4.1 General characterisation of solid matrices

The solid matrices used as sorbents in the sorption experiments were chosen for their varied physico-chemical properties (Table 4). The variety of sorbent properties in the selected matrices is useful to assess the sorbent characteristics that play an important role in the mobilisation of PGE in the natural environment. The selected clay minerals consist on very fine particles smaller than 3 μm in diameter and the Consol sand consist of predominantly coarse and medium sand size particles. The Malm sample has a predominant silt and fine sand fraction while in the Zandvlei sample the very fine sand and clay fraction predominate. The Tokai sample has a predominant coarse and medium sand fraction and is poor in clay and silt. As expected, the SSA-N₂ is inversely related with the particle size: the selected clay minerals have the highest SSA-N₂ while the Consol sand has the lowest SSA-N₂ of all solid matrices. The SSA-N₂ for the Malm and Zandvlei samples is lower than that of the isolated clay minerals since these samples are constituted of particles of all sizes.

The organic matter content was detectable in the Malm, Zandvlei and Tokai samples being 6, 11 and 23 %, respectively. The organic matter content is lower in the Malm sample which is due to less abundant vegetation in the area where the soil was sampled. The elevated organic carbon content in the Zandvlei sediment is an expected finding and it is thought to be a result of the

accumulation of organic materials in the estuary reaching this area as fine sediment particles with the river flow.

As expected the selected clay minerals differ in the CEC (Table 4). The Ca-bentonite has a high CEC due to exchangeable Ca^{2+} and Mg^{2+} in the interlayer structure while the Kaolin has a low CEC due to the low charge in its 1:1 layer and smaller surface area (Olson, 2000). The determined CEC of the Zandvlei is about three times higher than the one of the Malm sample. The clay content as well as the elevated organic carbon content of this wetland sediment is responsible for its high CEC. In the clay poor Tokai sample the CEC is mainly due to the high organic carbon content since organic materials have high surface area and high chemical reactivity (McBride, 1994; Chadwick, 2000).

The potentiometric titrations (Fig. 1) of the solid matrices did not show an intersection of the four curves of different electrolyte concentrations: the point of zero salt effect. If the mineral surfaces were positively charged the curves were expected to intersect at a single pH and diverge away from that pH in either direction as a result of the chemical and electrostatic effects involved in adsorption reactions (Drever, 1997). However, from the titration curves the different behaviour of each of the solid matrices on acid and base additions (buffering capacity) can be observed. The potentiometric titration curves of the Kaolin and Consol sand samples do not show any buffering capacity due to a very low CEC (Fig. 1a, c). In contrast the titration of the Tokai and Zandvlei samples show the highest buffering capacity (Fig 1e, f) which is explained by the high organic matter content (Table 4) that balances both acid and base additions to the solid matrix. At high pH organic acids are negatively charged due to a loss of H^+ while at low pH organic acids are protonated and therefore capable of anion exchange (McBride, 1994).

The PGE and Au background concentrations in the solid matrices leachates are mostly below the detection limit of ICP-MS method (Table 12 in Appendix). One exception to this is Os showing much higher background concentrations than expected. Abnormally high Os concentrations are also observed when analysing PGE and Au in the solid matrices solution (Table 13a-f in Appendix). This observation confirms the suspicion that these findings

are likely to be a result of an analytical artefact occurring at very low Os concentrations. Contamination with Os is very unlikely to happen but it is known that Os analysis by ICP-MS at very low concentrations may be more affected by the higher Os concentrations in the calibration standards (Andreas Spaeth, personal communication, September 2002).

4.2 Time course experiments

The time course batch experiments were used to compare the behaviour of the different PGE and Au over time. All PGE and Au were analysed in the supernatant aliquots sampled at specific time points (t_i) over the total reaction time of 24h (Fig. 3). This discussion is focussed on the behaviour of Rh, Pd and Pt since these elements are the ones used in the catalytic converters (Palacios et al., 2000). A selection of the time course data for Rh, Pd and Pt is presented in Figure 5.

Studying the plots of the concentrations of these elements (Pt, Pd and Rh), as measured after interaction with the selected solid matrices, allows visualisation of the different behaviours during the time course experiments and facilitates comparisons. As described in chapter 3.1, it was clearly shown that Rh and Pd have almost opposite sorption behaviours under these experimental conditions. While Pd is removed efficiently from solution, except in the Kaolin solid matrix, Rh concentration remains fairly constant over time (Fig. 5b, c). An exception to this is Rh behaviour seen with the Ca-bentonite and Zandvlei samples where the Rh concentration decreases slowly over the 24h experiment (Fig. 5c). Pt shows an intermediate sorption behaviour when compared to Rh and Pd: the interaction of Pt with the Zandvlei and Tokai samples lead to the most efficient decrease in Pt concentration in the supernatant (Fig. 5a). On the other hand Pt interaction with the Kaolin and Consol sand samples leads to a smaller decrease in Pt concentration in solution (Fig. 5a). The sorption behaviour described in Fig. 5 is surprising since PGE are generally considered to be fairly inert.

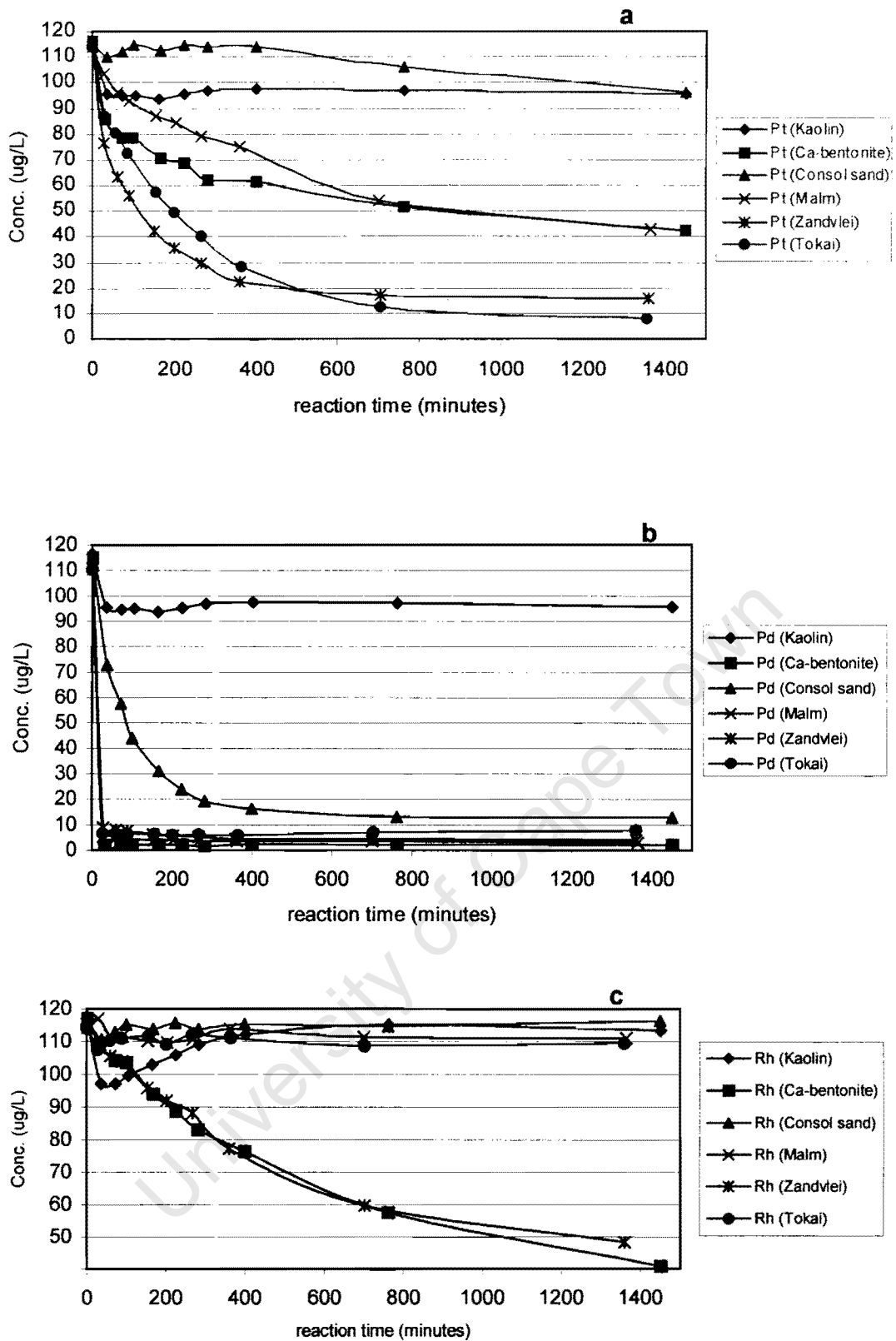


Figure 5 - Concentrations of (a) Pt, (b) Pd and (c) Rh ($\mu\text{g/L}$) in the supernatant of Kaolin, Ca-bentonite, Consol sand, Malm, Zandvlei and Tokai samples at correspondent reaction times over 24 h time course experiment.

In the metal form Pt and Pd are considered to be more reactive than other PGE and their noble character is known to predominate only in the absence of strongly complexing species (Cotton et al., 1999). Identification of the Pt, Pd and Rh species present in solution could bring some light over the different behaviours of these elements during the time course experiments.

Pt and Pd are expected to be predominately in the (+2) oxidation state while Rh is in the (+3) oxidation state, in the original stock solution (SpecPure® 100 mg/l PGE and Au in 20% HCl) (see Fig. 9). According to Wood (1990) and Fletcher et al. (1995), hydroxide and chloride are important anions responsible for Pt and Pd speciation but hydroxide is likely to be the most important anion in natural environments such as lakes, rivers and even surface seawater (Wood, 1992). Therefore, Pt and Pd hydroxide species of the type $\text{Pt}(\text{OH})_2$ and $\text{Pd}(\text{OH})_2$, may predominate in the reagent solution added to the solid matrices. It is noteworthy to remember that the stock solution was diluted 100 times when preparing the reagent solution used for the time course experiments. Furthermore, in the solid matrix/reagent solution mixture the predominant ions in solution originate from the solid matrix solution (3g:50ml). Most of these ions are at much higher concentrations than the added PGE and Au. The presence of organic complexes in solution may have a direct influence in Pt, Pd and Rh speciation.

It is known that Pt^{II} and Pd^{II} geochemistry have many similarities concerning the formation of cationic and anionic species but Pd^{II} complexes seem to be less stable than their Pt^{II} analogues (Cotton et al., 1999). Therefore, the formation of stable Pt-organic complexes rather than Pd-organic complexes could partially contribute to higher Pt concentrations in solution compared to Pd concentrations (Fig. 5a, b). Pd would tend to precipitate independently of the organic or clay content of the solid matrices and be removed rapidly from solution. However, in Fig. 5a it is clear that Pt interaction with organic rich matrices (Tokai and Zandvlei) leads to a gradual but more efficient removal of Pt from solution than the interaction with the other matrices. Fuchs and Rose (1974) findings support that Pt has a preference for organic materials since Pt/Pd ratio was higher in A and transition horizons (both organic rich) of the Stillwater Complex. Several other studies have also documented enrichment

of Pt in organic rich soils and sediments (Kucha, 1982; Dissanayake et al., 1984 and Plyusmina, 2000) even though the mechanism responsible for this is still not clear.

However, Pt was found to be immobile relatively to Pd and formation of a Pd-organic complex was suggested to explain leaching of Pd from the topsoil and accumulation in the B and C horizons (Fuchs and Rose, 1974). Another study found that metallic Pd seems to react much more quickly than metallic Pt in the presence of acetate, salicylate, phthalate, and fulvic acids (Wood, 1994). Rh sorption behaviour is particularly interesting since data on Rh speciation and interaction with soils is scarce and it contrasts with Pt and Pd behaviour (Fig. 5c). The main difference between Pt-Pd and Rh may be the oxidation state in solution (Cotton et al., 1999), influencing Rh adsorption behaviour. While Pt sorption behaviour seems to be positively correlated with organic rich solid matrices and Rh sorption is favoured in high surface area solid matrices (Ca-bentonite and Zandvlei). High surface area means more surface sites available for reactions with the sorbate. Since Rh is less reactive it is probably more dependent on sorbent physical properties such as surface area.

pH is a major variable is PGE speciation (Wood, 1992; Barefoot, 1999). The pH of the supernatant during the time course experiments was both influenced by the reagent solution added (from stock solution in 20% HCl) and by the solid matrix buffering capacity. The pH of the Ca-bentonite supernatant stayed fairly stable, while the pH in the Kaolin and Consol sand decreased after addition of reagent solution, from pH 6.5 to 3 and pH 7 to 4, respectively (Fig. 3). As expected from the potentiometric titrations (Fig.1), both the Kaolin and the Consol sand matrices have low buffering capacities. Therefore addition of reagent solution leads to the most pronounced initial decrease in pH that may additionally have influenced the low adsorption of PGE in both Kaolin and Consol sand matrices. The other solid matrices show less pronounced pH variations after reagent solution addition (Fig. 3). Variations such these are common in real soils and the supernatant pH can be considered fairly stable over the total reaction time .

In summary, we found that at least some of the PGE studied show considerable reactivity under the chosen experimental conditions. In

particular, we found that the Pd adsorbs very readily with all the matrices, Rh stays in solution and Pt shows a sorption behaviour in between these two extremes. Despite that the mechanism responsible for these findings is not clearly understood. However, results from the time course experiments in the present study are more of qualitative value than quantitative: repetitive sampling of supernatant over time introduces changes in the volume/solid matrix ratio that were not fully quantified. Despite that, this kind of experiment proved to be useful to compare the sorption behaviour of PGE and Au in the selected solid matrices.

4.3 Pt, Pd, and Rh isotherms and K_d calculation

Sorption isotherms were obtained for Pt, Pd, and Rh. These were then described and classified according to the observed isotherm patterns. The K_d was determined by plotting the amount of Pt, Pd and Rh sorbed by each solid matrix (C_s in mg/kg) as a function of its concentration in solution (C_w in mg/L) (Fig. 6). The amount of metal adsorbed (mg) was obtained by subtraction of the mass of that element present in solution after the total equilibration time (t_{1440} concentration) from the mass of that same metal in the reagent solution (t_0 concentration). This mass was then divided by the respective mass of sorbent for that solid matrix subsample.

Duplicate adsorption isotherms are plotted for each of the elements for the subsamples of the Malm, Tokai soils and Zandvlei sediment (Fig. 5). Since replicate subsamples did not show the same sorption patterns both trends are presented (Malm 1/Malm 2, Zandvlei 1/Zandvlei 2, and Tokai1/Tokai 2). A gradual increase in the amount adsorbed was observed with the increase of concentration of the elements in solution (Fig. 6). The curve is steepest for the lower concentration range which is typical of trace inorganic substances in natural waters (Langmuir, 1997). When observing the shape of the curves for the different elements and considering the whole C_w range, one notices that the flattening of the adsorption isotherm is not always achieved in the higher concentration range Pd and Pt interaction with Tokai solid matrix (Fig. 6a, b) as well as for Rh after interaction with the Malm solid matrix (Fig. 6c).

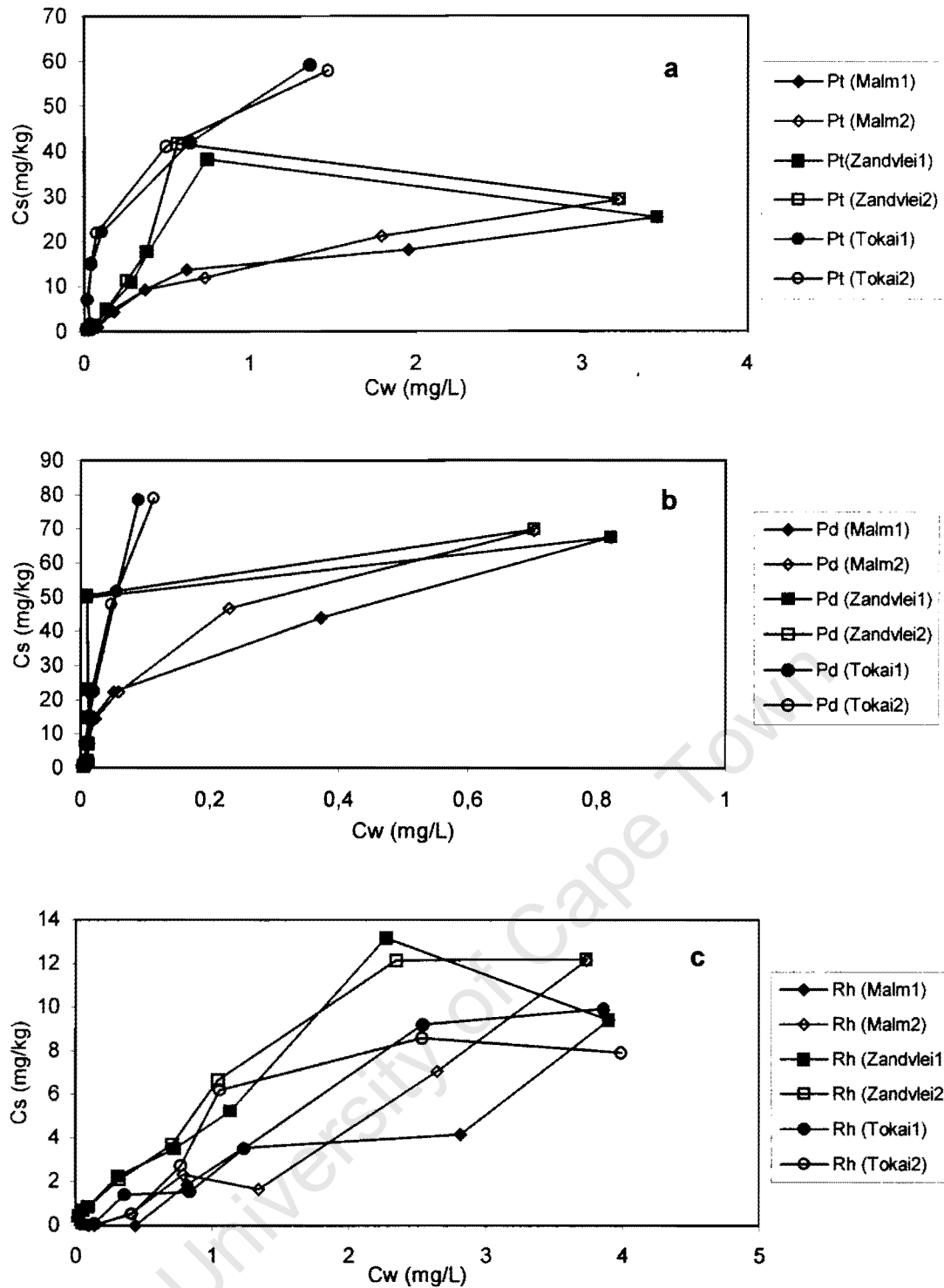


Figure 6 - Adsorption isotherms in duplicate: (a), Pt, (b) Pd and (c) Rh in the respective solid matrices. The adsorbed concentration C_s (mg element adsorbed / kg solid matrix) is plotted against the equilibrium concentration C_w (mg element in solution / volume of solution) after 24h reaction time.

An abrupt decrease in C_s for high values of C_w is pronounced for Pt in the Zandvlei matrix and for Rh in the Zandvlei and Tokai matrices (Fig. 6a, c).

This behaviour may be a result of a saturation of sites in the sorbent's surface. Duplicate measurements show that Rh behaves unpredictably at both the high and low concentration ranges in the Malm and Tokai samples (Fig. 5c). In contrast, a good agreement between duplicates for Pt and Pd in all solid matrices and Rh in the Zandvlei matrix was observed and an average value for C_S and C_W was calculated (Fig. 6a, b).

Despite the fact that all elements were present at the same concentration in the initial reagent solution (Table 7), the magnitude of C_W is different for each element and independent of the solid matrix (see C_W scale in Fig. 6a, b and c). This fact is directly related with the elements' affinity for the respective solid matrix. For example, Pd interaction with all solid matrices in the isotherm experiments not only shows the steepest isotherms, confirming its high affinity to be adsorbed but also the C_W values are 10 times lower than those of Pt and Rh (Fig. 6b). Pd shows a higher affinity for the Zandvlei and Tokai samples than for the Malm sample since the steepest isotherms are observed for the interaction with Zandvlei and Tokai samples (Fig. 6b). Pt interaction with the Tokai sample shows the steepest of the three isotherms following a similar pattern as observed for Pd (Fig. 6a). As mentioned above Rh behaviour is not the same for both duplicate samples. Despite this discrepancy, one can say that Rh shows a lower affinity for all solid matrices as compared to the affinity noted for Pt and Pd for the same solid matrix (Fig. 6c). This sorption behaviour of Pd, Pt and Rh is also observed for the high concentration range and is in accordance with the findings of the time course experiments (Fig. 2d-e).

McBride (1994) describes 4 general types of adsorption isotherms, suggesting a main type of sorbate-sorbent interaction according to the shape of the isotherm. For high affinity between the sorbate and the sorbent the so called L-type isotherm is steeper for the lowest C_W but it stabilises (flattening of the curve) as the C_W increases. This type of isotherm indicates that chemisorption may be the main mechanism responsible for the observed behaviour. The H-type is an extreme case of the L-type high affinity isotherm (Langmuir) showing a steeper curve for low C_W than the L-type isotherm. When the bonds between the sorbate-sorbate are stronger than between sorbate-sorbent the

sorbate is only adsorbed at higher equilibrium concentrations. When this occurs the isotherm can be classified as S-type isotherm indicating that cooperative sorption favours clustering of sorbate molecules at the surface. A constant relative affinity of the sorbate molecules for the sorbent results in a C-type isotherm and is usually observed only at the low range of concentrations. It can be a good description of the reality since many compounds of interest in soils are adsorbed at low concentrations (McBride, 1994).

According to this classification the adsorption isotherm for both Pt and Pd in the Zandvlei and Tokai samples could be classified as being of the H-type, although no flattening of the curve is observed for high C_w concentrations. The steep correlation between C_s and C_w for both Pt and Pd in the Zandvlei and Tokai solid matrices (Fig. 6a, b) suggests a strong sorbate-sorbent interaction. This interaction probably involves strong ionic or even covalent bonds with the soil colloids. On the other hand, Pt, Pd and Rh isotherms after interaction with the Malm sample are less steep than observed for Pt, Pd and Rh in the Zandvlei and Tokai samples. The relationship between C_s and C_w for all elements in the Malm sample suggests an L-shaped isotherm. The interaction of Pd with the Malm sample of the L-type suggests a high affinity of the sorbate for the sorbent but this is not so pronounced when compared to the behaviour of Pd in the other solid matrices (H-type).

In view of the above results there is a need to quantify the affinity of Pt, Pd and Rh for each solid matrix. The general approach is the calculation of the distribution coefficient K_d (or partition coefficient) from the individual isotherms:

$$K_d = \frac{C_s}{C_w} \quad \text{Eq. 1}$$

Since there is not a linear relationship between C_s and C_w for the whole adsorption data, both Freundlich and Langmuir isotherms are tested to fit the data and calculate K_d . As mentioned above, the instable behaviour of Rh, as noted from the replicates, does not allow the calculation of average C_s and C_w values and respective K_d except in the case of Rh in the Zandvlei sample.

The general equation of the Freundlich isotherm refers to a non-linear relationship between C_s and C_w of the form:

$$C_s = K \cdot C_w^n \quad \text{Eq. 2}$$

In order to calculate the respective K_d the general approach is to apply the linear form of the Freundlich equation:

$$\log C_s = n \log C_w + \log K \quad \text{Eq. 3}$$

The Freundlich equation linear form is applicable if the logarithmic form of the adsorption data will fall on a straight line with slope n and intercept $\log k$, where n and k are adjustable positive parameters (McBride, 2000).

This equation was tested to fit the data and Fig. 7 summarises the correlations found for the Freundlich linear equation. In the same way, the Langmuir equation (Eq. 4) can be used to describe adsorption isotherms. The non-linear equation for Langmuir isotherm is:

$$C_w = b \times \left(\frac{K \times C_w}{1 + K \times C_w} \right) \quad \text{Eq. 4}$$

where K is an adsorption constant related to the binding energy (L/mg) and b is the maximum amount of sorbate that can be adsorbed by the solid. The linear form of Eq. 4 is:

$$\frac{C_w}{C_s} = bK - K \times C_w \quad \text{Eq. 5}$$

If the Langmuir equation is applicable the data should fall on a straight line with slope $-K$ and x intercept bK . The plotting of the C_w/C_s against C_w result in the following correlations shown in Fig. 8.

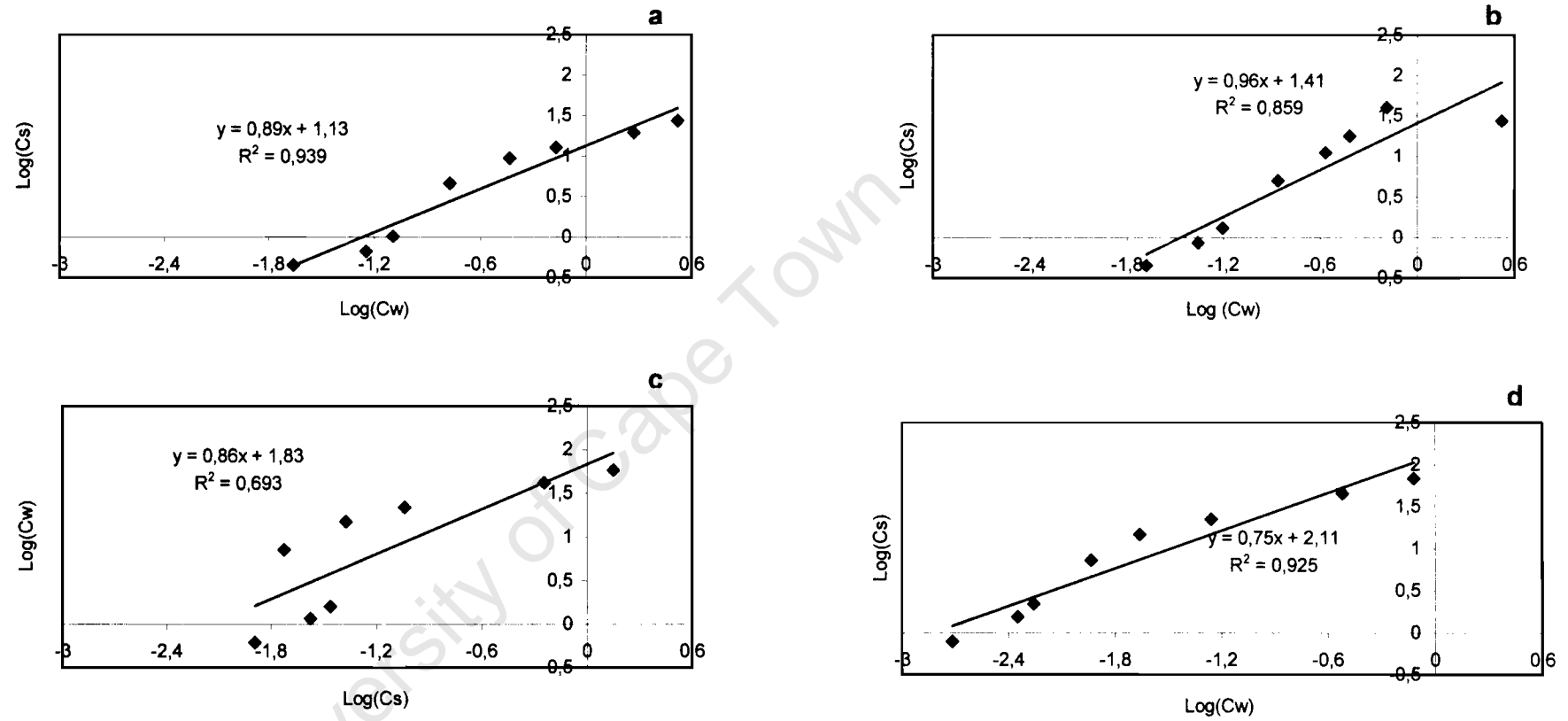


Figure 7 - Freundlich isotherms converted to the logarithmic form for Pt, Pd and Rh. Pt in the (a) Malm, (b) Zandvlei and (c) Tokai samples; Pd in the (d) Malm, (e) Zandvlei and (f) Tokai samples, and Rh in the (g) Zandvlei sample.

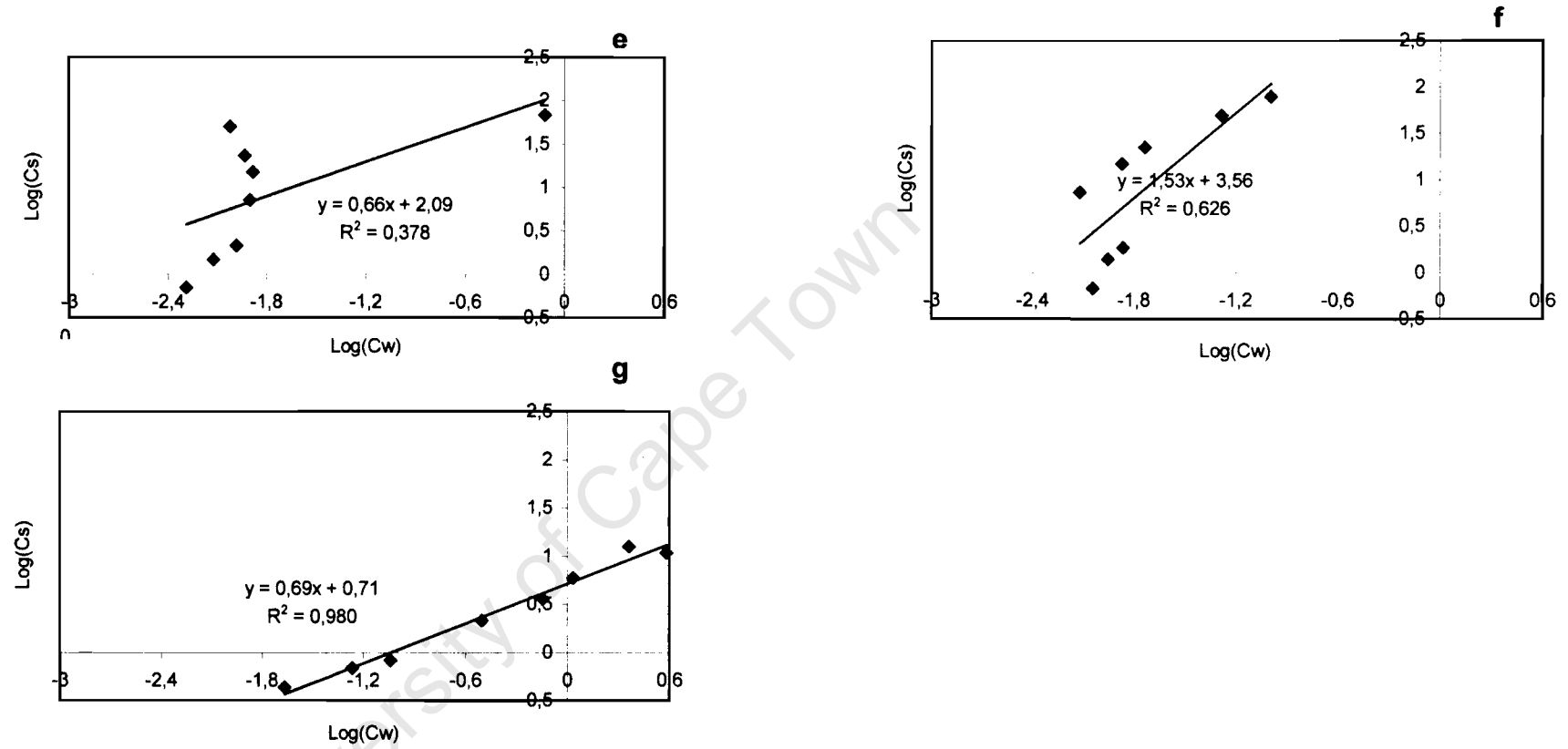


Figure 7 (cont.) - Freundlich isotherms converted to the logarithmic form for Pt, Pd and Rh. Pt in the (a) Malm, (b) Zandvlei and (c) Tokai samples; Pd in the (d) Malm, (e) Zandvlei and (f) Tokai samples, and Rh in the (g) Zandvlei sample.

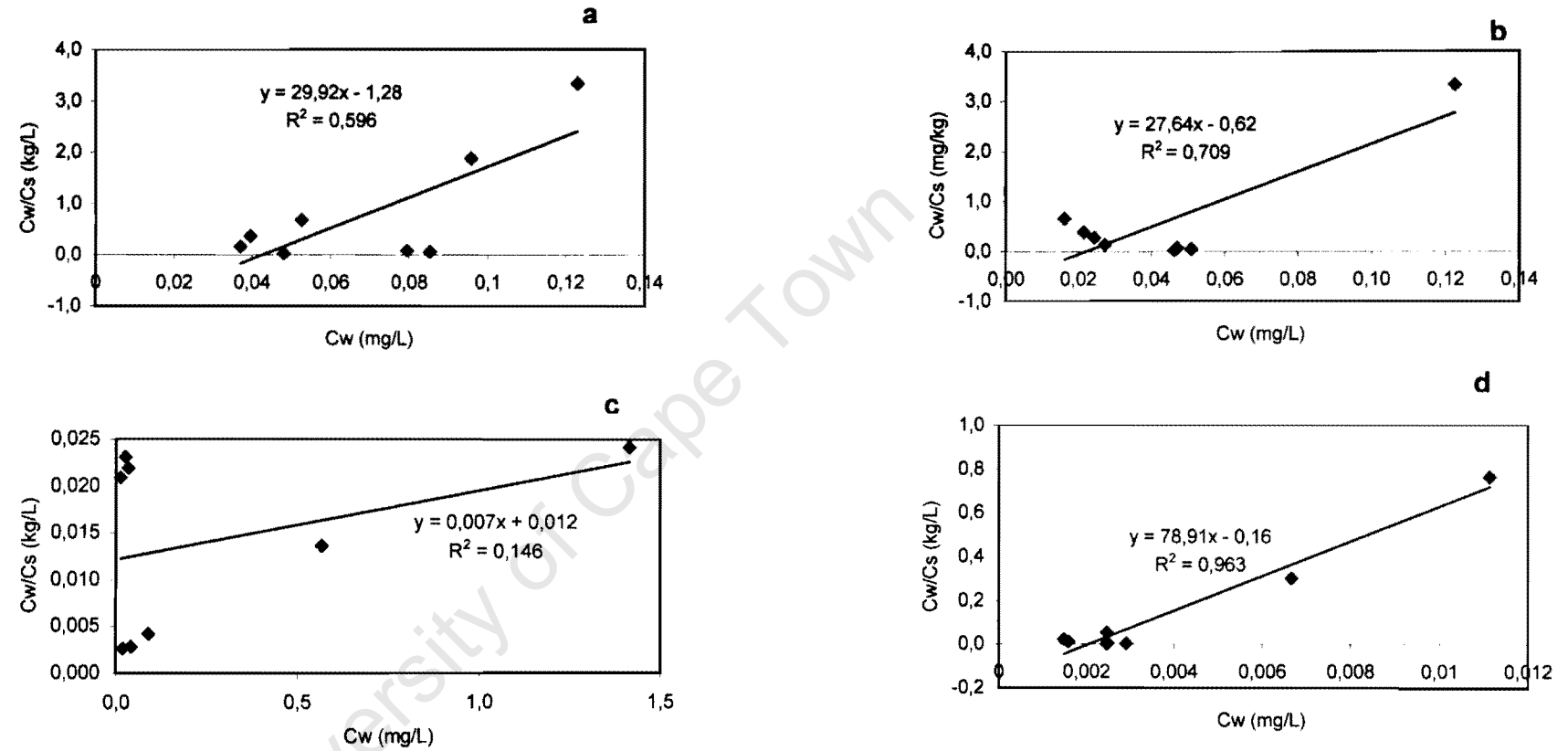


Figure 8 – Langmuir isotherms converted to the linear form $C_w/C_s = bK - KCw$ for Pt adsorption data in the (a) Malm, (b) Zandvlei and (c) Tokai samples; Pd in the (d) Malm, (e) Zandvlei and (f) Tokai samples, and Rh in the (g) Zandvlei sample.

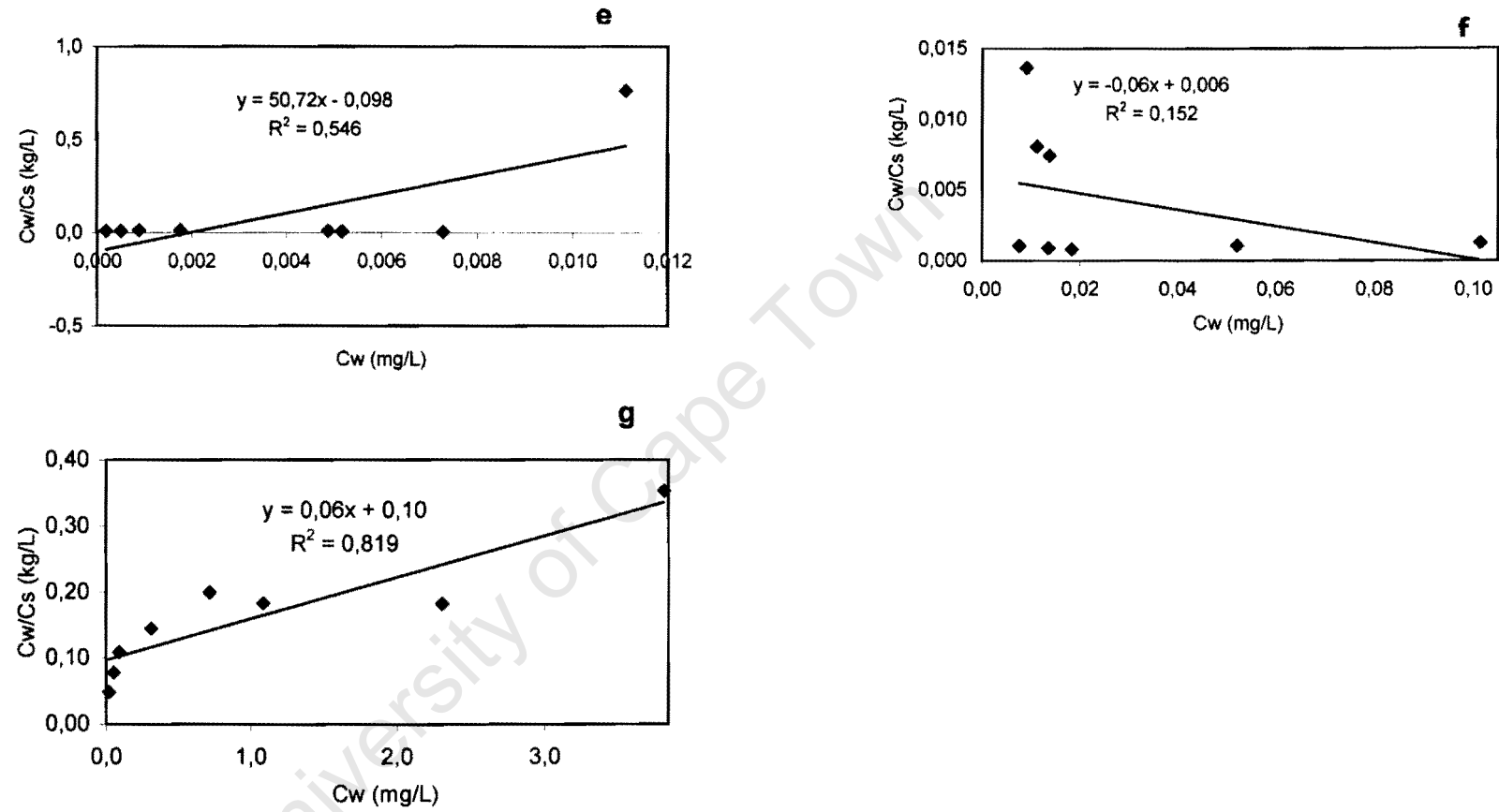


Figure 8 (cont.) – Langmuir isotherms converted to the linear form $C_w/C_s = bK - KC_w$ for Pt adsorption data in the (a) Malm, (b) Zandvlei and (c) Tokai samples; Pd in the (d) Malm, (e) Zandvlei and (f) Tokai samples, and Rh in the (g) Zandvlei sample.

All graphs are presented even if there is not a true correlation between the experimental data when applying either Freundlich or Langmuir equations (Fig. 7e and 8b, c, d and f). For these data the calculation of the respective K_d is not possible since none of the adsorption models can describe the behaviour of the elements in the solid matrix. However, as it can be observed in Fig. 7, reasonably high correlation coefficients are obtained for Pt in the Malm ($r^2=0.939$) and Zandvlei ($r^2=0.859$) samples as well as for Pd in the Malm ($r^2=0.925$) and Rh in the Zandvlei ($r^2=0.980$) samples. For these adsorption data the Freundlich isotherm is applicable to describe the adsorption behaviour observed. The Langmuir equation is only valid for Pd in the Malm sample ($r^2 = 0.963$), all the other r^2 are below 0.85.

Furthermore, the calculation of K_d value for Pt, Pd or Rh can be obtained for a given C_w since the Eq.1 cannot be applied directly. A given C_w value is substituted in Eq.3 and the respective C_s is used to calculate K_d . In the same way, when the Langmuir model is valid, the K_d can be obtained from a given C_w and the respective C_s calculated applying Eq. 5.

In this context it is important to have in mind the concentrations of Pt, Pd and Rh in soils exposed to exhaust fumes. Documented concentrations do not exceed 100 $\mu\text{g}/\text{kg}$ for Pt, 10 $\mu\text{g}/\text{kg}$ for Pd, and 35 $\mu\text{g}/\text{kg}$ for Rh, respectively (Table 1). Therefore, the lowest concentration range of initial reagent concentration (50 –1000 $\mu\text{g}/\text{L}$) is the one of most interest for this study since it is closest to the observed concentrations in contaminated soils. At such low concentrations and over narrow C_w ranges the relationship between C_s and C_w is usually linear both in the Freundlich and Langmuir non-linear isotherm models (Langmuir, 1997; Fetter, 1999). A linear correlation was tested to fit the adsorption data selecting C_w values in the low concentration range. The selected experimental C_w values (first five values of C_w) were plotted against the correspondent adsorbed concentration (C_s) in Fig. 9. A linear trend fitted the data for Pd, Pt and Rh in at least one of the selected solid matrices with a reasonably acceptable correlation coefficient ($r^2>0.98$). In this case K is equal to the partition coefficient K_d for that concentration range.

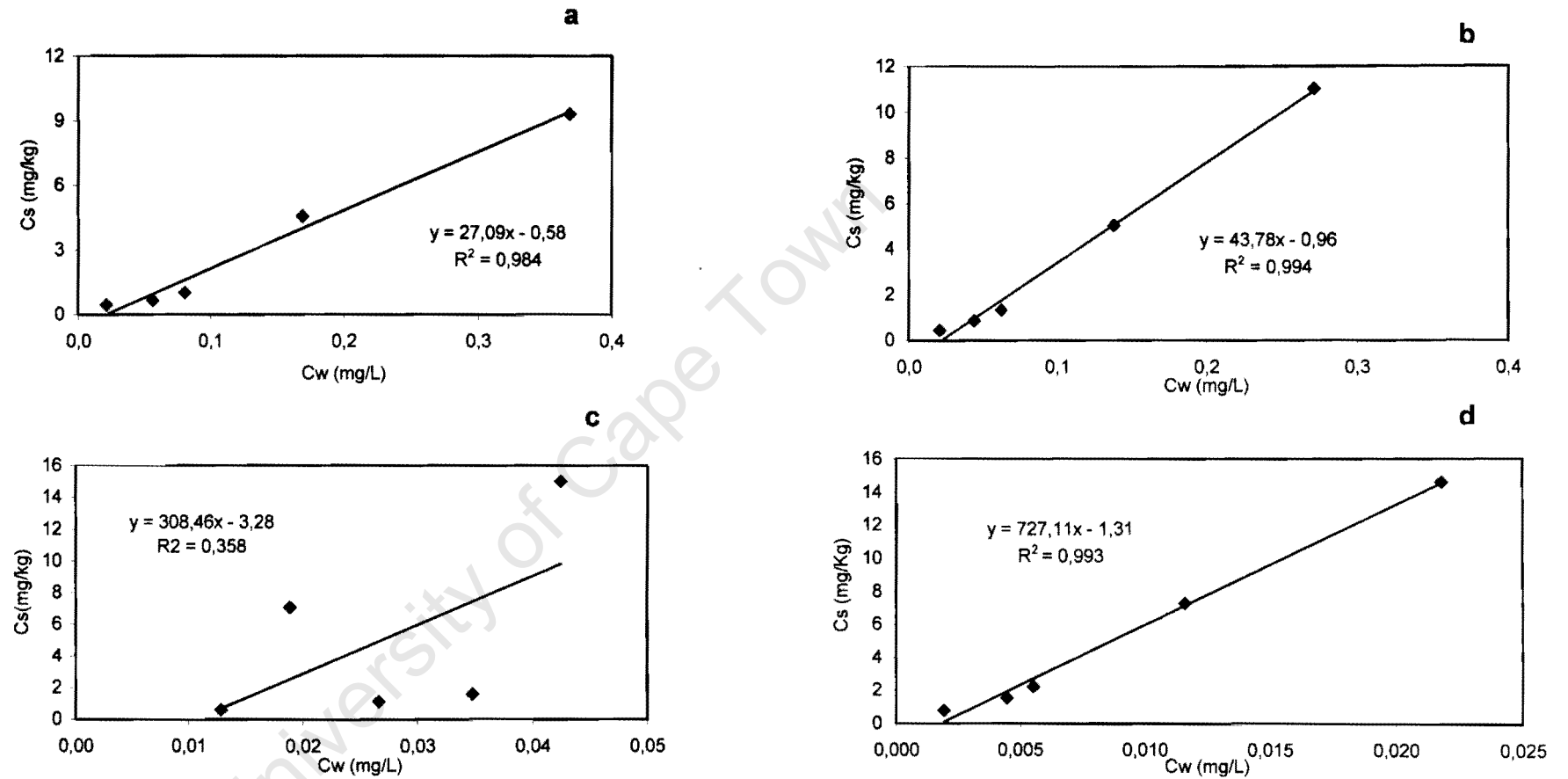


Figure 9 – Linear isotherm for Pt, Pd and Rh selected adsorption data. $C_w = KC_s + b$. for Pt, adsorption data in the (a) Malm, (b) Zandvlei and (c) Tokai samples; Pd in the (d) Malm, (e) Zandvlei and (f) Tokai samples, and Rh in (g) Zandvlei sample.

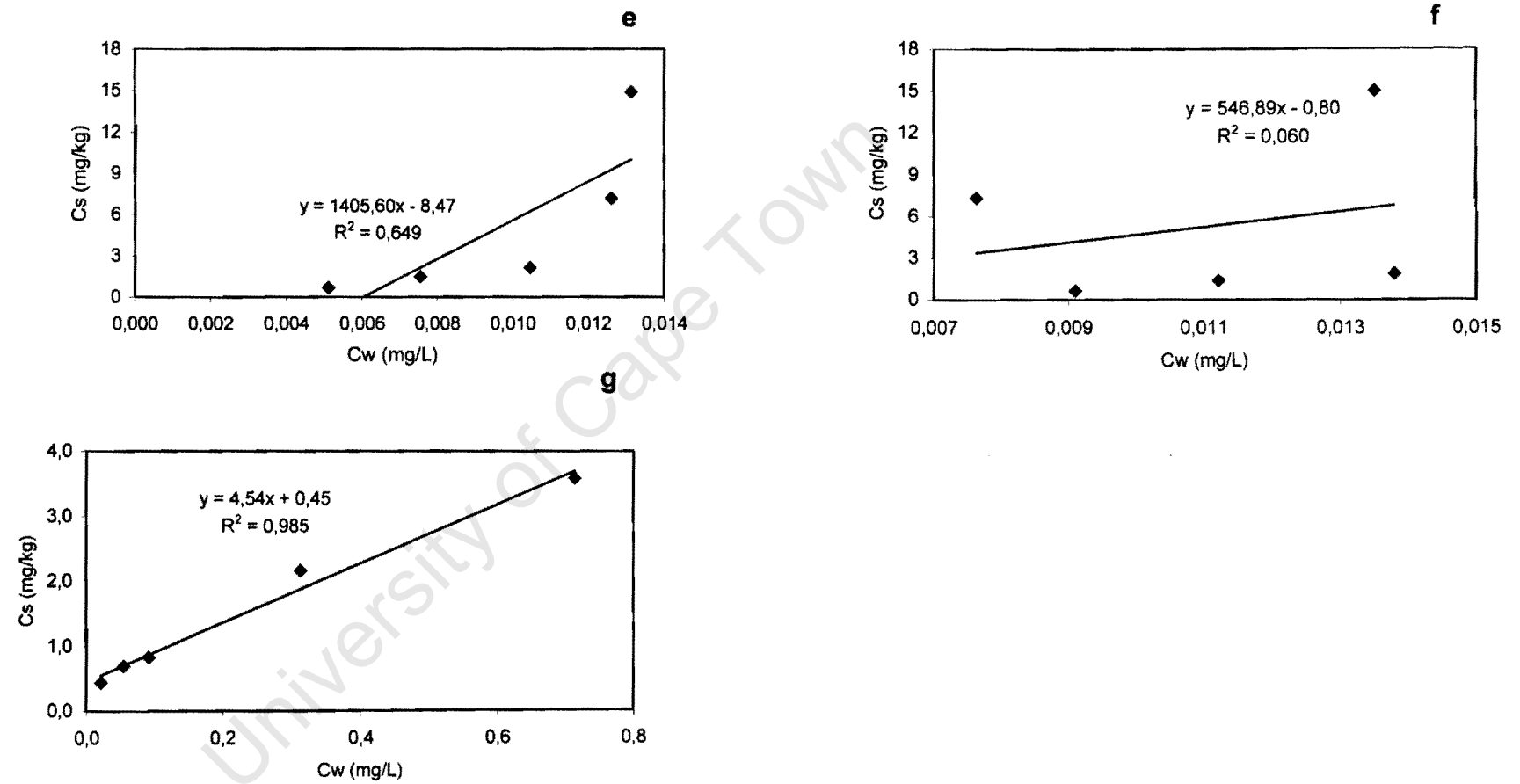


Figure 9 (cont.) – Linear isotherm for Pt, Pd and Rh selected adsorption data. $C_w = KC_s + b$. for Pt, adsorption data in the (a) Malm, (b) Zandvlei and (c) Tokai samples; Pd in the (d) Malm, (e) Zandvlei and (f) Tokai samples, and Rh in (g) Zandvlei sample.

For the selected data set applying the linear model for the lower C_w range the C_w value for Pd after 24 h is 10 times lower than the one of Pt and 100 times lower than the one of Rh for the same C_i (Fig. 9). Therefore, Rh behaviour contrasts with the high reactivity of Pd, remaining in solution (high C_w) even for the lowest C_s . Although the K_d linear relationship is valid for Pt and Pd in the Malm and Zandvlei samples and Rh in the Zandvlei sample the respective K_d values are of completely different magnitudes (Table 9). After interaction with the Malm soil (Fig. 5c) a much higher slope (K_d) is obtained for Pd than for Pt. This value confirms the higher affinity of Pd for the Malm solid matrix than that of Pt as expected from the time course experiments: Pd concentration decreased abruptly within the first 30-60 min. to $C_w < 10$ ppb while Pt decreased gradually to values around 40 ppb.

A summary of K_d values obtained for a chosen C_w is shown in Table 9.

Table 9 – Comparison of Pt, Pd and Rh K_d values obtained using the Freundlich, Langmuir and linear isotherm models (when applicable) to describe adsorption behaviour in the batch adsorption experiments. Using $C_w = 0.03$ mg/L.

Solid matrix	Langmuir Eq.	Freundlich Eq.			Linear Eq.		
	Pd	Pt	Pd	Rh	Pt	Pd	Rh
Malm	0.45 ($r^2=0.963$)	19.84 ($r^2=0.939$)	25.7 ($r^2=0.925$)	<i>n.a.</i>	27.09 ($r^2=0.984$)	727.11 ($r^2=0.993$)	<i>n.a.</i>
Zandvlei	<i>n.a.</i>	29.57 ($r^2=0.859$)	<i>n.a.</i>	15.20 ($r^2=0.980$)	43.78 ($r^2=0.994$)	1405.60 ($r^2=0.649$)	4.54 ($r^2=0.985$)
Tokai	<i>n.a.</i>	110.46 ($r^2=0.693$)	556.07 ($r^2=0.629$)	<i>n.a.</i>	<i>n.a.</i>	<i>n.a.</i>	<i>n.a.</i>

Note: *n.a.* not applicable

The adsorption coefficients calculated applying the linear isotherm (Fig. 9) are only valid for the specified concentration range. No extrapolations can be made for higher concentrations since the behaviour of Pt, Pd, and Rh follows a different trend in the equilibrium isotherm (Fig. 6). The K_d obtained for the selected C_w range confirms that Pt, Pd and Rh behave differently from one another (Table 9). For Pt the K_d is roughly similar for the Malm and Zandvlei samples, the same is true for Rh in the Zandvlei and Tokai samples. This confirms that the K_d is a characteristic of the element more so than of the actual solid matrix. There are differences in the K_d , which distinguish the

elements affinity for the specific solid matrix for which it was calculated. For example: K_d for Pt in the Zandvlei sample is higher than the K_d in the Malm sample (Fig. 9).

Since there are differences between the K_d for the different solid matrices it may be interesting to correlate a value used in the calculation of K_d with sorbent properties such as % clay, SSA- N_2 and % Corg. The K_d was not chosen itself, instead the maximum C_s (in the C_w range considered) was arbitrarily chosen for the correlations as a measure of affinity of that element for the matrix.

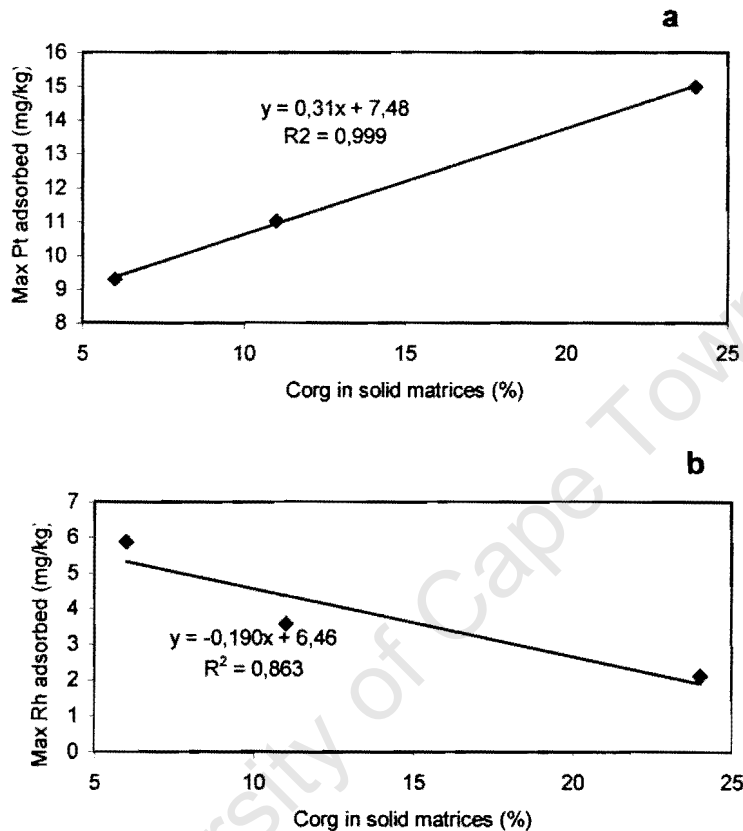


Figure 10 – Correlation between % C_{org} in the solid matrices (Malm, Zandvlei and Tokai) with the maximum (a) Pt and (b) Rh adsorbed concentration (mg/kg).

Although the correlations were obtained with only three data points (three solid matrices) Fig. 10a and b show an interesting directly proportional correlation between the % C_{org} of the solid matrices and the maximum adsorbed Pt in the solid matrices ($R^2=0.9993$) while for Rh the correlation is inversely proportional with $R^2=0.86$. Other sorbent properties such as % clay

and SSA-N₂ did not show a linear correlation with the maximum C_S for Pt and Rh. In addition, there was no correlation between the maximum C_S for Pd and any of the sorbent properties mentioned above.

4.4 Data quality

The present study used ICP-MS as the method of choice to analyse PGE and Au in solution in batch adsorption experiments. The use of ICP-MS has important advantages: a large number of samples of supernatant (more than 50) can be analysed simultaneously for all PGE and Au in less than 12h hours. However, analysis of PGE and Au concentrations in the ng/L range seems to be difficult to reproduce as observed in replicates of PGE and Au background concentrations (Table 12a-f). The present study intended to use PGE and Au concentrations in the ppt range following the same methodology described in section 2.2.1. In order to test the feasibility of using such low concentrations in the interaction with the selected solid matrices a preliminary batch experiment was conducted. Even though it was considered a “failed” experiment a brief description is presented here since the results influenced the PGE and Au concentration range chosen for the following time course and isotherm experiments.

The preliminary batch experiment used Ca-bentonite duplicate subsamples in interaction with several PGE and Au solutions in the ng/L range (50, 100, 500, 1000 ng/l) instead of a single concentration. The procedure was performed as described in section 2.2.1 with exception of the volume sampled and the preservation step: aliquots of 3 ml were sampled from each vial after centrifuging at 5500 r.p.m. for 2 minutes and 15 µl of 5% HNO₃ was immediately added. Due to the large number of samples and to avoid loss of metals from solution, all aliquots sampled before the 6h reaction time were analysed on the same day while the other aliquots were analysed the following day (in a different ICP-MS run). The results obtained showed non reproducible time course PGE and Au concentrations for all the concentrations as well as abnormally higher concentrations (3 to 5 times) than

the ones initially added to the solid matrices (t_0). Although the reagent solution concentrations at t_0 were fairly close to the expected values the solution was not stable since t_{1440} concentrations were also abnormally higher. In order to investigate possible contamination from the Ca-bentonite all solid matrices were analysed for PGE and Au background concentrations. Since there was no evidence of contamination it was concluded that PGE and Au of such low concentration leads to unreliable results. Due to time constraints the above experiment was not repeated. The following experiments used PGE and Au concentrations in the ppb range. Further research using PGE and Au concentrations in the ng/L should use a pre-concentration step for better results.

In the time course experiments only duplicate subsamples of each solid matrix in interaction with the PGE and Au reagent solution were used. Due to procedure and time-related constraints it was not possible to sample the supernatant from each vial simultaneously, resulting in slightly different reaction times between duplicates (see Table 13a-f in Appendix). Therefore, the standard deviation depends mainly on the differences in reaction time between duplicates. This will have influenced directly the sorbate concentration in solution more so than procedure-related errors resulting from centrifuging and pipetting.

5. CONCLUSIONS

Batch experiments using different solid matrices and PGE containing solutions proved to be a useful method to study sorption behaviour of PGE with special emphasis on Pt, Pd and Rh:

- Two different groups of elements could be distinguished in the time course experiments: (1) Elements with inert behaviour (IB) namely Rh, Re, Os, and Ir. These elements were less adsorbed under these experimental conditions than (2) the elements with reactive behaviour (RB), which were found to be Au, Pd, Pt, and Ru.

Adsorption isotherms were obtained for Pt, Pd and Rh from 24-hour batch experiments in the Malm, Zandvlei and Tokai samples:

- The Freundlich adsorption model could be applied to the adsorption data while Langmuir model was not valid.
- A linear fit was applied to the lowest C_w range for Pt, Pd and Rh (only in the Zandvlei sample): higher K_d values were obtained for Pd, clearly differentiating Pd sorption behaviour from that of Pt.

The adsorption experiments performed clearly show that the affinity of Pt, Pd and Rh for the selected matrices follows the sequence: (Pd>Pt)>>>Rh. The high K_d values obtained for Pd and Pt indicates that a strong sorbent-sorbate interaction is probably responsible for Pd and Pt adsorption behaviour. Both elements show a clear preference for organic rich solid matrices (high K_d) while the opposite is true for Rh. Rh erratic behaviour did not allow to calculate specific K_d for most adsorption data but Rh lower reactivity compared to Pt and Pd was confirmed in the adsorption experiments.

This study shows interesting results that add something new to what is known about PGE geochemistry. However, the mechanisms responsible for the observed adsorption behaviour are not clear and merit further investigation. For example it would be interesting to use the PGE of interest (Pt, Pd and Rh) in more batch studies using other solid matrices and over longer time periods in order to confirm the conclusions presented here. Column leaching studies may also add further evidence to the present observations and may confirm some of these findings with a methodology that approximates better the

situation encountered in the natural soil environment. Furthermore, it would be interesting to study Pt, Pd and Rh in the same proportions present in the catalytic converters and separated from the influence of the other PGE in solution.

University of Cape Town

REFERENCES

- Artelt S, Creutzenberg O, Kock H, Levsen K et al. (1999) Bioavailability of fine dispersed platinum as emitted from automotive catalytic converters: a model study. *The Science of the Total Environment* 228:219-242
- Artelt S, Levsen K, Koenig P and Rosner G (2000) Engine tests bench experiments to determine platinum emissions from three-way catalytic converters, *Fresenius Journal of Analytical Chemistry*, 346:693-696
- Azaroual M, Romand B, Freyssinet P and Disnar J-R (2001) Solubility of platinum in aqueous solutions at 25 °C and pH 4 to 10 under oxidising conditions. *Geochimica et Cosmochimica Acta* 65:443-4466
- Begerow J, Dunemann L and Turfeld M (1996) Determination of physiological platinum levels in human urine using magnetic sector field inductively coupled plasma spectrometry in combination with ultraviolet photolysis. *Journal of Analytical Atomic Spectrometry* 11:913-916
- Cabri L (1989) Platinum group elements-Mineralogy Geology Recovery. Canadian Institute for Mining and Metallurgy CIM: 7-22
- Caroli S, Alimonti A, Perucci F, Bocca B et al. (2001) assessment of exposure to platinum group metals in urban children. *Spectrochimica Acta Part B: atomic Spectrometry* 56:1241-1248
- Carter DL, Mortland MM and Kemper WD (1989) Specific surface In: Klute A (ed.) *Methods of soil analysis: part 2, physical and mineralogical methods* 2nd ed. Soil Science Society of America, Madison, Wis. 413-423
- Chadwick OA and Graham RC Pedogenic processes In: Summer ME (ed.) of *soil science* 2nd ed., CRC Press, Boca Raton (Florida) E41-48
- Cotton FA, Wilkinson G, Murillo CA and Bochman M (1999) *Advanced Inorganic Chemistry* 6th ed. John Wiley and Sons, New York 1001-1082
- Cubelic M, Pecoroni R, Schaefer J Eckhart J-D et al. (1997) Verteilung verkehrsbedingter Edelmetallemissionen in Boden UWSF-Z *Umweltchem. Okotox.* 5:249-258

- Dissanayake CB, Kritsotakis K and Tobchall HJ (1984) Enrichment of platinum and associated elements in organic seepage soils of the Tulameen ultramafic complex, southern British Columbia. *Journal of Geochemical Exploration* 54:39-47
- Drever JI (1997) *The geochemistry of natural waters* Prentice Hall, New Jersey 84-99
- Ely JC, Neal CR, Kulpa CF, Schneegurt, et al. (2001) Implications of platinum group elements accumulation along US roads from catalytic-converter attrition. *Environmental Science Technology* 35:3816-3822
- Engineering news (2001) SA beats autocat forecasts. (publisher) in [http://www.southafricaembassy.fi/transport technology.htm](http://www.southafricaembassy.fi/transport%20technology.htm),
- Farago ME, Kavanagh P, Blanks R et al. (1998) Platinum concentrations in urban road dust and soil, and in blood and urine in the United Kingdom. *The Analyst* 123:451-454
- Fetter CW (1999) *Contaminate hydrogeology* 2nd ed. Prentice Hall, New Jersey 120-133
- Fletcher WK, Cook SJ, Hall GEM et al. (1995) Enrichment of platinum and associated elements in organic seepage soils of the Tulameen ultramafic complex, southern British Columbia. *Journal of Geochemical Exploration* 54:39-47
- Fuchs WA and Rose AW (1974) The geochemical behaviour of platinum and palladium in the weathering cycle in the Stillwater Complex, Montana. *Economical Geology* 69:332-346
- Gebel T (2000) Toxicology of platinum, palladium, rhodium and their compounds In: Zeirini F and Alt F (eds.) *Anthropogenic platinum group elements emissions: their impact on man and in the environment*. Springer Verlag 245-255
- Gómez MB, Gómez MM and Palacios MA (2000) Control of interferences in the determination of Pt, Pd and Rh in airborne particulate matter by inductively coupled plasma mass spectrometry. *Analytica Chimica Acta* 404:258-294

- Gómez MB, Gómez MM, Sanchez JL Fernández R et al. (2001) Platinum and rhodium distribution in airborne particulate matter and road dust. *The Science of the Total Environment*, 269: 131-144
- Gubevu JS (1997) A study of the pH dependent charge of a selection of highly weathered humic soils *MSc thesis* University of Cape Town, South Africa
- Heinrich E, Straub G and Kratz KL (1996) Determination of Pt-group elements (PGE) from catalytic converters in soil by docimasy and INAA emissions from three-way catalyst-equipped gasoline engine. *Atmospheric Environment* 5:741-745
- Jones RT (1999) Platinum smelting in South Africa.
<http://www.mintek.ac.za/Pyromet/Platinum/Platinum.htm>,
- Koenig P, Hertel RF, Koch W and Rosner G (1992) Determination of platinum emissions from three-way catalyst-equipped gasoline engine. *Atmospheric Environment* 5:741-745
- Krachler M, Alimonti A, Petrucci F, Irgolic KJ et al. (1998) Analytical problems in the determination of platinum-group metals in urine by quadrupole and magnetic sector field inductively coupled plasma mass spectrometry. *Journal of Analytica Chimica Acta* 363:1-10
- Kucha H and Przybylłowicz W (1999) Noble metals in organic and clay-organic matrices, Kupferschiefer, Poland. *Economic Geology* 94:1137-1162
- Langmuir D (1997) *Aqueous Environmental Geochemistry* Prentice Hall, New Jersey 343-365
- Lustig S, Zang S, Michalke B, Beck W et al. (1998) Platinum speciation with hyphenated techniques: high performance liquid chromatography and capillary electrophoresis on-line coupled to an inductively coupled plasma-mass spectrometer-application to aqueous extracts from platinum treated soil. *Fresenius Journal of Analytical Chemistry* 360:18-25
- Lustig S, Zang S, Michalke B, Schramel P et al. (1996) Transformation behaviour of different platinum compounds in a clay-like humic soil: speciation. *Fresenius Journal of Analytical Chemistry* 188:195-204

- Lustig S, Zang S, Michalke B, Schramel P et al. (1997) Platinum determination in nutrient plants by inductively coupled plasma mass spectrometry with special respect to the hafnium oxide interference. *Fresenius Journal of Analytical Chemistry* 357:1157-1163
- McBride MB (1994) Environmental chemistry of soils. Oxford University Press, New York 110, 143-150, 344-354
- McBride MB (2000) Chemisorption and precipitation reactions. In: Summer ME (ed.) 2nd ed. Handbook of soil science, CRC Press, Boca Raton (Florida) B265-B302
- McDonald I (1998) The need for a common framework for collection and interpretation of data of platinum and palladium geochemistry. *Geostandards Newsletter* 22: 85-91
- McLeod DB (1996) Platinum group metal mines in South Africa. Republic of South Africa Department of Mineral and Energy affairs, Minerals Bureau 1-19
- Messerschmidt J, Alt F, Tolg G, Angerer J et al. (1992) Adsorptive voltametry procedure for the determination of platinum baseline levels in human body fluids. *Fresenius Journal of Analytical Chemistry* 343:391
- Morton O, Puchelt H, Hernández H and Lounejeva E (2001) Traffic-related platinum group elements (PGE) in soils from Mexico City. *Journal of Geochemical Exploration* 72:223-227
- Mountain BW and Wood SA (1998) Chemical controls on the solubility, transport and deposition of platinum and palladium in hydrothermal solutions: a thermodynamic approach. *Economic Geology* 83: 492-510
- Nachtigall D, Artelt S and Wunsh G (1997) Speciation of platinum-chloro complexes and their hydrolysis products by ion chromatography. Determination of platinum oxidation states. *Journal of Chromatography A* 775:197-210
- Nachtigall D, Kock H, Artelt S, Levsen K et al. (1996) Platinum solubility of a substance designed as a model for emissions of automobile catalytic converters. *Fresenius Journal of Analytical Chemistry* 354:742-746

- Nelson DW and Sommers LE (1982) Total carbon, organic carbon and organic matter. In: Page AL, Miller RH and Keemey DR (eds.) *Methods of soil analysis: Part 2 Chemical and microbiological properties* 2nd ed. Am. Soc. Agron. Madison, Wis. 539-577
- Olson CG, Thompson ML and Wilson MA (2000) Phyllosilicates In: Summer ME (ed.) 2nd ed. *Handbook of Soil Science*, CRC Press, Boca Raton (Florida) F77-97
- Palacios MA, Moldovan M and Gomez MM (2000) The automobile catalyst as an important source of PGE in the environment In: Zereini F and Alt F (eds.) *Anthropogenic Platinum group elements emissions: their impact on man and in the environment*. Springer Verlag 3-14
- Plyusmina LP, Kyz'mina TV, Likhoidov GG and Narnov GA (2000) Experimental modelling of platinum sorption on organic matter. *Applied Geochemistry* 15:777-784
- Rhoades JD, 1982 Soluble salts. In: Page AL, Miller RH and Keemey DR (eds.) *Methods of soil analysis Part 2 Chemical and microbiological properties* 2nd ed., Am. Soc. Agron. Madison, Wis. 167-171
- Schaefer J and Puchelt H (1998) Platinum-Group-Metals (PGM) emitted from automobile catalytic converters and their distribution in roadside soils, *Journal of Geochemical Exploration* 64:307-314
- Schaefer J, Hannker D, Eckhardt JD et al. (1998) Uptake of traffic-related heavy metals and platinum group elements (PGE) by plants, *The Science of The Total Environment* 215: 59-67
- Schierl R and Fruhmann G (1996) Airborne platinum concentrations in Munich city buses, *The Science of The Total Environment*, 182:21-23
- Schmidt G, Plame H, Kratz K-L (1997) Highly siderophile elements in impact melts from three European impact craters (Saaksjarvi, Mien and Dellen): clues to the nature of the impacting bodies. *Geochimica Cosmochimica Acta* 61:2977-2983
- Soil Science Society of South Africa (1990) *Handbook of standard soil testing methods for advisory purposes* 3-34

- Sparks DL (1999) Kinetics and mechanisms of chemical reactions at the soil mineral/water interface. In: Sparks DL (ed.) Soil physical chemistry 2nd Ed. CRC Press, Florida 135-157
- Weaver CE, Pollard LD (1973) The chemistry of clay minerals. (Developments in sedimentology 15) Elsevier, Amsterdam
- Wood SA (1990) The interaction of dissolved platinum with fulvic acid and simple organic acid analogues in aqueous solutions. *Canadian Mineralogist* 28: 665-6673
- Wood SA (1996) The role of humic substances in the transport and fixation of metals of economic interest (Au, Pt, Pd, U and V). *Ore Geology News* 11:1-31
- Wood SA, Mountain BW and Fenlon BJ (1989) Thermodynamic constraints on the solubility of platinum and palladium in hydrothermal solutions: reassessment of hydroxide, bisulphide and ammonia complexing. *Economic Geology* 84:2020-2028
- World Health Organisation (WHO) (eds) (1991) International Program of Chemical Safety, Environmental Health Criteria 125, Platinum, Geneva
- Zereini F, Skerstupp B, Alt F, Helmers E et al. (1997) Geochemical behaviour of platinum-group elements (PGE) in particulate emissions by automobile exhaust catalysts: experimental results and environmental investigations. *The Science of the Total Environment* 206:137-146

Appendix

University of Cape Town

Table 10 - Total data (duplicates) from solid matrices characterisation: CEC (Li⁺), LiCl extractable cations, and organic carbon content (%).

Type	Sample ID											
	Kaolin		Ca-Bentonite		Malm	Consol sand		Zandvlei	Tokai			
CEC (mmol _c /kg soil)	26	21	1016	1059	95	99	11	13	328	280	231	233
LiCl ext. cations (mmol _e /kg soil)												
Ca²⁺	19.36	22.37	244.01	243.01	68.30	55.32	7.13	7.20	108.28	118.26	58.71	-
Mg²⁺	4.02	4.10	364.68	364.68	32.40	33.49	0.25	0.27	162.25	163.90	50.34	-
Na⁺	3.82	3.63	37.62	9.01	4.52	3.98	6.63	6.22	298.56	275.94	5.50	-
K⁺	1.88	1.80	8.84	8.67	5.63	5.63	0.07	0.10	10.46	10.45	5.02	-
C org (%)	-	-	-	-	5.3	5.7	-	-	10.9	11.3	22.2	23.1

Table 11 – pH-readings at different electrolyte concentrations for Kaolin, Ca-Bentonite, Consol sand, Malm, Zandvlei, and Tokai samples. Duplicates (D) and triplicates (T) for the 0.01M KCl concentration are presented.

Kaolin						
	Electrolyte concentration					
Acid or base addition ($\mu\text{mol}_c/\text{l}$)	1.0M	0.10M	0.01M	D	T	0.001 M
1000	1.36	1.35	1.39	1.42	1.45	
800	1.41	1.43	1.48	1.44	1.44	1.44
600	1.50	1.55	1.57	1.55	1.57	1.6
400	1.70	1.78	1.77	1.77	1.76	1.78
100	4.26	4.21	4.92	4.56	4.88	4.84
0	6.19	6.69	7.02	7.05	7.15	7.27
100	7.51	7.43	7.38	7.27	8.06	7.99
400	12.12	12.15	12.18	12.27	12.16	12.11
600	12.42	12.49	12.52	12.50	12.51	12.51
Ca-bentonite						
	Electrolyte concentration					
Acid or base addition ($\mu\text{mol}_c/\text{l}$)	1.0M	0.10M	0.01M	D	T	0.001 M
1000	4.85	5.06	5.03	5.13	5.07	5.11
800	5.46	5.32	5.63	5.64	5.63	5.77
600	6.24	5.99	5.94	6.02	5.97	6.02
400	6.04	6.17	6.28	6.22	6.24	6.33
100	6.75	7.02	7.31	7.38	7.39	7.55
0	6.99	7.43	7.9	7.89	7.91	8.39
100	7.4	7.7	8.32	8.38	8.25	9.01
400	8.95	9.04	9.65	9.53	9.57	10.02
600	9.14	8.97	9.88	9.86	9.78	10.36
Consol sand						
	Electrolyte concentration					
Acid or base addition ($\mu\text{mol}_c/\text{l}$)	1.0M	0.10M	0.01M	D	T	0.001 M
1000	1.24	1.35	1.29	1.33		1.29
800	1.31	1.29	1.27	1.31		1.31
600	1.41	1.42	1.43	1.43		1.43
400	1.58	1.58	1.63	1.69		1.57
100	5.32	5.91	5.94	5.61		5.98
0	8.69	8.41	8.77	8.87		7.08
100	10.96	11.01	11.14	11.22		11.2
400	12.27	12.34	12.39	12.42		12.44
600	12.46	12.5	12.54	12.53		12.55

Table 11 (cont.) – pH-readings at different electrolyte concentrations for Kaolin, Ca-Bentonite, Consol sand, Malm, Zandvlei, and Tokai samples. Duplicates and triplicates for the 0.01M KCl concentration are presented.

Malm		Electrolyte concentration				
Acid or base addition ($\mu\text{mol/l}$)	1.0M	0.10M	0.01M	D	T	0.001 M
1000	1.81	1.84	1.88	1.83	1.87	1.83
800	2.03	2.04	2.08	2.10	2.12	2.05
600	2.34	2.32	2.37	2.37	2.36	2.37
400	2.85	3.90	3.03	2.98	3.10	3.25
100	5.02	5.44	5.45	5.24	5.34	5.64
0	5.51	6.08	6.16	6.22	6.13	6.37
100	5.84	6.29	6.21	6.53	6.45	6.86
400	8.30	8.70	9.22	9.35	9.30	9.65
600	9.31	9.76	10.31	10.40	10.26	10.55

Zandvlei		Electrolyte concentration				
Acid or base addition ($\mu\text{mol/l}$)	1.0M	0.10M	0.01M	D	T	0.001M
1000	6.27	6.25	6.26	6.27	6.27	6.29
800	6.34	6.41	6.39	6.38	6.38	6.41
600	6.43	6.47	6.52	6.50	6.49	6.50
400	6.54	6.64	6.66	6.69	6.65	6.68
100	6.99	7.10	7.26	7.21	7.20	7.27
0	7.21	7.23	7.27	7.31	7.33	7.32
100	7.15	7.14	7.48	7.44	7.41	7.46
400	8.30	8.47	8.79	8.74	8.68	8.59
600	8.74	9.04	9.11	9.18	9.05	9.08

Tokai		Electrolyte concentration				
Acid or base addition ($\mu\text{mol/l}$)	1.0M	0.10M	0.01M	D	0.001 M	
1000	1.99	2.15	1.88	1.87	1.87	
800	2.35	2.33	1.98	2.08	4.81	
600	2.48	2.65	2.33	2.50	2.78	
400	2.95	3.21	3.07	3.07	3.09	
100	3.78	4.15	4.70	4.50	3.77	
0	3.94	4.24	4.95	4.55	5.18	
100	4.06	4.42	5.11	4.90	6.08	
400	4.96	5.67	6.32	5.99	6.46	
600	5.40	6.10	6.32	6.55	7.23	

Sorption of the Platinum group elements in selected solid matrices - Appendix

Table 12 - Total PGE and Au concentrations ($\mu\text{g}/\text{kg}$) in the solid matrices acid digestion leachates determined by ICP-MS: Kaolin (single subsample), Ca-bentonite (single subsample), Consol sand (single subsample), Malm (triplicate subsamples), Zandvlei (duplicate subsamples), and Tokai (duplicate subsamples) solid matrices. Triplicate runs in ICP-MS (1, 2, and 3)

	Kaolin			Ca-Bentonite			Consol sand			Malm					
Element	1	2	3	1	2	3	1	2	3	1	2	3	1	2	3
Ru	bdl	bdl	bdl	0.0750	bdl	bdl	0.0042	0.0046	bdl	0.0364	bdl	bdl	bdl	bdl	bdl
Rh	0.0079	0.0095	0.0082	0.0091	0.0062	0.0097	0.0012	0.0012	0.0010	0.0055	0.0049	0.0049	0.0060	0.0072	0.0063
Pd	bdl	bdl	bdl	bdl	bdl	bdl	bdl	bdl	bdl	bdl	bdl	bdl	bdl	bdl	bdl
Re	bdl	bdl	0.0046	bdl	bdl	0.0010	bdl	bdl	0.0002	bdl	0.0016	0.0020	bdl	bdl	0.0018
Os	0.7472	0.7068	0.7493	0.7472	1.1546	1.2027	0.1037	0.0956	0.1024	0.3672	0.3335	0.3481	0.2868	0.2234	0.2529
Ir	0.0380	0.0274	0.0338	0.0380	0.0300	0.0293	0.0036	0.0029	0.0028	0.0271	0.0206	0.0254	0.0217	0.0158	0.0210
Pt	0.0069	0.0038	bdl	0.0069	bdl	0.0115	0.0028	0.0017	0.0015	bdl	0.0064	bdl	0.0088	0.0027	bdl
Au	0.0343	0.0408	0.0653	0.0343	0.0675	0.0821	0.0052	0.0090	0.0088	0.0391	0.0324	0.0616	0.0220	0.0256	0.0486
	Malm(cont.)			Zandvlei						Tokai					
Element	1	2	3	1	2	3	1	2	3	1	2	3	1	2	3
Ru	bdl	bdl	bdl	0.0188	0.0187	0.0113	0.0238	0.0263	0.0132	bdl	0.0008	0.0022	bdl	bdl	0.0016
Rh	0.0066	0.0030	0.0052	0.0114	0.0120	0.0113	0.0117	0.0105	0.0103	0.1094	0.0321	0.1713	0.0946	0.0284	0.2152
Pd	bdl	bdl	bdl	0.0051	0.0117	bdl	0.0438	0.0377	bdl	0.0060	0.0015	0.0037	0.0070	0.0025	0.0077
Re	bdl	bdl	0.0010	bdl	bdl	0.0018	bdl	bdl	0.0022	0.0106	0.0021	0.0080	0.0039	0.0026	0.0081
Os	0.2292	0.1680	0.1782	0.1761	0.1057	0.1784	0.1381	0.0779	0.1559	0.0170	0.0078	0.0914	0.0152	0.0053	0.0838
Ir	0.0177	0.0193	0.0206	0.0101	0.0087	0.0083	0.0104	0.0068	0.0046	bdl	0.0008	0.0022	bdl	bdl	0.0016
Pt	0.0049	bdl	0.0081	0.0083	0.0011	0.0028	0.0075	bdl	bdl	0.1094	0.0321	0.1713	0.0946	0.0284	0.2152
Au	0.0170	0.0147	0.0409	0.0092	0.0032	0.0549	0.0048	bdl	0.0260	0.0060	0.0015	0.0037	0.0070	0.0025	0.0077

Table 13a - PGE and Au background concentrations (ng/L) in the Kaolin subsamples supernatant in the time course adsorption experiments. Solid matrix/ MQ water ratio: 3 g: 50 ml.

Element	t ₃₅	t ₇₅	t ₁₀₅	t ₁₆₁	t ₂₂₆
Ru	bdl	15.00	bdl	bdl	107.03
Rh	bdl	2.86	bdl	bdl	43.48
Pd	bdl	bdl	bdl	bdl	29.35
Re	bdl	51.20	bdl	48.52	10.21
Os	1995.33	bdl	2683.44	bdl	737.62
Ir	bdl	4.92	bdl	bdl	532.16
Pt	bdl	27.63	bdl	10.49	bdl
Au	bdl	50.87	bdl	bdl	37.36

Element	t ₂₂₆	t ₂₈₅	t ₄₀₄	t ₇₆₅	t ₁₄₅₃
Ru	bdl	bdl	bdl	6.11	28.46
Rh	bdl	bdl	1.21	2.53	0.42
Pd	5.60	31.91	17.72	bdl	bdl
Re	0.58	17.95	bdl	bdl	bdl
Os	bdl	bdl	bdl	bdl	bdl
Ir	3.50	bdl	bdl	3.98	bdl
Pt	bdl	bdl	bdl	bdl	3.69
Au	32.61	43.62	29.64	90.27	46.67

Table 13b - PGE and Au background concentrations (ng/L) in the Ca-bentonite subsamples supernatant in the time course adsorption experiments. Solid matrix/ MQ water ratio: 3 g: 50 ml.

Element	t ₂₇	t ₇₃	t ₁₀₀	t ₁₆₆	t ₂₂₆
Ru	bdl	bdl	bdl	16.93	6.36
Rh	bdl	3.42	bdl	1.39	11.44
Pd	bdl	bdl	bdl	bdl	5.44
Re	bdl	50.73	bdl	34.81	bdl
Os	3716.37	bdl	4775.50	bdl	2373.37
Ir	bdl	8.39	bdl	1.59	10.66
Pt	bdl	2.91	bdl	14.96	bdl
Au	bdl	22.16	bdl	bdl	bdl

Element	t ₂₂₆	t ₂₈₂	t ₄₀₀	t ₇₆₂	t ₁₄₅₁
Ru	bdl	bdl	bdl	bdl	169.62
Rh	5.53	7.91	7.93	30.07	23.55
Pd	bdl	bdl	bdl	bdl	18.29
Re	bdl	22.09	bdl	11.08	bdl
Os	bdl	bdl	bdl	bdl	1527.55
Ir	12.45	13.28	14.00	31.91	20.99
Pt	bdl	bdl	bdl	bdl	26.88
Au	28.21	68.36	15.35	101.37	26.68

Note: bdl (below detection limit)

Table 13c - PGE and Au background concentrations (ng/L) in the Consol sand subsamples supernatant in the time course adsorption experiments. Solid matrix/ MQ water ratio: 3 g: 50 ml.

Element	t ₄₀		t ₇₅		t ₁₀₅		t ₁₇₃		t ₂₂₇
Ru	bdl	40.43	bdl	bdl	30.37	12.23	9.05	bdl	126.18
Rh	bdl	6.76	bdl	4.38	bdl	3.24	bdl	bdl	bdl
Pd	bdl	8.14	bdl	21.50	12.87	35.44	bdl	bdl	28.78
Re	bdl	48.25	bdl	25.62	bdl	bdl	13.33	bdl	11.66
Os	9334.97	bdl	10378.20	bdl	7618.05	6074.80	bdl	bdl	517.30
Ir	bdl	19.62	bdl	bdl	bdl	bdl	4.20	4.94	bdl
Pt	bdl	11.75	bdl	8.36	bdl	bdl	5.42	bdl	bdl
Au	bdl	103.72	bdl	12.39	4.19	17.78	55.95	76.89	bdl
Element	t ₂₂₇	t ₂₈₄		t ₄₀₂		t ₇₆₄		t ₁₄₅₂	
Ru	bdl	bdl	bdl	21.70	136.10	bdl	bdl	5.57	bdl
Rh	2.99	4.11	4.43	116.48	111.10	6.44	1.87	bdl	8.12
Pd	bdl	33.91	61.96	30.91	26.92	20.81	13.79	27.29	1.11
Re	bdl	bdl	7.68	113.80	93.73	bdl	bdl	bdl	bdl
Os	102.48	bdl	bdl	1179.12	1221.05	5546.00	5134.46	1386.98	1111.75
Ir	4.04	2.78	0.59	23.28	19.67	5.27	bdl	bdl	bdl
Pt	3.86	bdl	bdl	99.73	94.17	13.75	bdl	bdl	18.32
Au	43.50	46.56	17.04	40.66	38.02	9.20	bdl	41.30	20.42

Table 13d - PGE and Au background concentrations (ng/L) in the Malm subsamples supernatant in the time course adsorption experiments. Solid matrix/ MQ water ratio: 3 g: 50 ml.

Element	t ₃₅		t ₇₅		t ₁₀₅		t ₁₈₁		t ₂₂₆
Ru	bdl	221.52	146.94	14.36	68.50	bdl	132.69	509.84	bdl
Rh	5.27	2.83	8.80	5.25	9.09	10.89	bdl	bdl	bdl
Pd	62.37	73.59	119.00	146.74	bdl	0.22	bdl	bdl	bdl
Re	bdl	28.98	bdl	38.94	bdl	bdl	bdl	bdl	3.24
Os	8237.88	bdl	1710.42	bdl	2597.82	1969.34	bdl	bdl	bdl
Ir	15.56	3.66	7.88	bdl	2.19	0.83	bdl	0.37	2.87
Pt	1.77	bdl	18.84	14.75	16.31	5.74	0.61	bdl	17.73
Au	118.90	164.69	208.00	493.91	83.28	95.46	75.39	196.97	8.22
Element	t ₂₂₆	t ₂₈₅		t ₄₀₄		t ₇₈₅		t ₁₄₅₃	
Ru	128.02	302.71	bdl	203.59	303.60	bdl	bdl	123.13	260.52
Rh	7.12	bdl	bdl	8.28	1.73	9.78	3.92	11.62	2.86
Pd	bdl	bdl	bdl	bdl	bdl	bdl	bdl	bdl	bdl
Re	bdl	0.27	bdl	11.94	2.84	3.98	3.95	2.27	3.86
Os	bdl	bdl	bdl	139.47	bdl	918.28	595.24	990.50	499.73
Ir	0.88	1.76	bdl	11.46	6.24	1.49	0.38	18.05	bdl
Pt	4.42	bdl	bdl	bdl	bdl	16.81	bdl	2.67	bdl
Au	14.46	40.53	16.48	11.63	21.61	11.40	43.02	27.29	63.72

Note: bdl (below detection limit)

Table 13e - PGE and Au background concentrations (ng/L) in the Zandvlei subsamples supernatant in the time course adsorption experiments. Solid matrix/ MQ water ratio: 3 g: 50 ml.

Element	t ₃₅	t ₇₅	t ₁₀₅	t ₁₈₁	t ₂₂₆
Ru	31.47	8.66	146.94	14.36	136.03
Rh	5.23	4.45	8.80	5.25	10.04
Pd	119.63	272.59	119.00	146.74	81.67
Re	bdl	24.28	bdl	38.94	7.23
Os	3560.21	bdl	1710.42	bdl	976.71
Ir	8.46	bdl	7.88	bdl	bdl
Pt	1.57	bdl	18.84	14.75	6.25
Au	378.14	1911.06	208.00	493.91	237.76

Element	t ₂₂₆	t ₂₈₅	t ₄₀₄	t ₇₈₅	t ₁₄₅₃
Ru	75.93	97.10	805.99	103.90	372.87
Rh	5.47	4.20	2.66	6.56	3.66
Pd	89.04	156.13	145.71	136.63	124.23
Re	bdl	7.81	2.59	2.59	bdl
Os	bdl	bdl	bdl	bdl	bdl
Ir	bdl	bdl	bdl	bdl	bdl
Pt	bdl	bdl	bdl	bdl	bdl
Au	378.42	320.50	524.32	211.28	326.18

Table 13f - PGE and Au background concentrations (ng/L) in the Tokai subsamples supernatant in the time course adsorption experiments. Solid matrix/ MQ water ratio: 3 g: 50 ml.

Element	t ₃₅	t ₇₅	t ₁₀₅	t ₁₈₁	t ₂₂₆
Ru	66.77	bdl	226.13	bdl	33.60
Rh	0.84	bdl	2.34	bdl	3.38
Pd	5.50	bdl	14.61	bdl	5.98
Re	bdl	23.59	bdl	36.14	bdl
Os	2122.80	bdl	1087.53	bdl	326.23
Ir	7.71	bdl	4.42	bdl	bdl
Pt	bdl	bdl	15.59	bdl	bdl
Au	40.24	bdl	36.80	bdl	22.59

Element	t ₄₀₄	t ₇₈₅	t ₁₄₅₃
Ru	220.56	286.63	8.82
Rh	3.06	bdl	bdl
Pd	bdl	bdl	bdl
Re	bdl	8.01	bdl
Os	bdl	bdl	bdl
Ir	bdl	bdl	bdl
Pt	bdl	bdl	bdl
Au	5.85	bdl	bdl

Note: bdl (below detection limit)

Table 14a – Average PGE and Au concentrations ($\mu\text{g/l}$) and pH readings and respective standard deviation between duplicate for the Kaolin subsamples supernatant at specific time sampling points (t_i) in the time course experiments.

Element	t_{37}	t_{74}	t_{106}	t_{166}	t_{225}	t_{284}	t_{402}	t_{764}	t_{1451}
Ru	32.67 \pm 1.82	30.92 \pm 0.31	31.64 \pm 0.64	32.25 \pm 0.96	33.12 \pm 1.06	33.52 \pm 1.50	34.71 \pm 0.12	34.97 \pm 1.09	33.92 \pm 0.25
Rh	97.09 \pm 1.63	97.16 \pm 2.07	99.70 \pm 3.00	102.91 \pm 0.80	105.94 \pm 1.61	109.13 \pm 5.21	112.20 \pm 0.22	115.17 \pm 1.57	113.33 \pm 0.04
Pd	95.52 \pm 3.70	86.55 \pm 5.06	80.30 \pm 1.56	72.23 \pm 4.71	69.23 \pm 4.63	67.45 \pm 3.27	61.22 \pm 3.65	46.32 \pm 0.83	33.63 \pm 0.19
Re	115.80 \pm 2.43	113.67 \pm 1.60	114.72 \pm 2.93	112.91 \pm 0.69	115.52 \pm 0.39	117.85 \pm 2.91	117.68 \pm 2.07	118.51 \pm 0.28	115.68 \pm 0.45
Os	98.39 \pm 0.20	96.50 \pm 1.40	96.24 \pm 1.96	92.83 \pm 0.94	94.15 \pm 0.44	97.59 \pm 5.04	96.38 \pm 0.84	95.29 \pm 2.44	92.16 \pm 0.45
Ir	6.09 \pm bdl	6.61 \pm 0.31	7.32 \pm 0.36	8.07 \pm 0.53	9.24 \pm 0.74	10.43 \pm 1.21	12.95 \pm 0.14	24.16 \pm 0.84	31.25 \pm 0.38
Pt	95.58 \pm 3.31	94.65 \pm 1.02	95.07 \pm 2.40	93.83 \pm 0.82	95.29 \pm 0.44	96.97 \pm 1.86	97.63 \pm 1.56	97.19 \pm 0.69	95.62 \pm 1.07
Au	48.86 \pm 2.00	27.09 \pm 28.03	2.57 \pm 2.73	0.40 \pm 0.02	0.33 \pm bdl	0.26 \pm 0.01	0.22 \pm 0.05	0.22 \pm 0.06	0.08 \pm 0.01
pH	2.71 \pm 0.01	2.73 \pm 0.01	2.84 \pm 0.01	2.86 \pm 0.0	2.86 \pm bdl	2.92 \pm 0.01	3.02 \pm bdl	3.15 \pm 0.04	2.67 \pm 0.04

Table 14b – Average PGE and Au concentrations ($\mu\text{g/l}$) and pH readings and respective standard deviation between duplicate for the Ca-bentonite subsamples supernatant at specific time sampling points (t_i) in the time course experiments.

Element	t_{32}	t_{73}	t_{100}	t_{168}	t_{225}	t_{282}	t_{400}	t_{762}	t_{1451}
Ru	27.41 \pm 0.05	25.59 \pm 0.15	24.61 \pm 0.47	20.69 \pm 0.62	17.53 \pm 6.48	14.58 \pm 0.10	10.96 \pm 0.24	4.36 \pm 0.10	2.74 \pm 0.11
Rh	109.00 \pm 0.53	104.20 \pm 1.28	103.55 \pm 1.61	94.00 \pm 0.42	88.83 \pm 32.26	83.05 \pm 0.31	76.48 \pm 0.49	57.53 \pm 0.64	40.84 \pm 1.51
Pd	1.76 \pm 0.01	2.03 \pm 0.04	2.18 \pm 0.03	2.14 \pm 0.14	2.18 \pm 0.68	1.52 \pm 0.20	2.38 \pm 0.26	2.16 \pm 0.11	2.12 \pm 0.03
Re	118.44 \pm 1.31	117.12 \pm 0.06	122.36 \pm 1.46	118.08 \pm 0.16	120.14 \pm 43.25	120.41 \pm 0.76	121.37 \pm 1.09	120.10 \pm 1.73	118.17 \pm 1.30
Os	98.66 \pm 1.27	80.53 \pm 0.76	78.85 \pm 0.60	74.06 \pm 0.86	70.32 \pm 25.38	70.54 \pm 0.58	73.14 \pm 0.27	65.55 \pm 0.65	63.31 \pm 2.55
Ir	115.71 \pm 0.76	114.71 \pm 1.13	119.27 \pm 2.28	112.48 \pm 0.51	114.74 \pm 40.55	116.88 \pm 0.79	117.60 \pm 0.04	115.70 \pm 1.42	113.74 \pm 1.81
Pt	85.52 \pm 1.02	78.30 \pm 1.16	78.43 \pm 2.01	70.63 \pm 0.45	68.34 \pm 25.02	61.97 \pm 0.23	61.22 \pm 0.10	51.24 \pm 0.28	42.16 \pm 0.55
Au	9.84 \pm 0.13	8.00 \pm 0.59	7.34 \pm 0.23	5.82 \pm 0.19	4.92 \pm 1.72	4.52 \pm 0.71	3.78 \pm 0.70	1.81 \pm 0.80	1.07 \pm 0.41
pH	6.41 \pm 0.01	6.42 \pm 0.01	6.47 \pm 0.01	6.77 \pm 0.04	6.90 \pm 0.06	6.84 \pm 0.06	7.17 \pm 0.11	7.10 \pm 0.18	6.44 \pm 0.56

Table 14c – Average PGE and Au concentrations ($\mu\text{g/l}$) and pH readings and respective standard deviation between duplicate for the Consol sand subsamples supernatant at specific time sampling points (t_i) in the time course experiments.

Element	t_{38}	t_{73}	t_{101}	t_{168}	t_{225}	t_{282}	t_{400}	t_{762}	t_{1450}
Ru	97.75±0.75	90.56±2.24	81.25±1.64	71.23±0.58	65.58±0.27	58.55±0.76	53.10±2.40	42.26±0.80	39.1±0.81
Rh	110.72±7.05	112.95±1.12	115.14±0.67	113.81±1.56	115.76±2.27	113.85±1.12	115.4±0.66	114.62±0.46	116.32±0.63
Pd	72.82±8.80	57.76±3.41	43.91±2.61	30.95±0.76	23.84±1.26	19.26±0.50	16.31±0.10	13.18±0.49	12.99±0.26
Re	112.68±7.20	115.49±1.99	117.32±0.64	115.60±1.78	117.60±1.49	117.48±1.80	119.36±0.41	118.37±0.06	120.32±0.93
Os	109.34±11.35	112.02±4.52	113.63±2.72	111.60±6.51	109.20±3.05	111.59±6.09	110.60±2.06	92.30±1.44	95.38±2.99
Ir	108.48±6.58	110.80±1.22	113.04±0.71	110.61±1.54	113.45±2.72	114.31±1.04	113.90±0.37	114.82±0.57	116.25±1.15
Pt	109.93±6.38	112.38±0.67	114.46±1.20	112.50±2.28	114.49±1.75	113.76±1.43	114.24±0.05	106.39±2.58	95.96±4.88
Au	38.24±1.51	28.87±2.71	12.26±4.76	7.74±1.57	13.87±4.70	13.50±8.63	13.05±1.71	16.25±1.76	18.45±0.87
pH	2.66±0.02	2.75±0.07	3.08±0.09	3.35±0.13	3.56±0.13	4.33±0.36	4.36±1.92	6.14±0.56	2.61±0.01

Table 14d – Average PGE and Au concentrations ($\mu\text{g/l}$) and pH readings and respective standard deviation between duplicate for the Malm subsamples supernatant at specific time sampling points (t_i) in the time course experiments.

Element	$t_{29\pm 2}$	$t_{60\pm 2}$	$t_{90\pm 2}$	$t_{155\pm 1}$	$t_{204\pm 1}$	$t_{268\pm 2}$	$t_{363\pm 0}$	$t_{701\pm 1}$	$t_{1364\pm 1}$
Ru	35.3±5.40	30.83±0.89	30.36±0.70	29.17±1.89	29.27±1.69	29.1±0.34	29.69±0.37	28.62±0.56	28.09±9.62
Rh	116.98±10.98	111.88±0.30	111.64±1.07	110.30±4.17	109.77±5.12	110.73±1.27	113.92±3.17	111.40±1.35	111.03±39.02
Pd	5.34±1.24	4.73±0.74	4.58±0.23	3.85±0.57	4.00±0.59	3.62±0.26	3.49±0.21	3.60±0.01	3.02±0.70
Re	118.34±11.86	113.6±0.73	113.89±0.52	112.93±4.87	113.33±4.45	113.44±1.97	118.83±3.90	115.36±0.12	113.19±39.99
Os	81.56±9.35	77.91±0.73	77.58±1.18	76.04±3.03	76.23±3.37	77.13±1.93	81.11±1.16	77.50±1.29	78.27±27.49
Ir	92.57±7.99	91.77±0.65	94.25±1.86	93.84±3.53	95.02±4.84	97.10±2.13	103.67±3.08	102.97±0.49	103.45±36.10
Pt	103.43±10.15	96.38±0.24	93.05±0.71	87.34±4.08	84.27±5.27	79.23±3.17	74.87±0.73	54.31±2.28	42.61±14.32
Au	1.4±0.07	1.7±0.21	2.04±0.19	1.62±0.02	2.02±0.22	1.71±0.16	1.71±0.20	2.16±0.21	1.74±0.35
pH	4.54±0.18	4.65±0.22	4.79±0.11	4.81±0.09	4.80±0.23	4.97±0.16	4.82±0.05	4.88±0.13	4.41±0.09

Table 14e – Average PGE and Au concentrations ($\mu\text{g/l}$) and pH readings and respective standard deviation between duplicate for the Zandvlei subsamples supernatant at specific time sampling points (t_i) in the time course experiments.

Element	$t_{29\pm0}$	$t_{60\pm0}$	$t_{89\pm0}$	$t_{153\pm1}$	$t_{202\pm0}$	$t_{267\pm0}$	$t_{360\pm0}$	$t_{703\pm0}$	$t_{1360\pm0}$
Ru	31.99 \pm 0.48	29.26 \pm 0.65	28.35 \pm 0.01	23.94 \pm 0.42	22.12 \pm 0.65	19.29 \pm 0.09	14.29 \pm 0.76	7.82 \pm 0.19	5.16 \pm 0.17
Rh	108.42 \pm 1.61	105.62 \pm 0.42	103.93 \pm 1.16	95.83 \pm 1.31	91.95 \pm 3.32	88.17 \pm 2.11	77.31 \pm 2.81	59.78 \pm 1.30	48.29 \pm 0.29
Pd	8.92 \pm 3.62	8.06 \pm 2.43	7.58 \pm 2.40	6.07 \pm 1.28	5.70 \pm 1.04	5.24 \pm 0.46	4.51 \pm 0.06	4.43 \pm 0.37	4.06 \pm 0.51
Re	114.39 \pm 3.32	114.65 \pm 0.23	114.83 \pm 1.20	112.38 \pm 2.60	113.90 \pm 3.92	116.67 \pm 1.73	115.27 \pm 1.88	114.72 \pm 3.12	114.48 \pm 1.40
Os	94.39 \pm 1.10	90.29 \pm 2.37	83.68 \pm 4.69	69.01 \pm 1.84	52.77 \pm 2.78	41.31 \pm 2.04	23.83 \pm 1.02	14.02 \pm 0.42	13.57 \pm 0.01
Ir	110.99 \pm 1.77	109.51 \pm 0.15	109.66 \pm 1.59	106.96 \pm 2.33	108.54 \pm 4.15	110.30 \pm 1.34	110.66 \pm 2.84	110.85 \pm 2.17	111.92 \pm 0.91
Pt	76.40 \pm 2.08	63.56 \pm 0.76	56.12 \pm 2.45	42.35 \pm 3.09	35.52 \pm 5.22	29.45 \pm 6.63	22.55 \pm 6.17	17.05 \pm 7.19	16.00 \pm 6.95
Au	23.88 \pm 0.33	20.15 \pm 0.14	16.55 \pm 0.85	10.15 \pm 0.90	7.98 \pm 0.36	6.36 \pm 0.19	5.55 \pm 0.29	4.90 \pm 1.30	3.09 \pm 0.01
pH	6.59 \pm 0.06	6.6 \pm 0.01	6.72 \pm 0.11	6.84 \pm 0.06	6.73 \pm 0.01	6.94 \pm 0.14	6.74 \pm 0.13	6.76 \pm 0.03	6.41 \pm 0.08

Table 14f – Average PGE and Au concentrations ($\mu\text{g/l}$) and pH readings and respective standard deviation between duplicate for the Tokai subsamples supernatant at specific time sampling points (t_i) in the time course experiments.

Element	$t_{27\pm1}$	$t_{5\pm2}$	$t_{88\pm3}$	$t_{156\pm6}$	$t_{201\pm1}$	$t_{267\pm2}$	$t_{365\pm5}$	$t_{703\pm3}$	$t_{1359\pm2}$
Ru	42.66 \pm 5.63	37.73 \pm 1.22	36.74 \pm 0.45	34.92 \pm 0.33	33.94 \pm 0.34	34.24 \pm 0.80	33.61 \pm 0.51	32.19 \pm 0.32	31.94 \pm 0.02
Rh	107.55 \pm 21.70	110.35 \pm 1.86	111.11 \pm 0.49	111.78 \pm 2.52	109.29 \pm 4.02	112.21 \pm 0.64	111.26 \pm 0.66	108.67 \pm 4.88	109.53 \pm 1.34
Pd	6.62 \pm 1.44	6.50 \pm 0.07	6.35 \pm 0.10	6.31 \pm 0.56	5.94 \pm 0.79	6.17 \pm 0.27	5.86 \pm 0.27	6.89 \pm 0.78	7.78 \pm 1.33
Re	106.52 \pm 20.54	110.12 \pm 0.37	110.20 \pm 0.68	111.83 \pm 2.00	110.25 \pm 4.32	112.22 \pm 1.32	113.36 \pm 0.24	109.33 \pm 4.39	110.40 \pm 0.37
Os	78.85 \pm 18.49	82.77 \pm 0.65	81.44 \pm 0.80	79.86 \pm 2.43	76.29 \pm 5.89	77.43 \pm 0.76	75.28 \pm 1.10	71.45 \pm 3.55	78.23 \pm 2.77
Ir	90.50 \pm 18.86	92.99 \pm 1.47	92.21 \pm 2.51	92.77 \pm 2.95	91.83 \pm 5.06	93.16 \pm 1.45	96.48 \pm 1.65	96.80 \pm 5.87	99.64 \pm 3.18
Pt	86.75 \pm 16.47	80.77 \pm 0.98	72.65 \pm 0.98	57.38 \pm 0.01	49.16 \pm 1.60	40.04 \pm 3.11	28.17 \pm 2.51	12.39 \pm 1.85	7.69 \pm 1.18
Au	5.41 \pm 1.80	6.19 \pm 0.48	6.29 \pm 0.90	6.72 \pm 0.61	6.72 \pm 1.03	7.29 \pm 0.47	8.00 \pm 1.13	8.45 \pm 1.51	9.42 \pm 2.26
pH	4.27 \pm 0.22	4.30 \pm 0.13	4.30 \pm 0.17	4.41 \pm 0.01	4.32 \pm 0.06	4.60 \pm 0.14	4.21 \pm 0.07	4.25 \pm 0.12	4.21 \pm 0.13

Table 15 – PGE and Au concentration ($\mu\text{g/l}$) in the reagent solution at the beginning (t_0) and end (after 1440 minutes) of the time course experiments: (A) using the Kaolin, Ca-bentonite, and Consol sand and (B) using the Malm, Zandvlei and Tokai samples. ICP-MS replicates of duplicate aliquots: upper/lower panel.

A					B			
Element	t_0	t_0	t_{1440}	t_{1440}	t_0	t_0	t_{1440}	t_{1440}
Ru	125.96	127.94	115.11	112.86	110.21	112.40	113.96	114.04
Rh	129.35	129.37	117.29	115.41	112.51	114.28	116.25	114.95
Pd	126.51	126.66	113.33	112.10	108.77	109.82	113.09	112.22
Re	131.24	128.81	116.12	120.09	113.43	113.66	117.34	115.72
Os	123.15	125.27	112.15	104.35	115.94	113.08	123.08	115.54
Ir	125.82	128.20	114.93	114.88	112.80	110.82	116.47	114.76
Pt	128.15	130.20	115.06	115.59	112.79	113.34	118.48	116.14
Au	80.63	88.37	73.07	57.10	67.38	67.18	91.54	86.35
Element	t_0	t_0	t_{1440}	t_{1440}	t_0	t_0	t_{1440}	t_{1440}
Ru	116.85	115.12	116.93	114.21	113.90	112.94	110.33	114.31
Rh	118.71	115.31	119.13	114.65	115.10	113.79	115.16	115.84
Pd	116.41	113.56	115.11	113.61	110.03	110.73	114.15	113.32
Re	118.43	116.44	118.98	116.98	114.65	111.23	118.86	115.55
Os	121.48	118.56	119.61	111.09	123.64	119.15	135.63	125.55
Ir	116.58	114.64	117.48	115.21	112.88	110.28	116.92	114.17
Pt	117.41	115.26	116.61	116.93	114.80	110.20	118.72	117.47
Au	64.77	67.38	75.02	66.96	62.40	62.24	95.30	94.02

Table 16 – Masses (mg) of each solid matrices used in the adsorption isotherm experiments for the respective reagent solution concentration (A. B. C. D. E. F. G. H).

Reagent solution	Sample ID					
	Malm		Zandvlei		Tokai	
A	1.497	1.395	1.484	1.499	1.392	1.447
B	1.475	1.494	1.503	1.483	1.465	1.542
C	1.516	1.493	1.454	1.506	1.480	1.947
D	1.476	1.483	1.502	1.494	1.494	1.477
E	1.498	1.506	1.485	1.493	1.498	1.455
F	1.499	1.495	1.495	1.496	1.511	1.564
G	1.505	1.488	1.507	1.487	1.434	1.551
H	1.503	1.503	1.503	1.497	1.524	1.507

Table 17 – PGE and Au concentration ($\mu\text{g/l}$) of the respective reagent solution: A, B, C, D, E, F, G, and H used in the adsorption isotherm experiments. ICP-MS replicates of single aliquots: upper/lower panel.

Reagent solution								
Element	A	B	C	D	E	F	G	H
Ru	42.45	95.16	142.90	433.35	926.41	1437.76	3022.44	5027.73
Rh	47.01	95.33	142.24	436.10	923.85	1446.86	3068.98	4502.74
Pd	46.46	94.38	138.01	437.73	900.17	1387.70	2996.44	4858.26
Re	48.31	97.90	146.52	447.72	933.88	1459.02	3147.60	4775.02
Os	106.29	119.25	113.69	643.66	1290.73	1745.98	4331.03	7673.03
Ir	47.12	92.98	139.69	424.42	918.71	1432.63	3063.55	4672.55
Pt	47.76	95.02	139.60	434.47	921.97	1445.48	3022.65	4988.87
Au	28.13	68.17	76.29	414.40	913.18	789.63	3197.49	5276.91
Element	A	B	C	D	E	F	G	H
Ru	43.26	94.05	140.33	439.56	914.18	1412.83	3010.72	4808.93
Rh	47.89	95.81	139.60	447.25	932.62	1435.24	3062.73	4435.65
Pd	47.49	95.06	139.84	445.75	897.32	1388.34	3028.32	4888.70
Re	47.75	97.01	143.39	452.10	939.71	1434.94	3085.25	4660.24
Os	82.35	86.27	72.97	558.90	1352.73	1823.21	4909.29	7895.10
Ir	47.68	95.89	140.22	439.99	932.82	1446.67	3146.16	4648.96
Pt	47.93	96.93	143.69	443.65	933.60	1431.97	3073.68	4948.81
Au	26.17	60.87	72.37	427.72	929.44	630.43	3238.36	5360.78

Table 18a – PGE and Au equilibrium concentration ($\mu\text{g/l}$) and standard deviations from ICP-MS replicate analysis, after interaction of the Zandvlei sample with the respective reagent solution (A, B, C, D, E, F, G, and H) in the adsorption isotherm experiments. Duplicate aliquots: upper/lower panel.

Element	Reagent solution							
	A	B	C	D	E	F	G	H
Ru	8,46±1.33	25,47±1.00	40,36±0.07	219,06±0.09	576,81±6.37	960,96±1.72	2589,75±9.41	4143,40±23.48
Rh	38,50±0.06	94,81±0.82	139,42±1.47	440,97±1.99	816,53±4.08	1229,70±5.99	2816,33±94.75	3903,30±25.23
Pd	1,87±0.43	4,26±0.71	4,93±0.70	13,20±0.21	20,45±0.52	51,42±1.76	372,94±1.62	822,15±1.76
Re	41,83±1.97	98,88±0.24	142,56±4.42	422,22±3.43	736,08±5.26	1096,28±4.85	2536,75±54.15	3739,84±76.43
Os	577,43±772.68	606,99±771.08	607,33±736.41	182,47±3.05	337,47±8.93	554,50±29.59	2036,16±231.21	2964,06±144.99
Ir	39,09±0.50	89,20±0.03	120,03±1.76	154,10±2.35	240,16±1.42	432,69±2.46	1375,87±36.08	2638,09±7.61
Pt	19,51±0.36	57,05±1.05	82,28±1.21	178,06±1.68	369,79±3.81	619,29±1.43	1958,18±40.31	3453,29±22.18
Au	0,81±1.14	0,90±1.28	0,54±0.76	0,83±0.14	0,85±0.07	2,13±0.06	9,96±0.28	18,73±2.90
Element	A	B	C	D	E	F	G	H
Ru	9,84±0.95	26,16±0.70	41,58±1.27	197,98±1.37	556,32±5.23	1073,35±9.91	2440,83±22.56	3924,92±33.30
Rh	41,82±0.11	95,52±0.29	140,68±0.95	409,03±1.00	788,24±0.34	1342,10±12.85	2645,28±44.21	3739,64±59.75
Pd	1,99±0.59	4,69±0.54	6,11±0.67	10,01±0.55	23,10±0.16	59,19±0.33	231,24±0.46	702,77±11.87
Re	45,46±1.16	98,77±1.80	142,15±3.17	387,10±7.97	715,15±5.43	1221,85±4.31	2337,53±32.78	3522,80±10.04
Os	589,06±787.62	609,37±774.96	608,77±742.20	169,57±2.40	327,41±13.65	668,75±36.79	1803,65±166.28	2766,77±157.25
Ir	42,55±0.53	90,90±0.14	119,82±0.66	142,23±1.08	232,37±0.09	488,50±6.61	1254,06±30.93	2395,37±39.03
Pt	23,98±0.25	56,48±1.11	79,05±0.07	160,27±0.15	367,68±2.75	728,22±12.06	1795,49±37.27	3220,47±85.98
Au	0,77±1.09	0,93±1.31	0,72±1.01	0,71±0.08	1,20±0.98	1,90±0.07	3,61±0.14	10,44±1.63

Table 18b – PGE and Au equilibrium concentration ($\mu\text{g/l}$) and standard deviations from ICP-MS replicate analysis, after interaction of the Zandvlei sample with the respective reagent solution (A, B, C, D, E, F, G, and H) in the adsorption isotherm experiments. Duplicate aliquots: upper/lower panel.

Element	Reagent solution							
	A	B	C	D	E	F	G	H
Ru	3,09±1.33	9,28±1.01	17,98±0.71	60,90±0.60	182,85±0.98	424,98±4.28	1332,26±11.89	2719,59±40.21
Rh	20,69±0.03	53,57±0.46	91,64±0.24	306,94±3.00	721,69±6.13	1128,88±14.16	2271,04±54.76	3695,15±32.70
Pd	5,67±0.99	7,65±0.27	10,00±1.21	13,20±0.29	13,40±1.08	11,94±1.56	9,71±1.44	21,46±0.71
Re	44,73±2.84	98,26±3.11	148,46±3.88	415,07±4.92	901,33±7.61	1331,57±21.25	2567,69±67.80	4118,62±98.93
Os	601,35±818.96	618,40±808.12	81,58±5.18	332,06±31.77	942,20±81.68	2111,79±256.60	2612,52±398.31	3154,33±40.72
Ir	42,41±0.13	93,27±0.22	144,25±3.42	400,87±2.65	868,81±6.10	1302,55±18.05	2447,16±39.35	4081,76±2.63
Pt	20,20±0.58	43,52±1.56	63,51±4.39	140,03±4.76	286,54±11.86	387,33±5.99	743,05±13.80	1302,69±20.37
Au	4,79±3.11	9,20±5.99	24,03±0.80	45,57±0.11	58,41±2.44	51,24±8.23	18,63±1.21	18,15±2.71
Element	A	B	C	D	E	F	G	H
Ru	4,13±0.37	9,19±1.51	17,71±1.54	65,55±0.33	177,31±0.55	448,23±2.31	1318,03±6.62	2326,04±34.00
Rh	22,40±0.15	55,04±0.11	90,36±1.34	318,35±0.45	707,78±10.51	1042,25±7.86	2343,74±56.67	3195,41±5.80
Pd	4,57±0.14	7,47±0.44	10,92±0.77	12,02±0.44	12,86±1.36	11,43±1.05	9,31±bdl	17,93±1.13
Re	49,64±1.75	97,63±1.49	145,62±1.66	435,32±0.23	885,39±0.89	1230,20±30.27	2680,32±69.70	3484,34±115.16
Os	608,35±829.55	618,80±801.52	81,59±5.79	328,91±44.92	983,22±103.35	2284,39±296.14	2560,14±311.66	2568,38±79.44
Ir	46,87±0.22	94,40±1.03	142,69±1.14	421,94±5.96	858,14±1.07	1190,18±4.98	2559,71±69.06	3046,67±30.99
Pt	21,65±0.62	44,96±1.95	61,16±2.52	135,64±4.66	256,14±8.88	377,09±4.22	562,27±16.64	946,24±7.12
Au	2,79±3.94	11,99±5.92	23,37±1.81	35,64±0.67	55,79±1.56	45,32±7.65	22,16±0.74	9,81±1.99

Table 18c – PGE and Au equilibrium concentration ($\mu\text{g/l}$) and standard deviations from replicate ICP-MS analysis, after interaction of the Tokai sample with the respective reagent solution (A, B, C, D, E, F, G, and H) in the adsorption isotherm experiments. Duplicate aliquots: upper/lower panel.

Element	Reagent solution							
	A	B	C	D	E	F	G	H
Ru	16,28±0.75	34,90±1.10	53,03±0.74	142,90±0.63	391,20±3.93	726,07±1.74	2589,75±9.41	3655,39±64.90
Rh	44,59±0.97	96,47±1.86	136,39±0.32	411,17±1.21	836,66±10.76	1231,21±12.35	2816,33±94.75	3864,42±2.25
Pd	9,44±1.16	11,02±1.18	13,89±0.49	8,11±0.42	13,96±0.13	20,54±0.16	372,94±1.62	89,79±0.08
Re	46,44±2.42	98,64±2.44	137,97±0.03	396,75±3.01	780,82±6.10	1109,63±21.42	2536,75±54.15	3692,74±47.53
Os	608,19±811.24	612,68±773.66	87,99±1.07	142,28±5.01	56,87±19.70	603,13±66.47	2036,16±231.21	2326,81±95.47
Ir	43,09±0.70	88,29±0.21	114,76±0.60	146,50±0.32	209,19±1.72	335,41±6.98	1375,87±36.08	1724,98±12.99
Pt	13,45±0.18	29,54±0.47	36,61±0.330	22,13±0.77	42,41±0.49	107,65±0.21	1958,18±40.31	1360,60±5.12
Au	4,83±6.83	4,32±6.10	7,81±0.06	1,17±0.25	3,75±1.29	3,73±0.08	9,96±0.28	5,74±2.07
Element	A	B	C	D	E	F	G	H
Ru	16,04±2.10	32,14±1.31	51,56±0.19	576,81±6.37	368,06±1.02	596,84±2.88	2440,83±22.56	3825,54±43.65
Rh	46,53±0.40	95,86±0.72	139,20±0.46	816,53±4.08	769,98±5.65	1053,51±0.12	2645,28±44.21	3992,48±7.12
Pd	8,76±1.10	11,42±0.92	13,71±1.06	20,45±0.52	13,07±0.22	16,35±0.41	231,24±0.46	113,18±0.47
Re	48,07±1.56	96,85±1.67	141,70±2.74	736,08±5.26	712,50±6.92	956,55±11.32	2337,53±32.78	3844,03±69.62
Os	611,40±812.83	612,66±776.41	86,35±0.89	337,47±8.93	40,13±19.53	294,63±8.50	1803,65±166.28	2518,43±134.72
Ir	45,87±0.57	88,88±0.73	118,50±0.84	240,16±1.42	193,09±2.68	264,59±3.02	1254,06±30.93	1898,32±5.77
Pt	12,33±0.53	23,75±0.34	32,96±0.07	369,79±3.81	42,49±0.74	75,45±0.07	1795,49±37.27	1471,69±9.79
Au	4,92±6.95	5,22±7.38	7,66±0.24	0,85±0.07	4,83±1.57	2,61±0.68	3,61±0.14	33,28±36.72

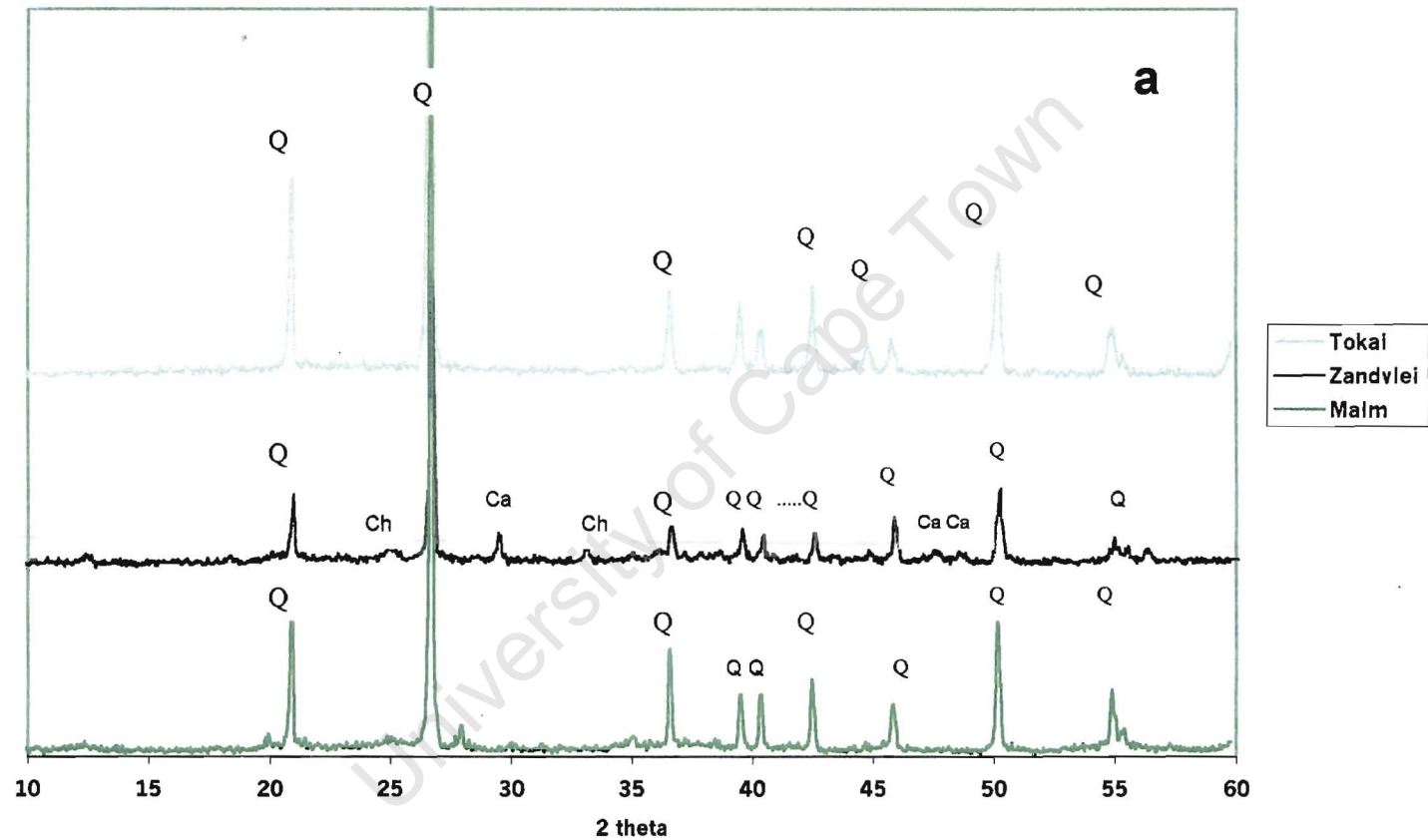


Figure 11 – X-ray diffractograms of the solid matrices: (a) X-ray diffractogram for Malm, Zandvlei, Tokai and Consol sand bulk sample (< 2 mm) and (b) X-ray diffractogram for Malm, Zandvlei and Tokai clay fraction. Note: Q-quartz, Ch-chlorite, Ca-calcite.

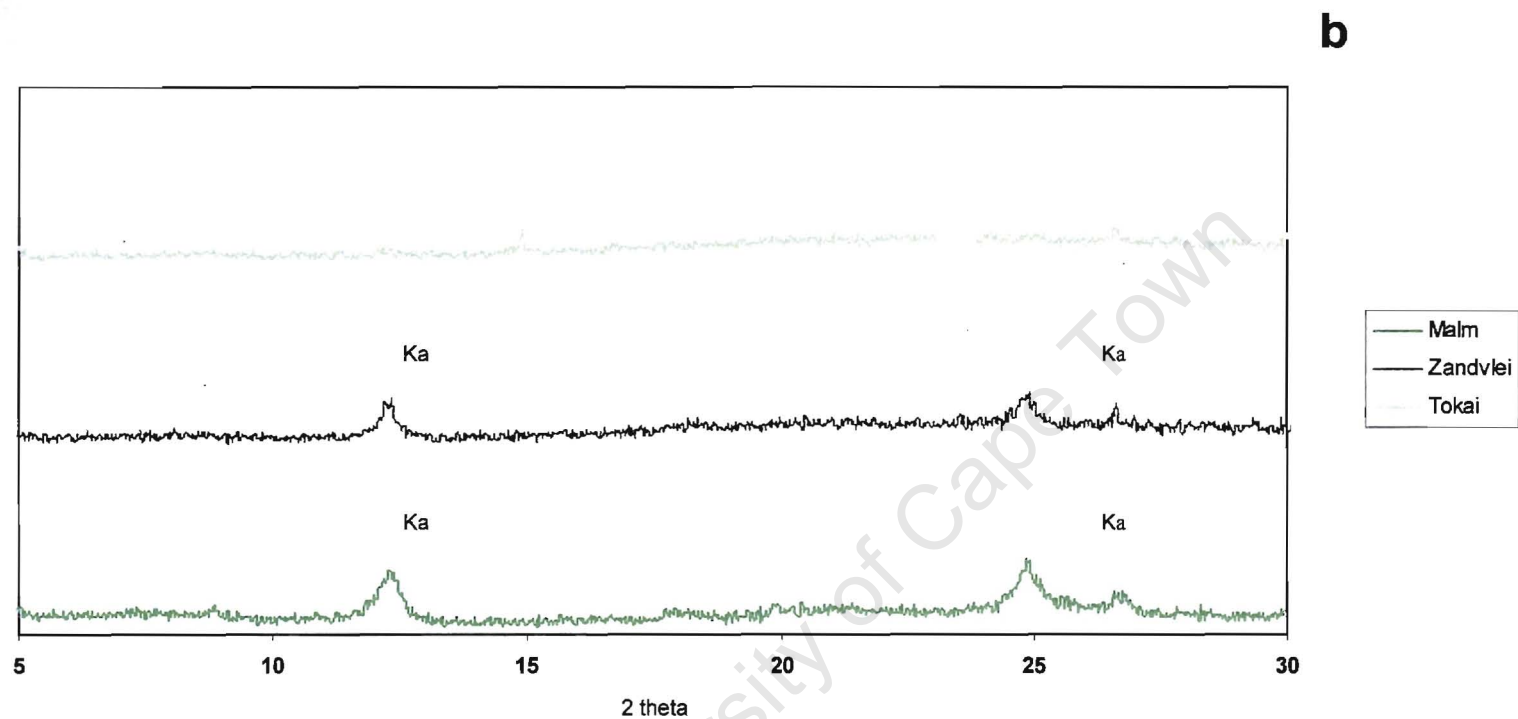


Figure 11 – X-ray diffractograms of the solid matrices: (a) X-ray diffractogram for Malm, Zandvlei, Tokai and Consol sand bulk sample (< 2 mm) and (b) X-ray diffractogram for Malm, Zandvlei and Tokai clay fraction. Note: Ka-kaolinite

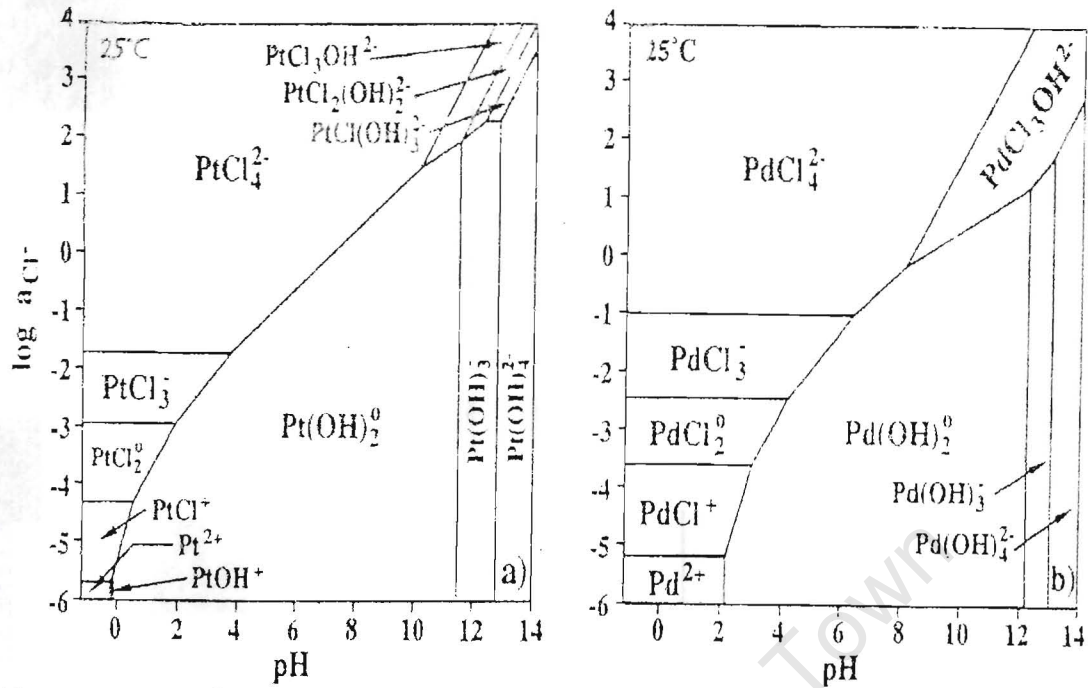


Figure 12 - Plot of $\log a_{Cl^-}$ versus pH for (a) Pt and (b) Pd at 25°C showing the various fields of predominance of the various chloride, hydroxide and mixed hydroxychloride complexes.
 Source: Wood et al. (1992).